NCSX

Design Basis Analysis

Modular Coil Bolted Joint Analysis

NCSX-CALC-14-008

13 July 2004

Prepared by:

Kevin Freudenberg
Digitally signed by Kevin Freudenberg
DN: cn=Kevin Freudenberg, c=US, o=Fusion Energy, ou=ORNL, email=fdk@ornl.gov
Date: 2008.07.01 15:05:32 -04'00'

Leonard Myatt (Myatt Consulting, Inc.)

K. Freudenberg, ORNL

I have reviewed this calculation and, to my professional satisfaction, it is properly performed and correct. I concur with analysis methodology and inputs and with the reasonableness of the results and their interpretation.

Reviewed by:

David Williamson
2008.07.02 08:31:50 -04'00'

D. Williamson, ORNL Engineer

Table Of Contents

Table Of Figures

1. Executive Summary

A structural analysis of the NCSX Modular Coil (MC) assembly is presented. The analysis focuses on the outboard coil-to-coil bolted connections (so-called A-A, A-B, B-C & C-C) in an effort to determine the acceptability of these mechanical joints. The analysis is based on an evolutional global ANSYS [1] model of the A-B-C half-field period [2], and detailed models of the so-called Type-1 (through-hole) & Type-2 (tapped-hole) bolted joints used to secure these flanged connections. An effective stiffness of each bolted joint type is determined and incorporated into the global model with equivalent beam elements. Various levels of friction are analyzed and the resulting bolt shear force and interface slip distributions are presented. The detailed models are also used to determine the stress range in the bolts from EM load cycles. A design-basis fatigue curve for the bolts is presented and used along with detailed model stresses to produce a bolt life (N) as a function of shear load (F) map for each joint configuration. The final analysis included a slight change to the Type 1 & 2 bolted joint design (increasing the shim clearance hole). Curves for each joint type indicate that the Type 1 joint shear loads should not exceed ~15 kip, while the Type 2 joint shear loads should not exceed ~9 kip for a 100,000 cycle design life.

The analysis shows that a friction coefficient of 0.4 is more than sufficient to provide a "no-slip" joint with a preload value of ~72 kip (kilo-pounds). With the Inner leg welded on the AA, AB and BC flanges, the entire outboard flange interfaces adjacent to the bolts remain "stuck" while subjected to what is thought to be the most demanding EM loading (2 Tesla high beta). In all cases, the bolt shear loads are held below 3 kips. The analysis for the three welded flanges (AA, AB, BC) was performed when the baseline design called for inboard bolts instead of in-board welds to impart the shear load in those areas. Here, the bolts are modeled identically to the outboard with the same friction coefficient. Thus, the analysis with the bolts presented here provides a conservative approach to the outboard bolts as it allows for some slippage in the inboard, which the welds analysis has shown to be near non-existent.

The CC Connection examines the outboard bolted joint using standard 1.375" bolts placed on the inboard side of the coil to impart the shear load and deflection. The exact number and location of these bolts remains in question pending a mock-up access study but it is shown that as long as six of the bolts are added the inboard shim does not slip on CC flange.

2. Introduction

The function of the NCSX modular coil system is 1) to provide specified quasi-axisymmetric magnetic field configurations, 2) to provide access for tangential neutral beam injection (NBI), radio frequency (RF) heating, and diagnostics, and 3) to provide a robust mechanical structure that minimizes non-symmetric field errors. The coil set consists of three field periods with six coils per period, for a total of 18 coils. Due

to stellarator symmetry, only three different coil shapes are needed to make up the complete coil set. The coils are connected electrically in three circuits according to type, and as such can produce alternate magnetic configurations by independently varying the current for each type.

The modular coils are wound onto stainless steel castings that are then bolted together to form a structural shell. As shown in Fig. 1, the winding cavity is a "tee" structure that is located on and integral with the plasma side of the shell. During operation, electromagnetic forces push the windings outward against the shell and laterally toward the "tee", so that only intermittent clamps are required for structural support.

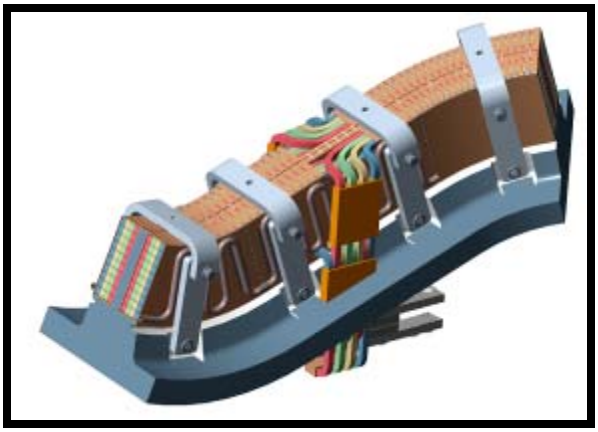

Fig. 1. Mod Coil Schematic showing the winding cavity (tee), winding and clamps

3. Analysis Approach

A CAD model of the MC half-field period assembly is shown in Fig. 2. and provides an overview of the modeling scope. This incarnation of the model represents the latest version of the model complete with individual shims, bolts and inner leg weld shims. This CAD version does not include any inboard bolt holes on the AA, AB and BC flanges but holes have been added to the CC Flange. Fig. 3. illustrates a detailed look at the bolt/shim/flange interface on C-C flange.

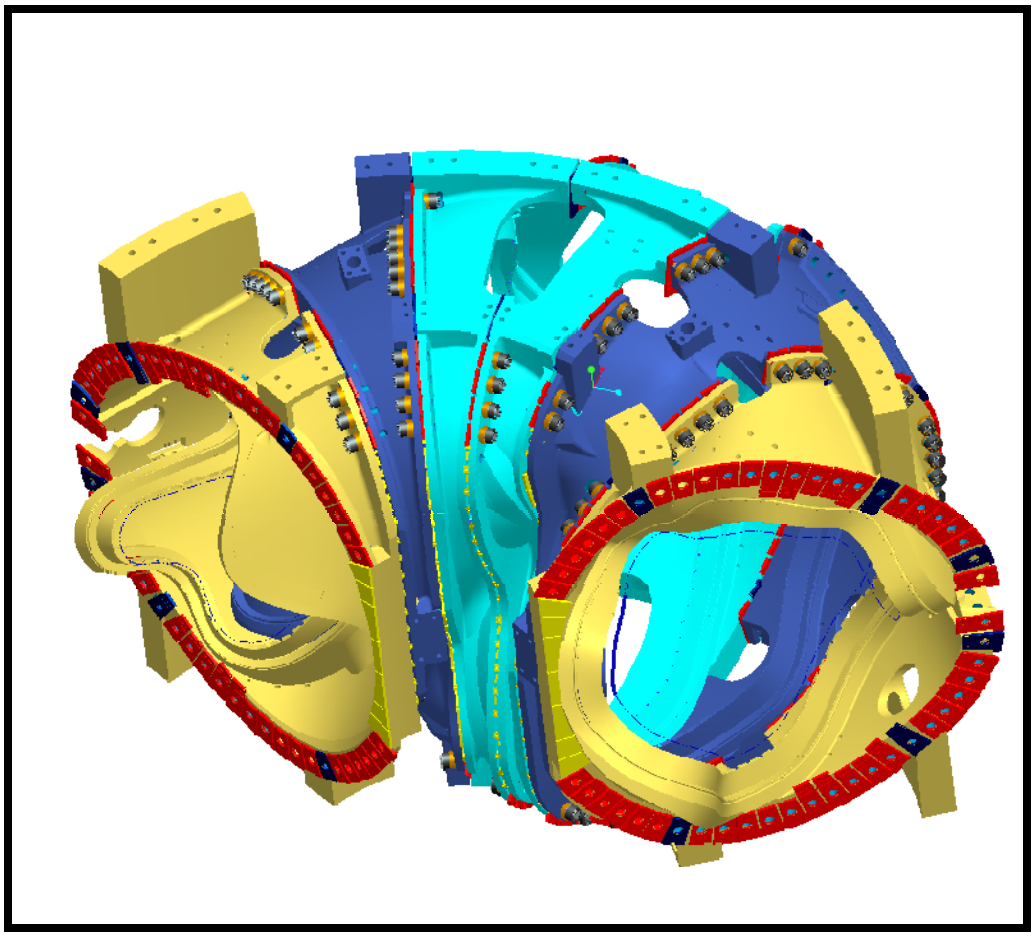

Fig. 2. Full Period Coil CAD Model (6 Coils)

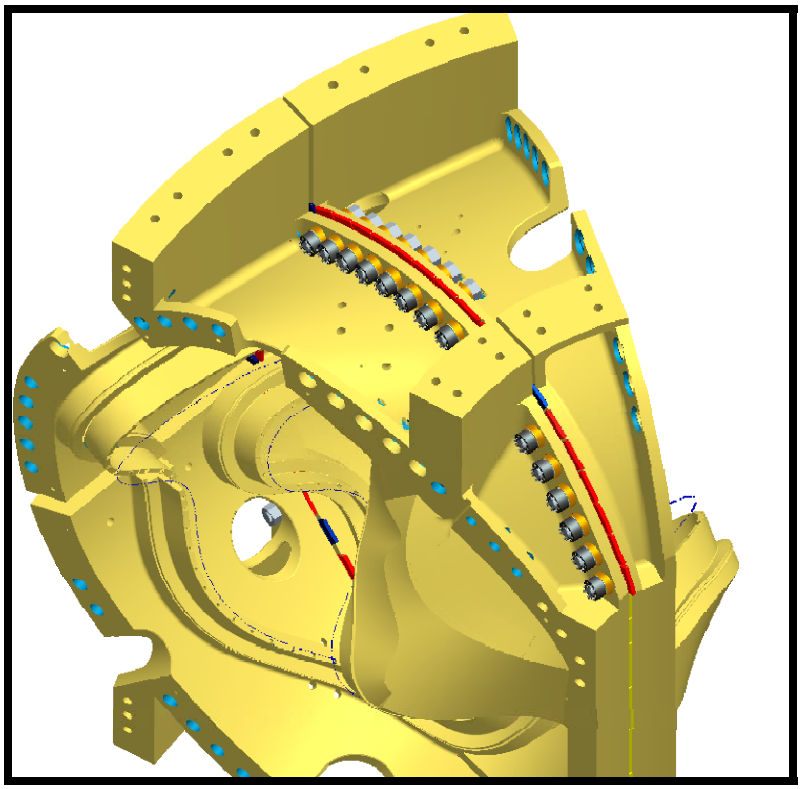

Fig. 3. C-C Interface CAD Model

3.1. Material Properties

The properties used assumed that the shell is made of stainless steel and the coil windings consist of a homogeneous copper/epoxy mixture. The properties are listed in Table 1. These values are used where when the thermal loading from a localized modular coil model is applied to the shell and the winding form.

TABLE 1: Material Properties.

	E (Mpa)	CTE /K	Poisson's Ratio
Tee/shell	151,000.00	0.00E+00	0.31
Modular Coil	58,600.00	1.00E-05	0.3
Toroidal Spacer	151,000.00	0.00E+00	0.31
poloidal spacer	151,000.00	0.00E+00	0.31
Wing bag	1,100.00	2.30E-04	0.42
Wing bag	1,100.00	2.30E-04	0.32
Clamp	151,000.00	0.00E+00	0.31
Top pad	21.28	1.25E-03	0

3.2 Magnetic Loading

Calculations to determine the fields and forces acting on all of the stellarator core magnets have been completed for seven reference operating scenarios. The worst case for determining forces in the modular coils appears to be the 2T high beta scenario at time=0.197-s. Two independent field calculations have been performed, one with the ANSYS code and the other with MAGFOR [3]. A comparison of magnetic flux density at 2-T indicates that the models are in good agreement, with only a 4% difference in peak field due primarily to mesh and integration differences.

3.3. Assumptions

The non-linear (frictional) analysis of this structure is based on the half-field period model shown in Fig. 4. Structural continuity between adjacent coils is handled two different ways to accommodate the computational limitations of this large problem:

1. At one particular interface, pipe elements with appropriate section properties are used to represent the characteristics of a bolted interface (see Attachment Section 4.1). Contact elements at this interface are allowed sliding contact (no separation). Fig. 5 shows the pipe elements used to model the bolt, connecting it to the hole via bar elements.
2. The other bolted interfaces are modeled with "Bonded Contact."

This un-bonded, sliding-only contact surface modeling approach seems to be the only way to get the analysis to complete in a reasonable amount of time (of order 12 hours). When the more general contact

behavior is implemented (stick-slip, open-closed), the model takes four days to reach 4% of the EM load case. The simplified approach is decent, with frictional shear only developing when a positive normal pressure occurs. So, shear loads in the bolts are reasonably accurate. However, since this approach simulates a "hooked" interface, it does not accurately represent the change in axial load on the bolts.

Simulating the 12-coil MC system with a half-field period (3-coil) model requires the application of displacement U(R,θ,Z) constraint equations (CE) to the cut boundaries (θ=0º & 60º). Nodes on these symmetry planes are rotated into a cylindrical coordinate system. Fig. 6 shows a graphical representation of this boundary condition which illustrates the following general rule. The vertical lines represent the link between the +Z nodes and -Z nodes. One node on the B shell is restrained in the vertical direction (z) to complete the required DOF constraints.

$$UR(R,\theta,Z) = +UR(R,\theta,-Z)$$
$$U\theta(R,\theta,Z) = -U\theta(R,\theta,-Z)$$
$$UZ(R,\theta,Z) = -UZ(R,\theta,-Z)$$

The electromagnetic loading (EM) is limited to one particular time-point (t=0.0s) within one particular current scenario (2T High-β). It is commonly thought that this represents the worst load case. However, there has been no attempt to verify this position. The nodal force files for each coil are read into the structural routine before the solution. Fig. 7 shows a plot of the coils and nodal force vectors (for visualization purposes).

Previous analysis [2,4] has shown that the non-linear contact interactions between the coils and winding forms do have an impact on stress. Running a non-linear sliding winding in this case is computationally difficult given the compute time required. Thus, to simulate this effect in a linear manner, a "wimpy" winding pack was used in these models. It has a modulus of 856 Mpa or 100 times less than that listed in Table 1. This allows for the brunt of the magnetic loading to transfer directly to the tee as the winding pack stiffness is reduced. This has a greater effect near the tee region than the flange interfaces but to be conservative, the value was used to simulate the maximum amount of magnetic loading the shell would ever experience.

3.4. Special Consideration

The purpose of this effort is to upgrade the global model to simulate the more realistic flange-to-flange connectivity. Previous modeling approaches assume bonded contact at flange connections which maintains a linear structure. Here, equivalent-property bolts and sliding contact are introduced at each flange interface (one at a time); A-A, A-B, B-C & C-C. This results in a non-linear analysis and adds substantial complexity to an already large model. Sliding, frictionless contact is the simplest embodiment of this upgrade. However, it ignores the most significant mechanical component to the bolted connection: joint shear capacity form friction. Adding friction to the simulation adds another complication which is not only non-linear, but path-dependent. Loads must be applied gradually to allow the model to initiate slippage when the shear load exceeds the frictional capacity of the interface. Embedded in the contact model are "normal"

and "transverse" stiffness values. ANSYS determines "appropriate" values of each. Of course, these default values handle a wide range of modeling scenarios, but not necessarily all situations.

Contact Stiffness

Following the presentation of numerous global model results which showed high shear loads in some of the bolts, a detailed review of the contact element characteristics uncovered a defect in the model. The default contact element shear stiffness (~0.17E11 N/m^3) was found to be too soft, and flange faces slipped when they should have been stuck. Over-riding the default shear stiffness value with incremental increases produced lower bolt shear loads and longer computer run-times for the representative A-A interface. This characteristic is shown in Fig. 2.0-6. A shear stiffness of 5E11 N/m^3 seems to provide a reasonable compromise in accuracy and run-time. All analyses presented here use this value which is ~30x larger than the default stiffness. However, when considering the CC added inner bolts, even the value of 5e11 N/m^3 is too small and larger values are used.

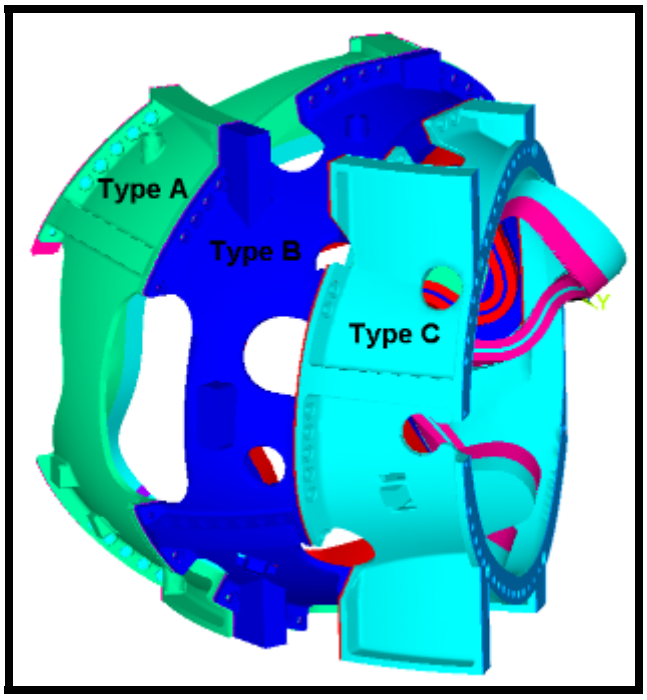

Fig. 4. Half-Field Period Global ANSYS Model.

Model Boundaries in a cylindrical coordinate system are at:
θ=0º (mid-thickness A-A shim)
θ=60º (mid-thickness C-C shim)

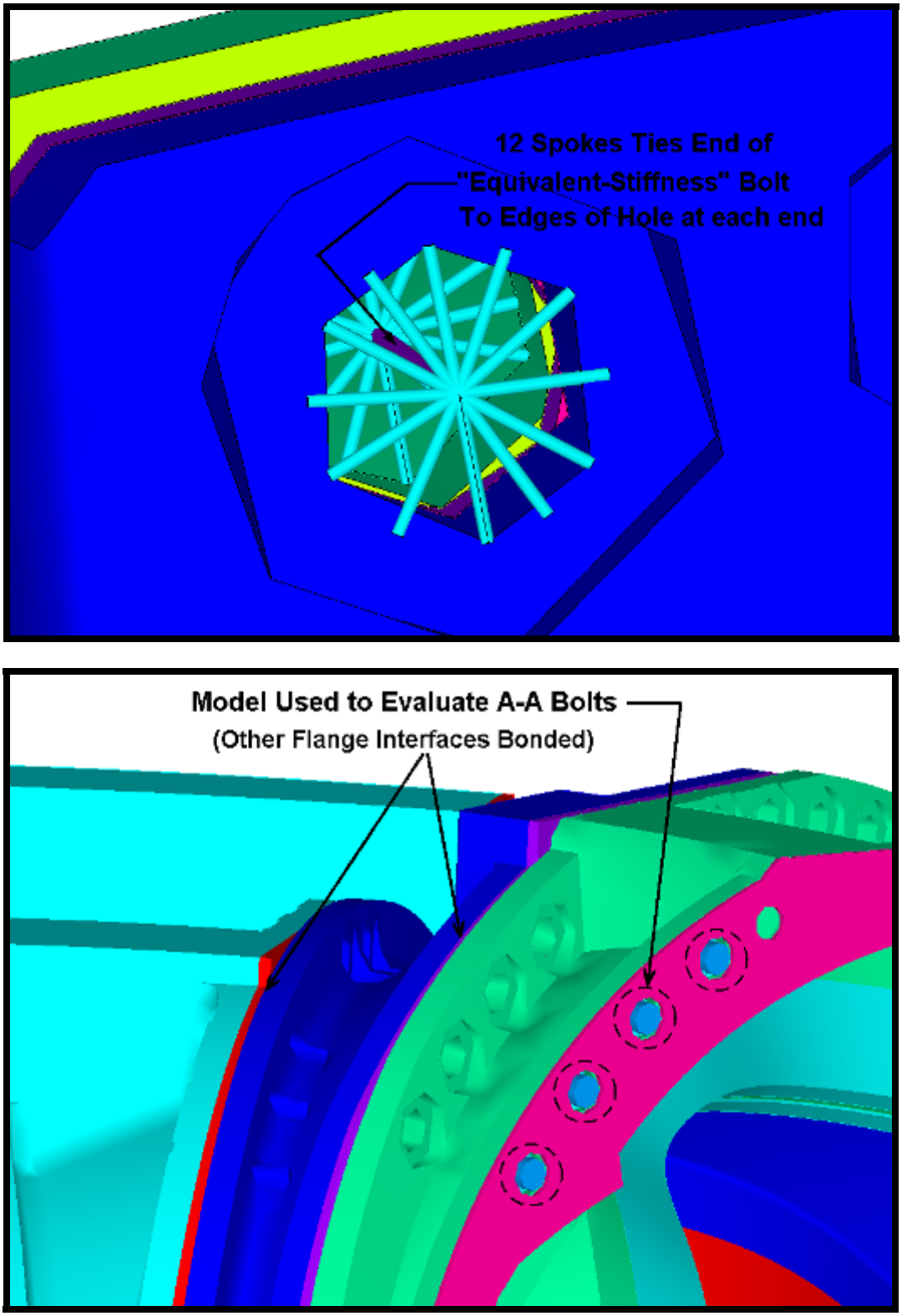

Fig. 5. Pipe Elements with Appropriate Section Properties Used to Simulated Bolted Connection Equivalent Pipe Elements Tie A-B Flanges (diameters scaled for visualization purposes)

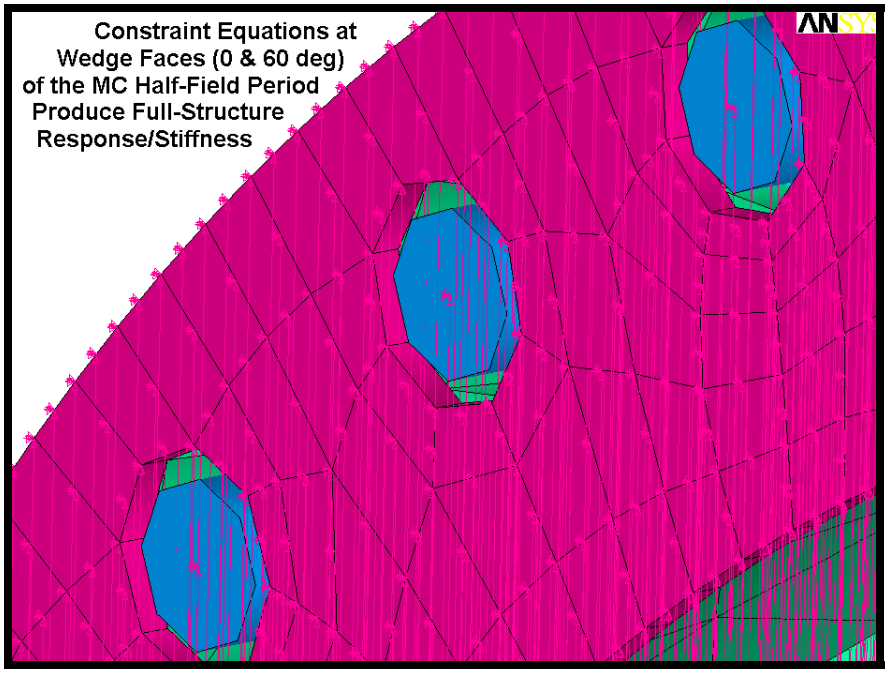

Fig. 6. Constraint Equation Symbols at A-A Shim Mid-Thickness

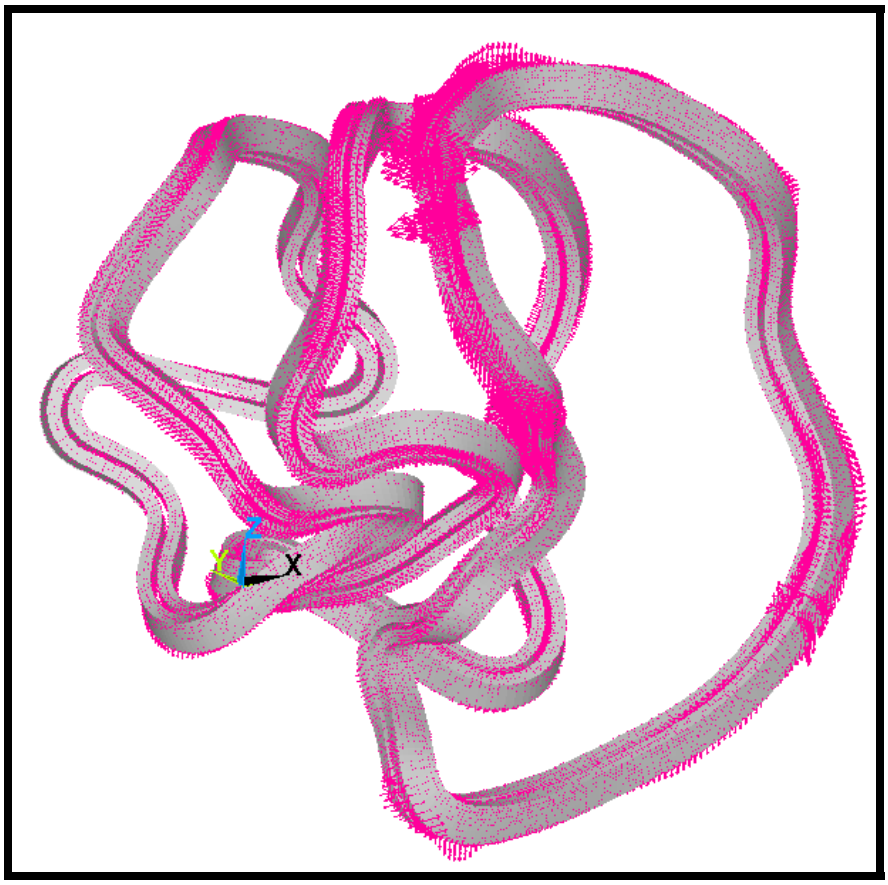

Fig. 7. Nodal Forces (t=0.0s of 2T, High-β)

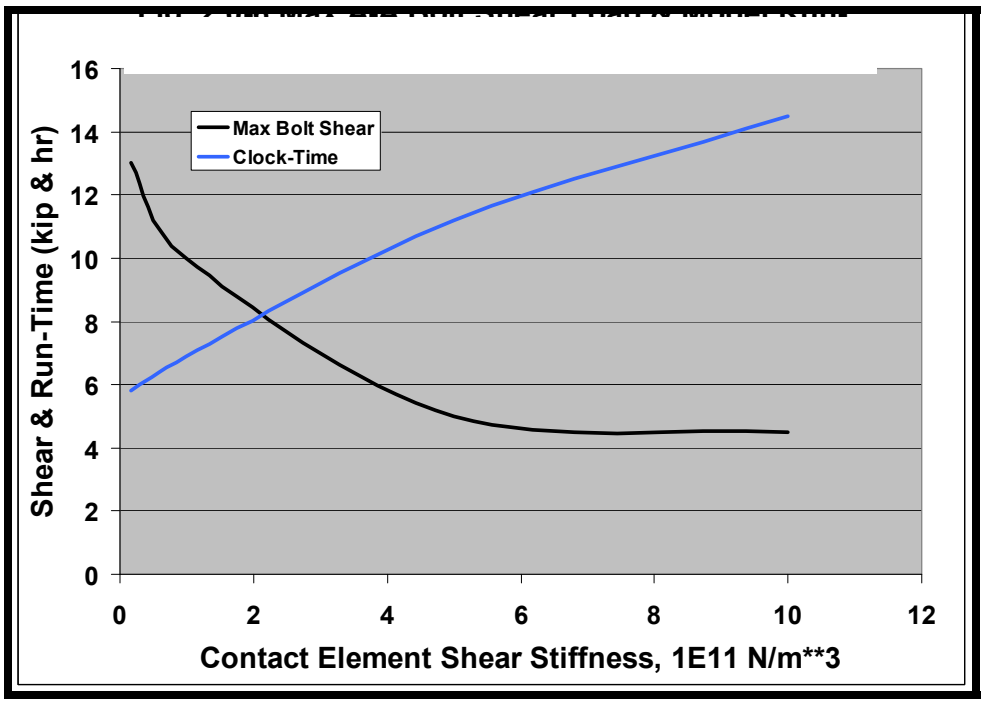

Fig. 8. Max A-A Bolt Shear Load & Model Run-Time vs Contact Stiffness

4. Global Model Results

4.1 Bolted Interfaces with Friction

Various analyses have indicated the need to improve structural continuity in the inboard leg region of the MC system. Designers have responded by modifications which include the addition of inboard leg bolts at A-A, A-B & B-C. The global model is exercised in an effort to quantify the shear load on the bolts.

Fig. 9 shows a bar chart of the tensile preload and transverse shear load form the EM load application in each of the 20 A-A bolts, and a model plot showing the bolt numbering system. The bolts are preloaded to roughly 75 kip (kilo-pounds), and the flange and shim surfaces have a finish which produces a design-basis friction coefficient of 0.4. Bolt numbers 5 & 6 carry the largest shear force at ~1.5 kip. This is indicative of the bolts being stuck and the loading transferred through friction as expected. The inner leg bolts are not plotted in the bar charts for any of the flanges but they were included in the analysis at the time. The now adopted inner leg weld will provide for a stiffer connection on the inboard side and thus these numbers and plots are conservative.

Fig. 10 shows a contour plot of the A-A interface slippage and the contact status plot bolt shear load vectors as a result of the EM load application. The blue regions of the contour plot are limited to the areas where bolts pull the flanges together and indicate little or no slippage. The slippage away from the inboard leg is quite small (< 0.05 mm).

A similar series of plots is included for the other flanged interfaces: A-B (Figs. 11 & 12), B-C (Figs. 13 & 14), and C-C (Figs. 15 & 16). Table 2 lists the salient numerical values. The plots show that most of the bolt shear loads are quite small (<3 kip). C-C has long regions without bolts, but the structure does not exhibit large slippage (<0.2 mm). The slippage numbers for the three welded flanges are approximate and very small away from the inboard region. All of the max shear values are under 3 Kips. The contact status plots indicate that the areas around all of the outboard holes are in deed in the "stuck" conduction for all of the coils.

Table 2. summary of MC Flange Interface Loads (75 kip Preload, μ=0.4)

Flange Set	Max Bolt Shear, kip	Max Slippage, mm
A-A	1.5	≈ 0.05
A-B	1.2	> 0.05
B-C	1.8	> 0.05
C-C	2.8	0.17

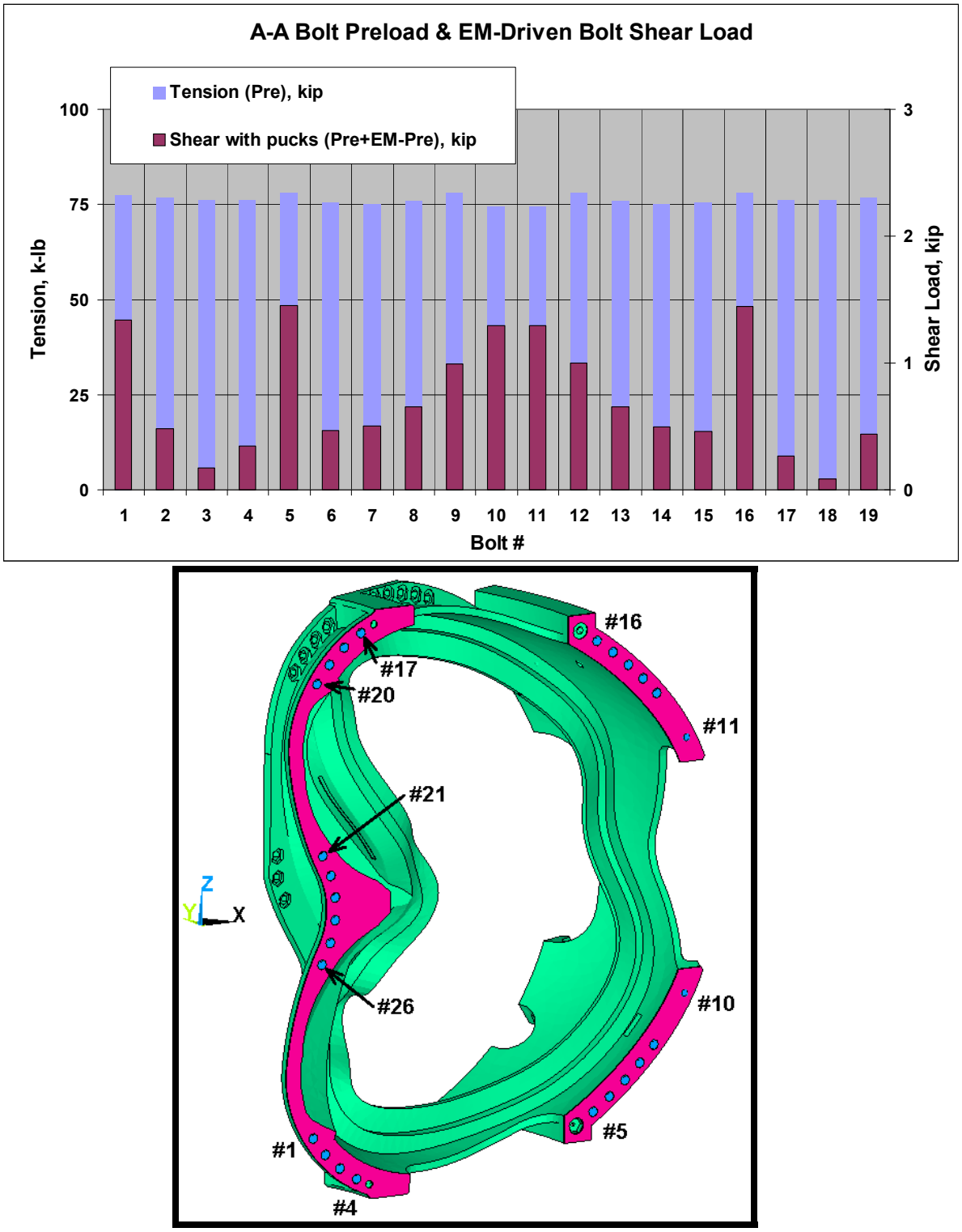

Fig. 9. A-A Bolt Preload & EM-Driven Shear Load (top) & Bolt Numbering (bottom)

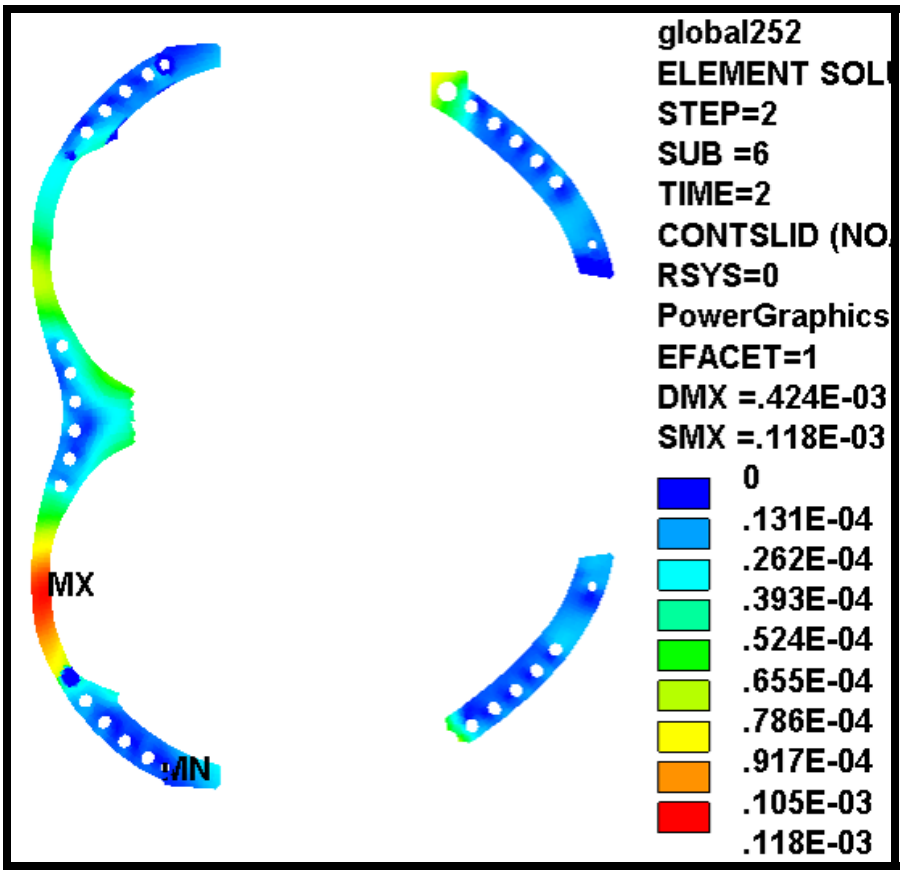

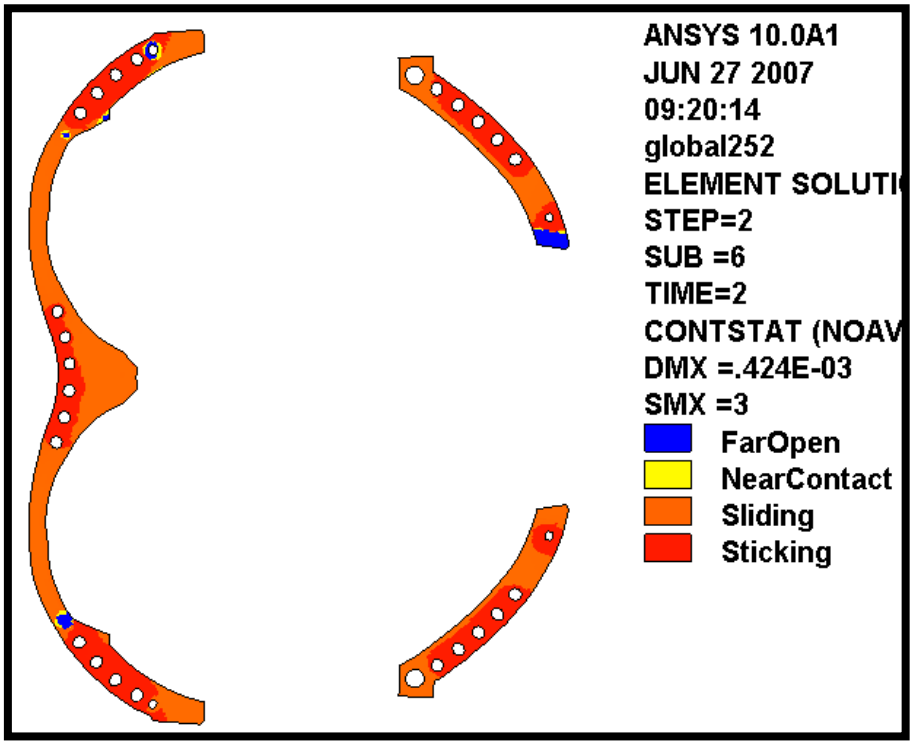

Fig. 10. A-A Slip [m] & Contact Status Plot from EM Load Application

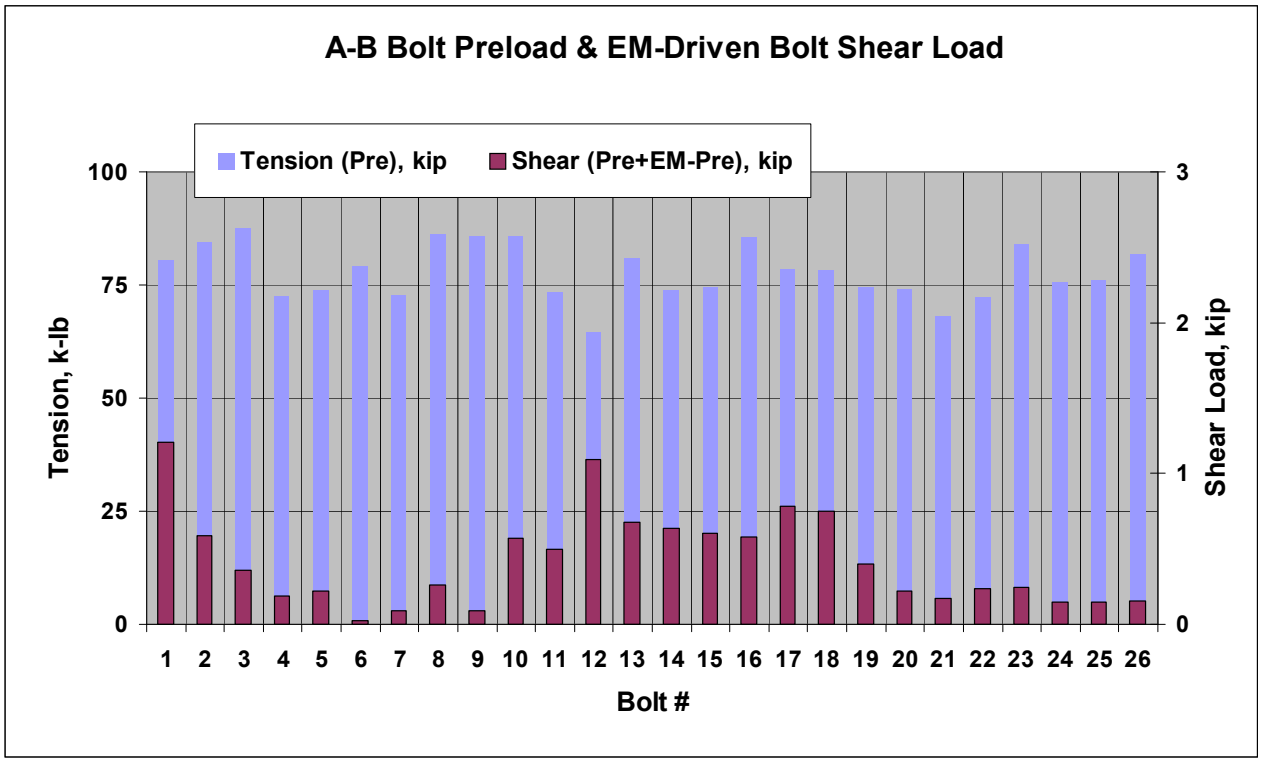

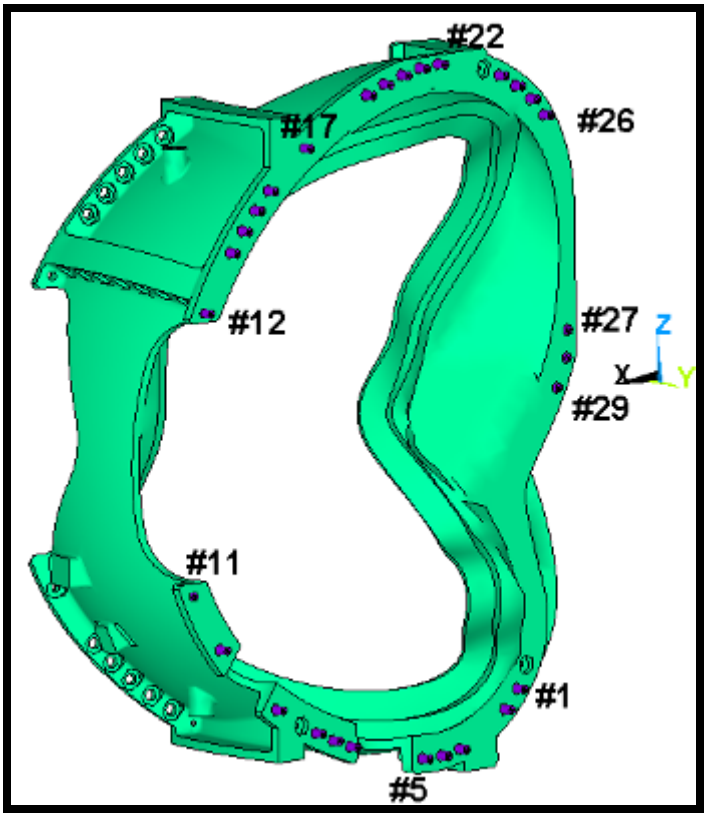

Fig. 11. A-B Bolt Preload & EM-Driven Shear Load (top) & Bolt Numbering (bottom)

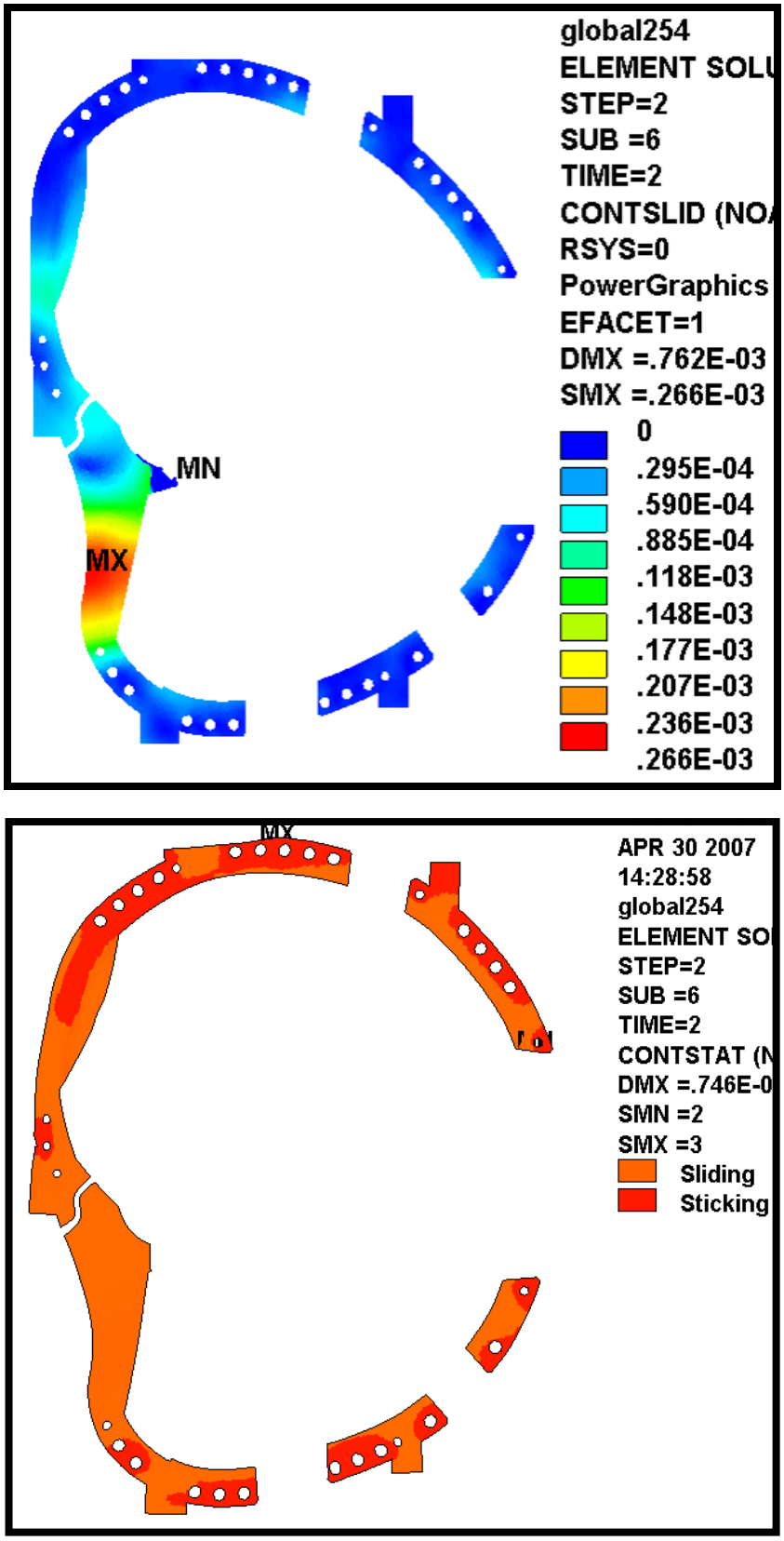

Fig. 12. A-B Slip [m] & Contact Status Plot from EM Load Application

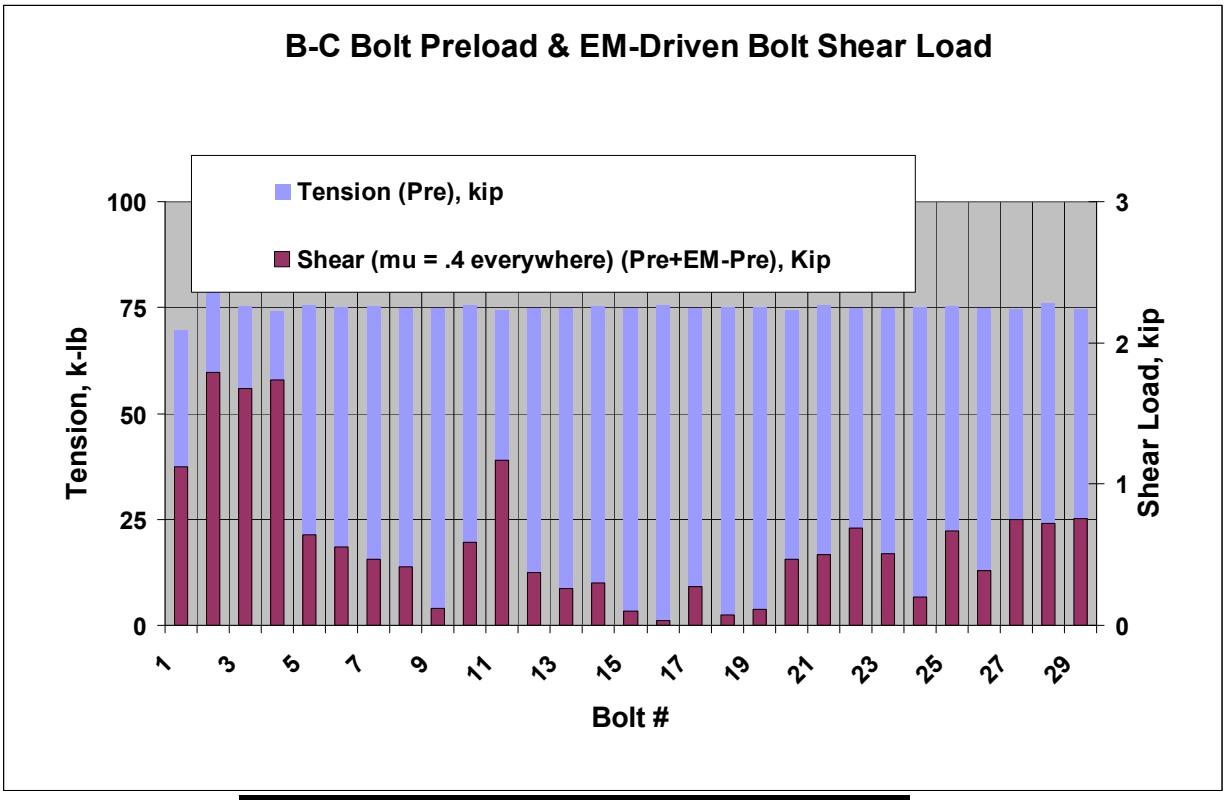

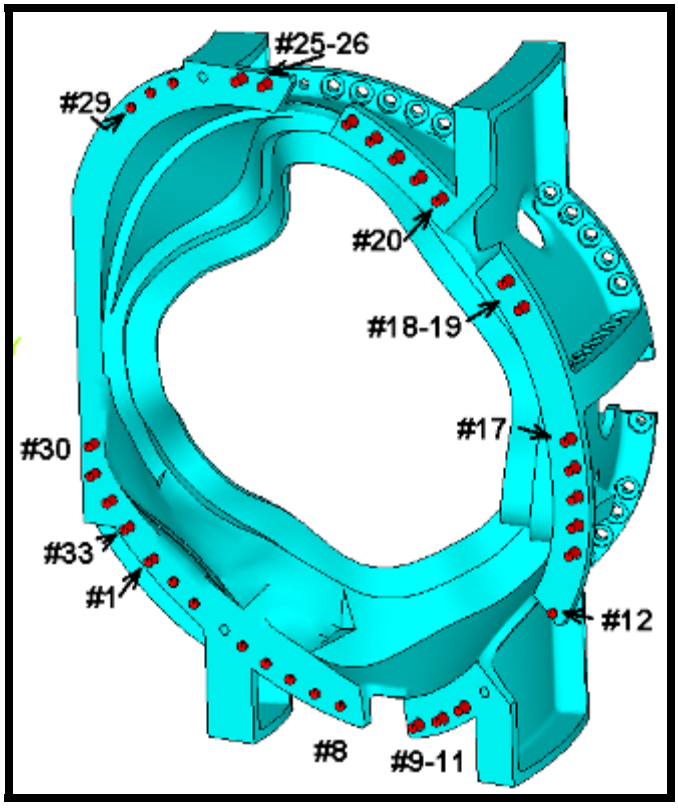

Fig. 13. B-C Bolt Preload & EM-Driven Shear Load (top) & Bolt Numbering (bottom)

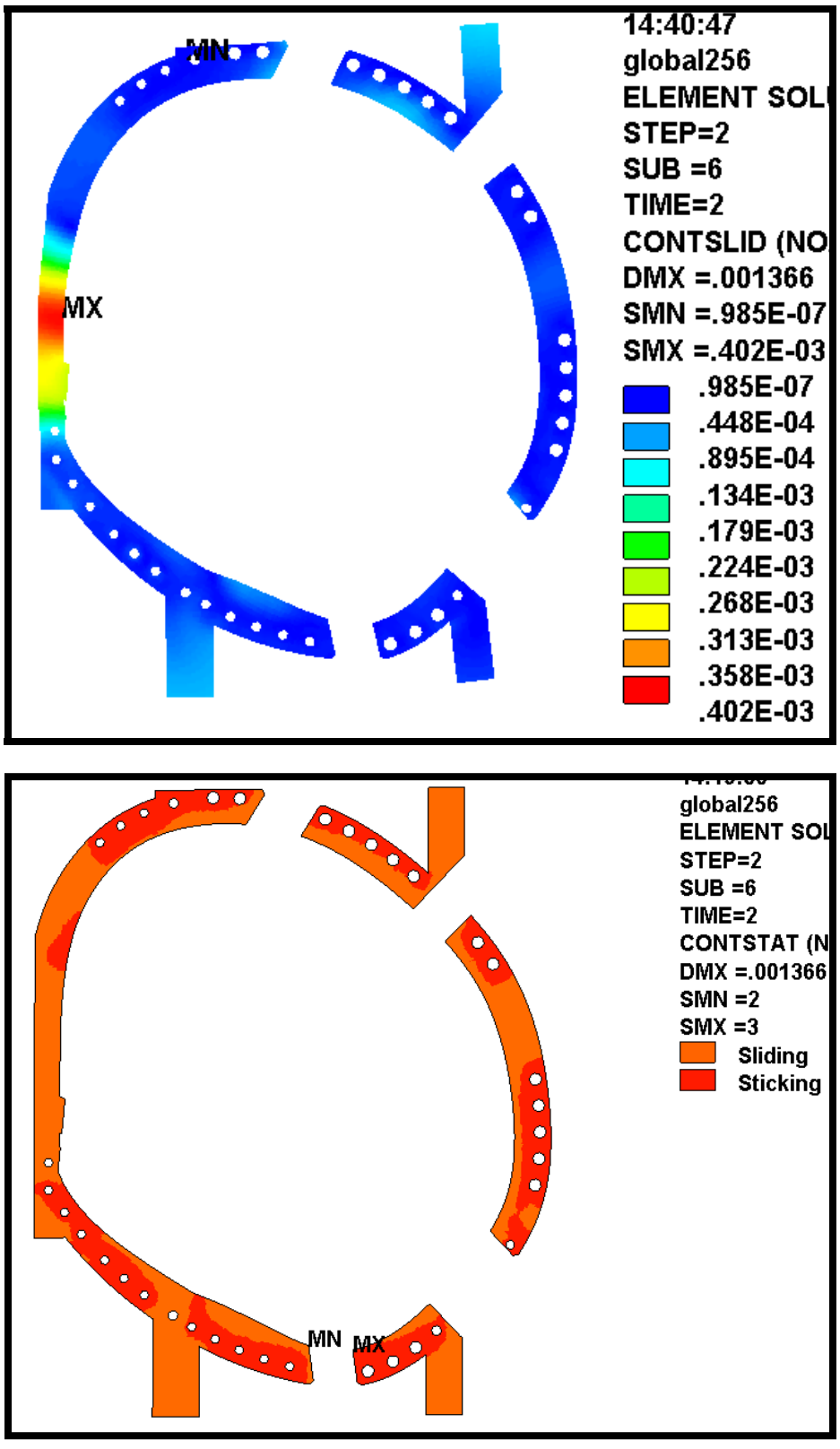

Fig. 14. B-C Slip [m] & Contact status Plot from EM Load Application

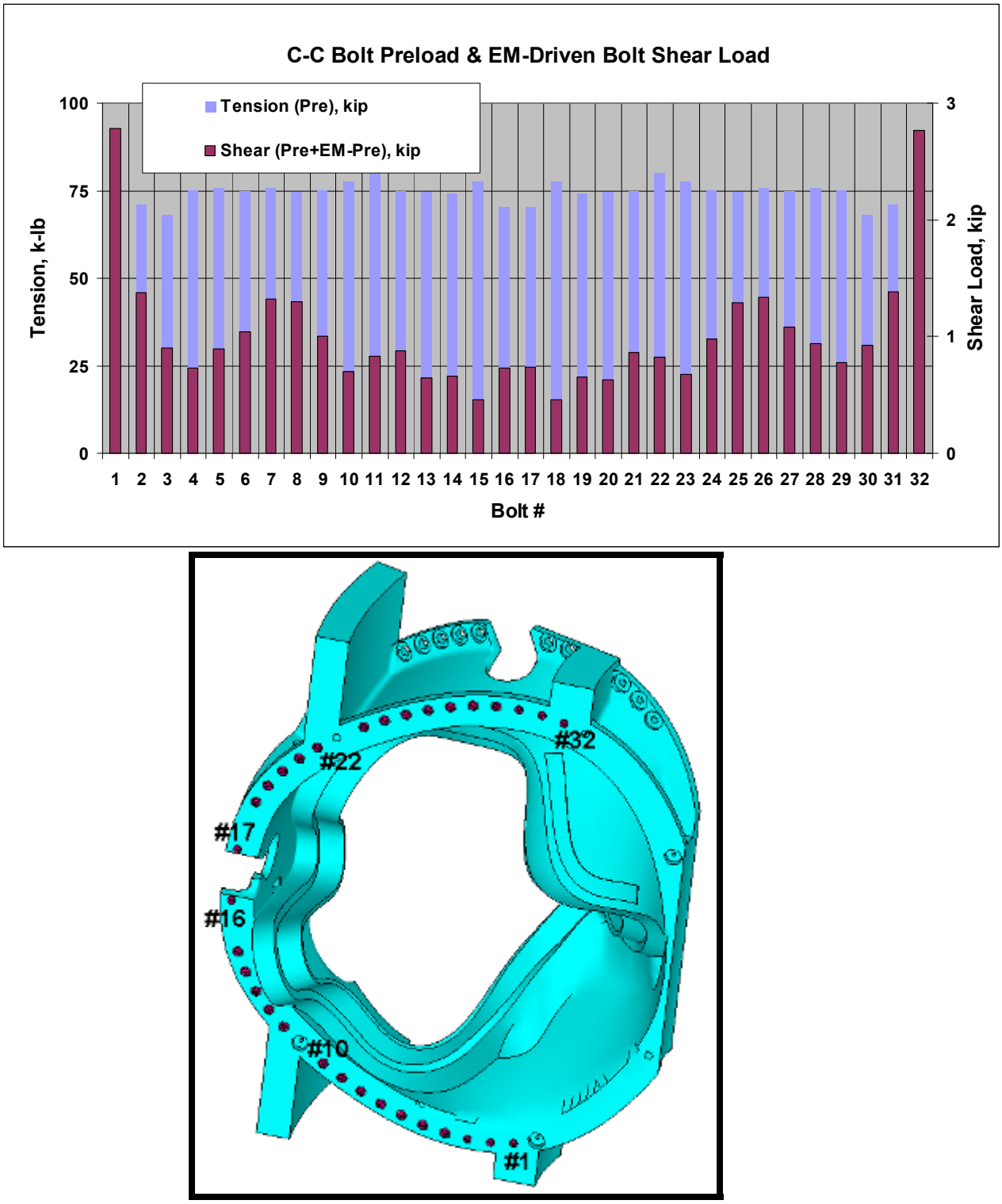

Fig. 15. C-C Bolt Preload & EM-Driven Shear Load (top) & Bolt Numbering (bottom)

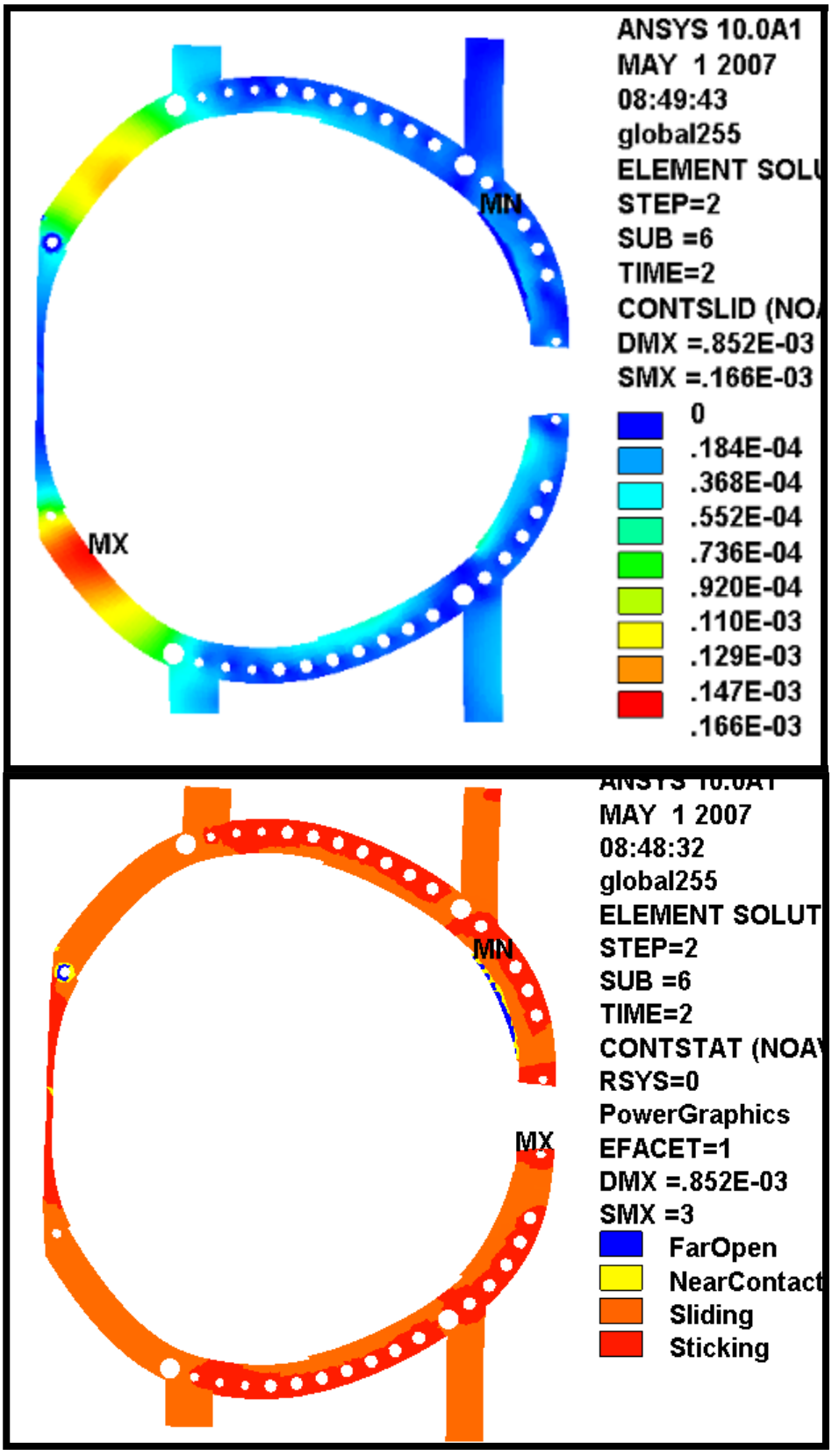

Fig. 16. C-C Slip [m] & Bolt Shear Loads [kip] from EM Load Application

4.2. Case Study 1> Results for the various CC inner leg options

The inner leg of the CC coil cannot be welded together like the other interfaces because of the electrical break isolation requirement. As such, the inner leg is outfitted with inner bolts. These bolts will be 1.375" diameter, which the same as the outer bolts. However, the exact number (a maximum of 12 per flange) is still in question pending an access study on a full scale mock up.

Fig. 18. shows a bar chart of the tensile preload and transverse shear load form the EM load application in each of the C-C bolts and a model plot of the friction scheme for the run. Here, 6 bolts have been added to the CC even though there are holes present for all 12. The additional holes (6 inner most holes indicated by x's) simply do not have any bar/pipe elements connecting them. The bolts are preloaded to roughly 75 kip (kilo-pounds), and the flange and shim surfaces have a finish which produces a design-basis friction coefficient of 0.4 under all of the bolts. The unbolted area on the extreme inboard has friction set to 0.04 friction. In further analysis the inboard friction is also set to 0.4. which allows for a bounding range for slippage. Fig 19 illustrates the sliding and contact behavior on the CC interface. A similar series of plots is included for the case of adding twelve bolts instead of six (Fig. 20 - Fig. 21).

Table 3 shows a summary of the max slip and shear loading from the set of analyses All of the outboard bolts have very low shear (<1.5 kip). This is indicative of the bolts being stuck and the loading transferred through friction as expected. Some of the inner leg bolts see higher shear (approx 5 Kips) but these bolts see little to no motion under them. This discrepancy is related to the contact stiffness problem defined above in section 3.4. The shear loads are most likely high by at least a factor of 2. Appendix 2 examines the inner leg of CC using 1.5" bolts and looks at a range of contact stiffness. The shear values drop by at least half on the inboard bolts as the stiffness increased by 10X. Larger bolts are used in the appendix because the added preload was thought to be beneficial from a shear load standpoint. However, the cost of the tooling required to achieve the 1.5" diameter threads is prohibitive. Also, given that the shear loads are overestimated due to the contact stiffness and that the bolts can withstand up to 8 Kips of shear from a fatigue standpoint (Section 5), all of the inboard bolts and outboard bolts are stuck and friction is able to transfer the shear. These bolts do experience some minimal residual shear form flange/flange deformation and typically this is under 1 Kip. Further, although the low contact stiffness value causes an overestimate of bolt shear it has a minimal effect on sliding.

All of the analysis on the CC joint, or any of the other joints, has always considered perfect fit up. To check this behavior, a 0.005" gap was instituted, (using an ANSYS contact element keyopt option), between the flange and the shim. The results for bolt load and shim are shown in Fig 22 which indicates that the effect of the gap is minimal. The max slippage still occurs in the same area after the coil has compressed down onto the flange. The inner leg with the gap has standard contact behavior so that it can close as opposed to the sliding behavior of the areas around the bolts.

Table 3: Max slippage and peak shear of the inboard bolts

Inboard Friction	# of inboard bolts	Max sliding distance (in)	Max Shear Force (kips)
0.4	0	0.0065	2.8
0.4	6	0.0047	2.4
0.4	12	0.0011	2.7
0.04	0	0.0199	4.9
0.04	6	0.0143	4.5
0.04	12	0.0024	3.5
Imperfect Fit-up gap of .005" on unbolted region	0	0.0193*	3.3

*sliding occurs after gap has closed

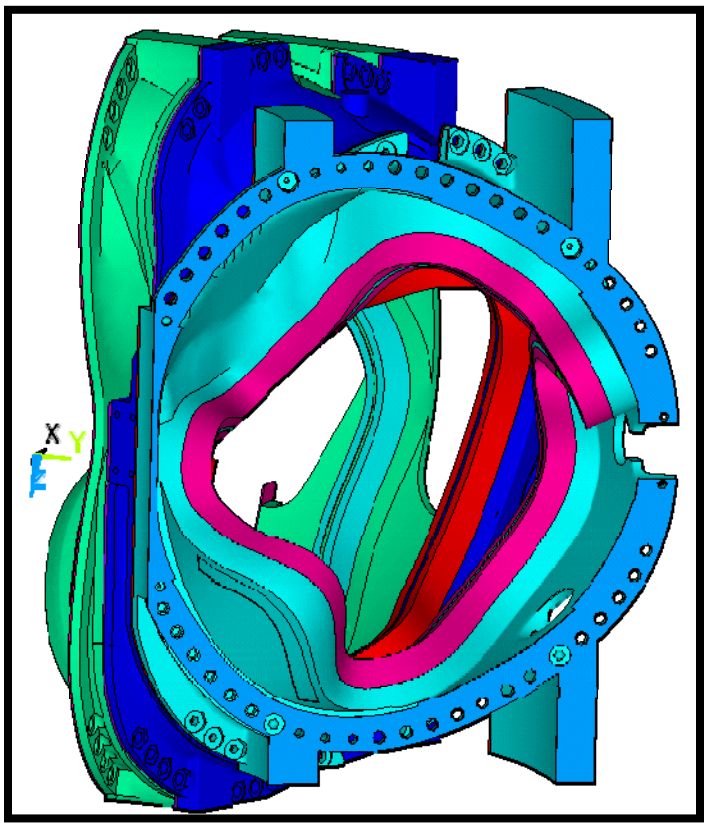

Fig. 17. Maximum added C-C bolt holes

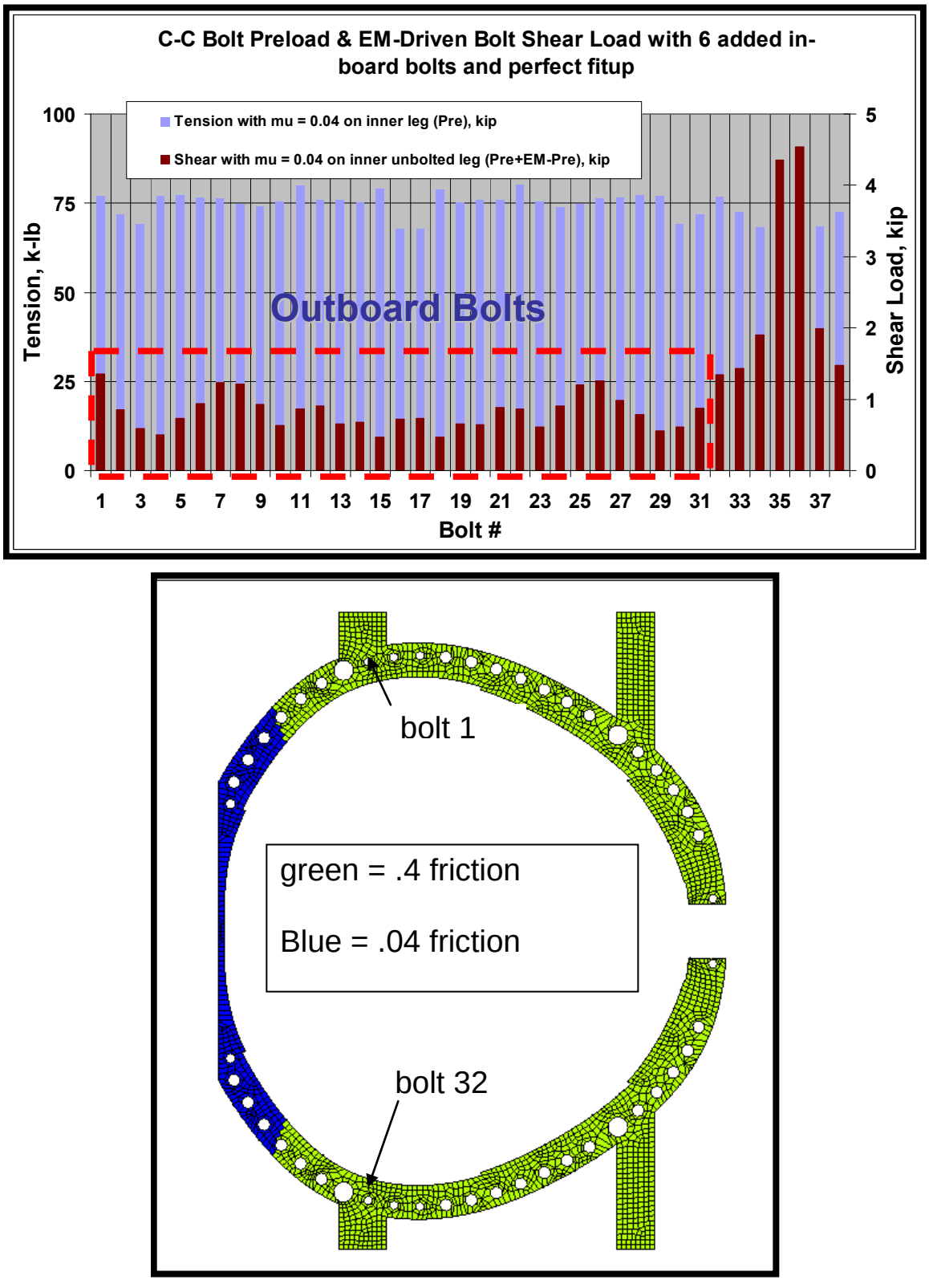

Fig. 18. C-C Bolt Preload & EM-Driven Shear Load (top) & Friction scheme [6 added in board bolts]

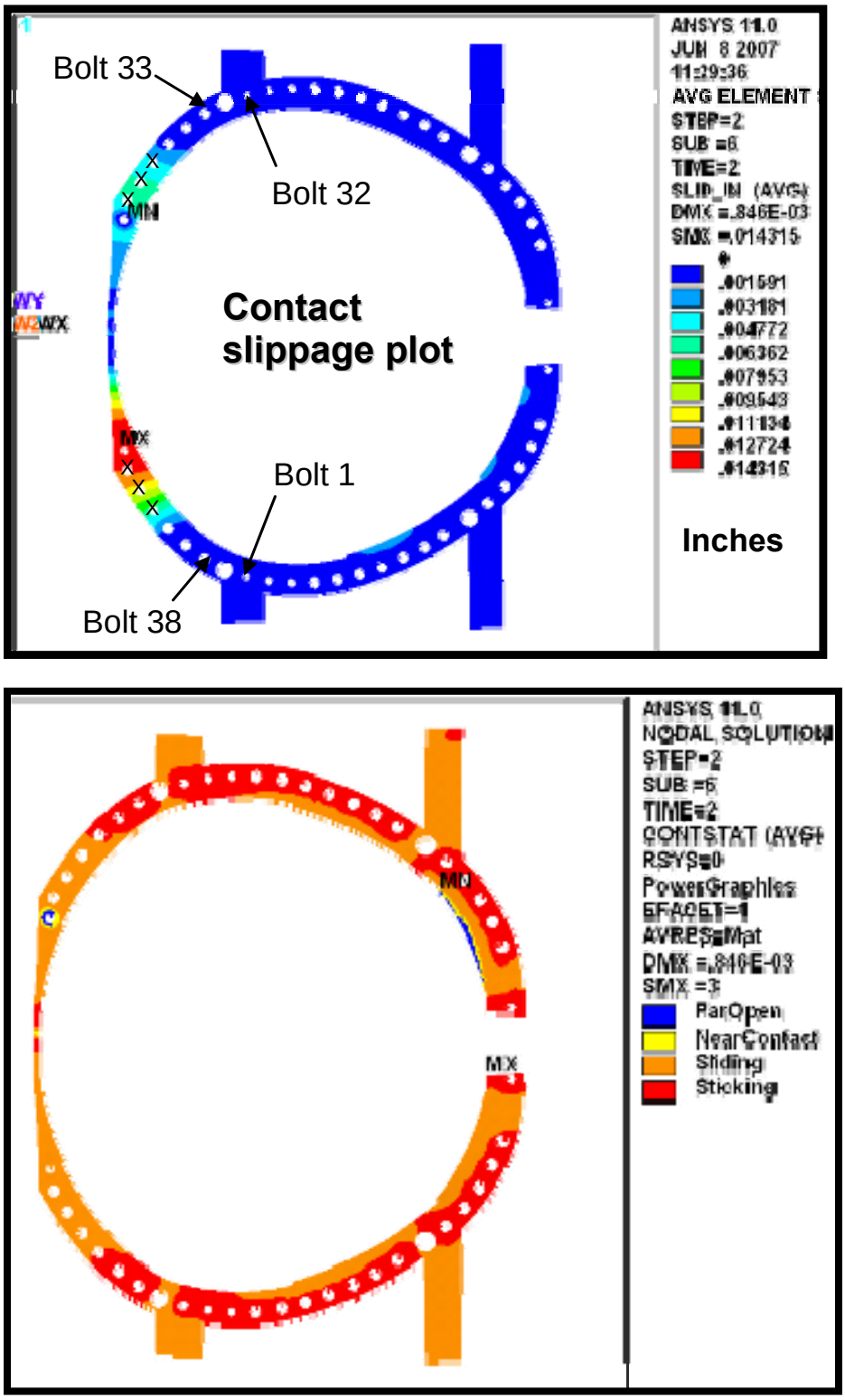

Fig. 19. C-C Slip [m] & Bolt Shear Loads [kip] from EM Load Application [6 added in board bolts]

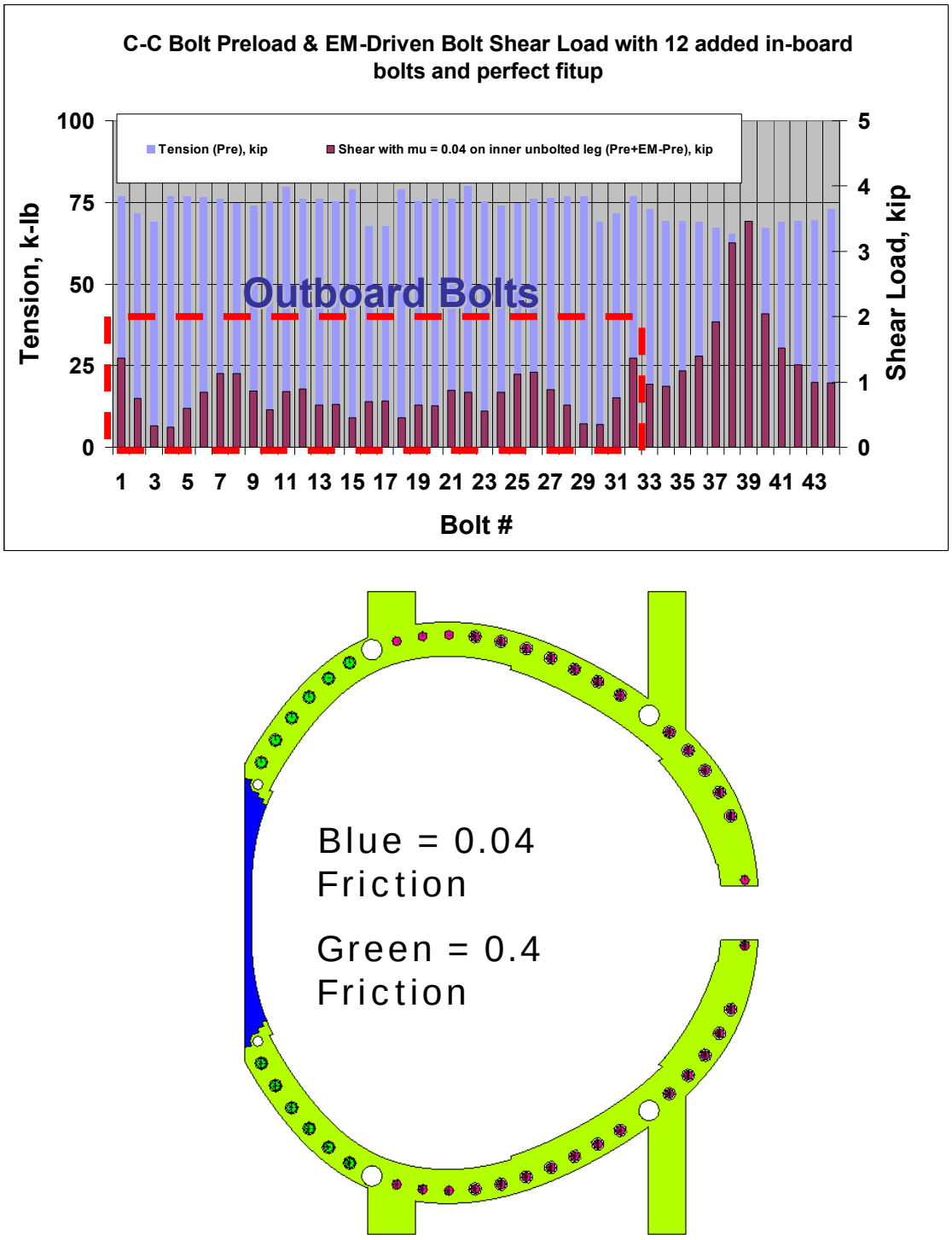

Fig. 20. C-C Bolt Preload & EM-Driven Shear Load (top) & Friction scheme [12 added in board bolts]

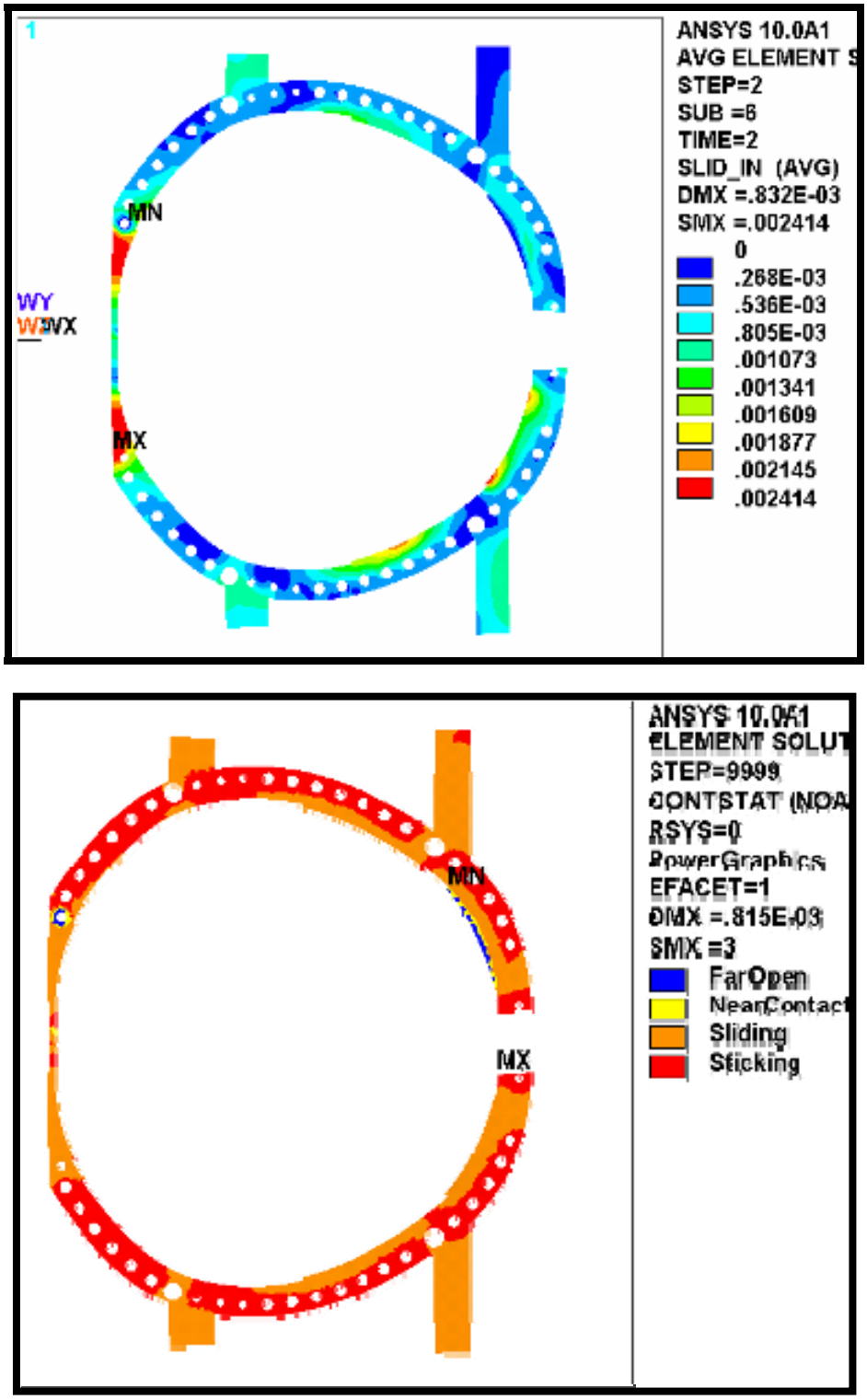

Fig. 21. C-C Slip [m] & Bolt Shear Loads [kip] from EM Load Application [12 added in board bolts]

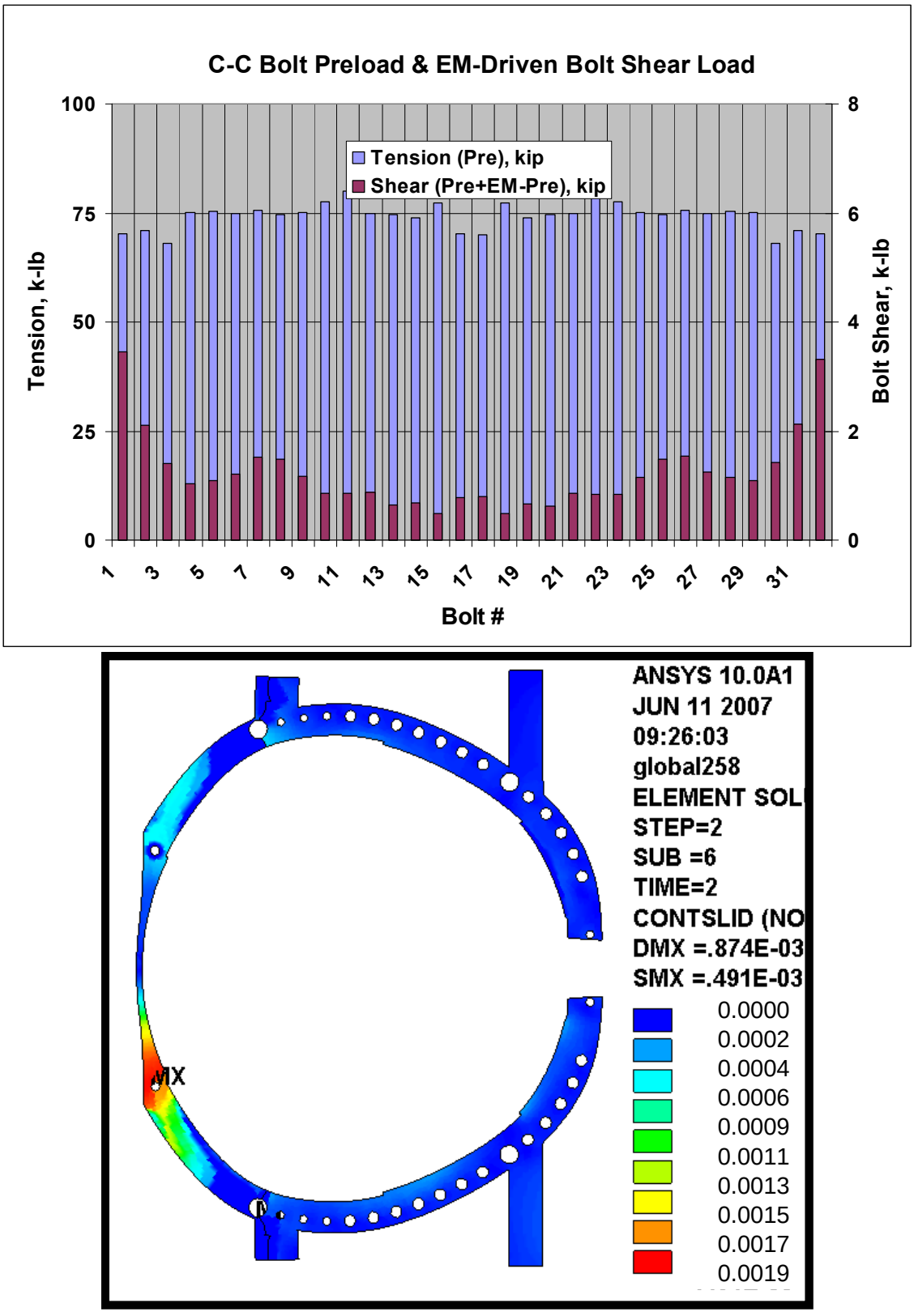

Fig. 22. C-C Slip [m] & Bolt Shear Loads [kip] and slippage (in)from EM Load Application [imperfect fit-up of .005" between flange and shim.]

4.3. Case Study 2> No preload on outer bolts with a welded (bonded) inner leg, AA, AB, BC.

The following figures (23-26) demonstrate the effect of welding the inner leg with bonded contact and letting the outer leg slip with the bolts having no preload applied to them. In the case of the C-C flange the added inner leg bolts (12) are held at their respective preload levels but the outboard bolts are relaxed. The friction on the outboard shims is set to 0.4 as before. The intent here is to indicate which bolts are candidates for active preload monitoring. Clearly, the situation where every bolt looses its preload is not expected to ever occur. Still, this study demonstrates that even if this occurs, there are only a handful of bolts (Table 4) that exceed that fatigue limit (Section 5) of approximately 9 Kips, which gives a high degree of confidence to the design. The bolts that have high shear loads are typically on the ends of their respective bolt patterns and are ideal candidates to be monitored with internal strain gages.

Table 4: Max Shear force and number of bolts exceeding fatigue limit of 9 Kips.

Interface Joint	Largest Shear Load (k-lb)	Number of Bolts Exceeding Fatigue Limit of 9 Kips	Max Slip (inches)
A-A	12	4	0.01
A-B	14	3	0.007
B-C	12	2	0.008
C-C	8	0	0.004

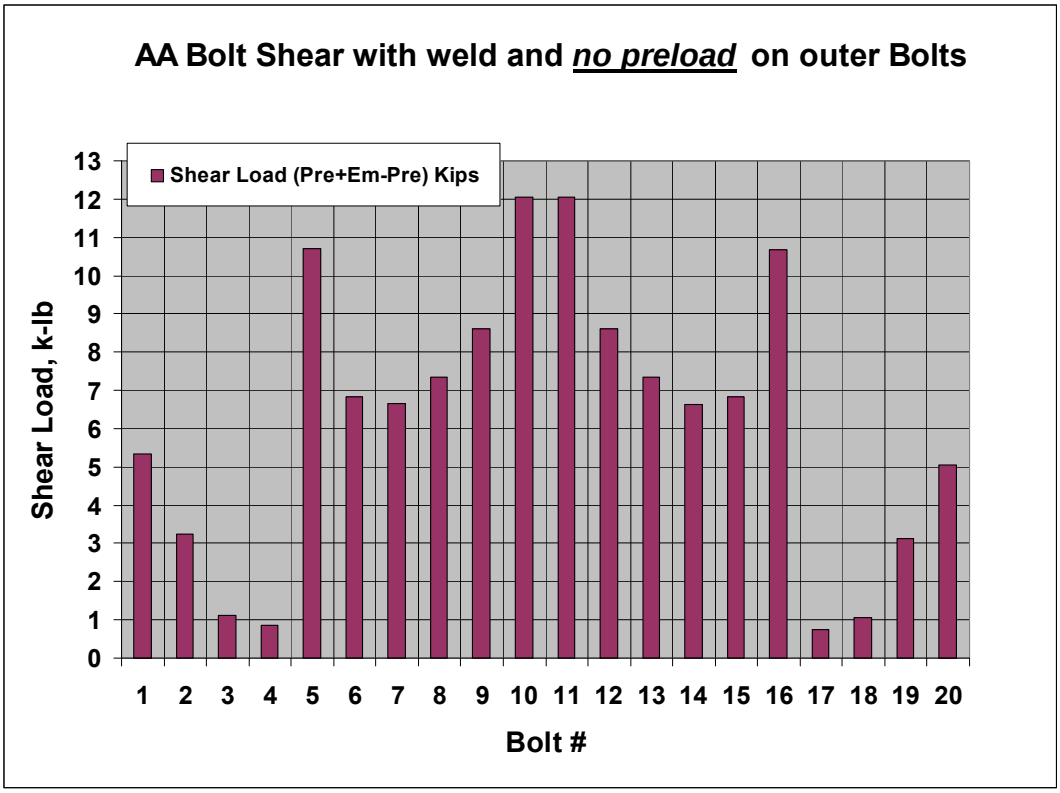

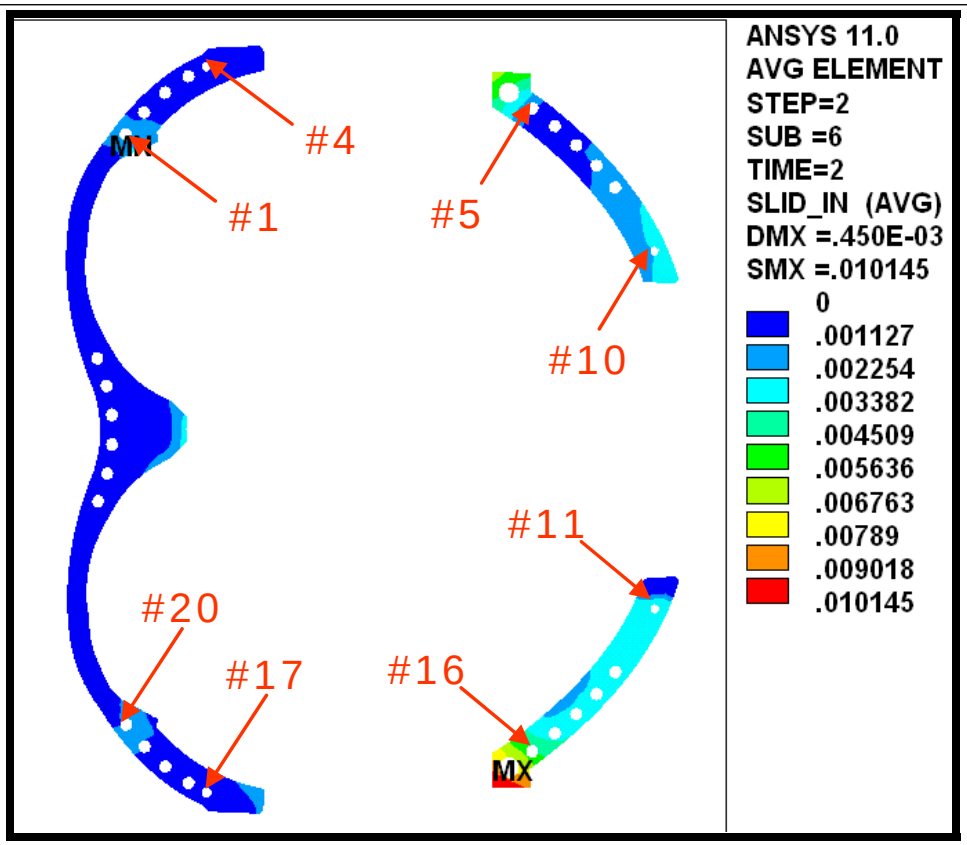

Fig. 23. A-A Bolt Preload & EM-Driven Shear Load (top) & Slippage (inches) (bottom)

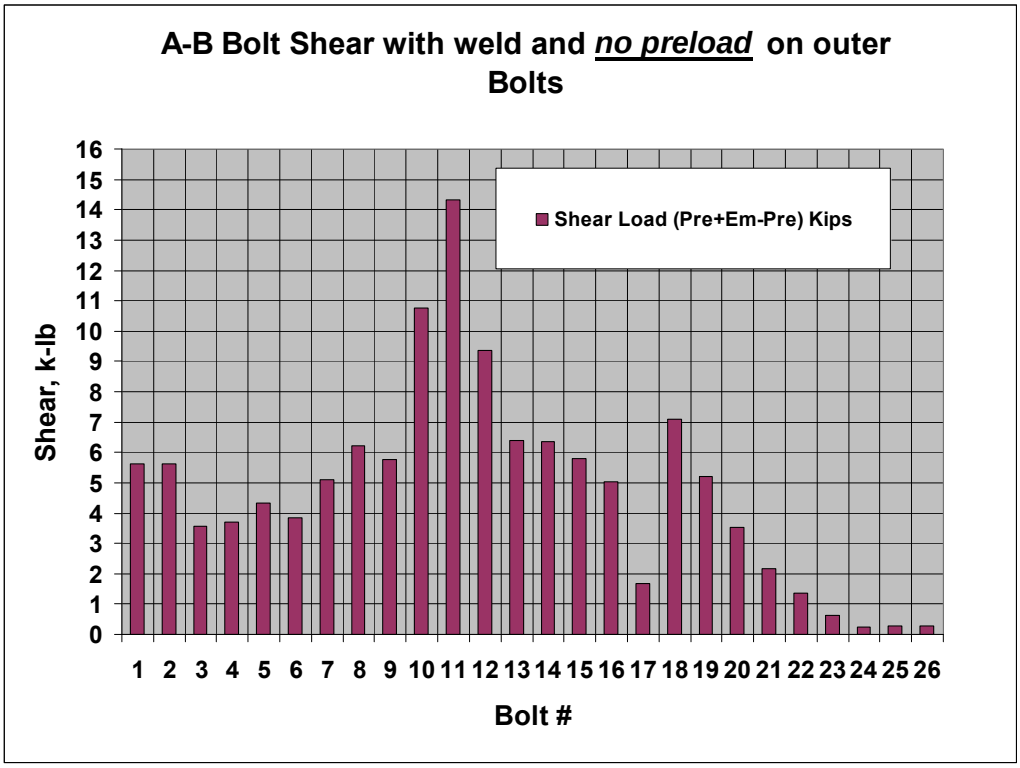

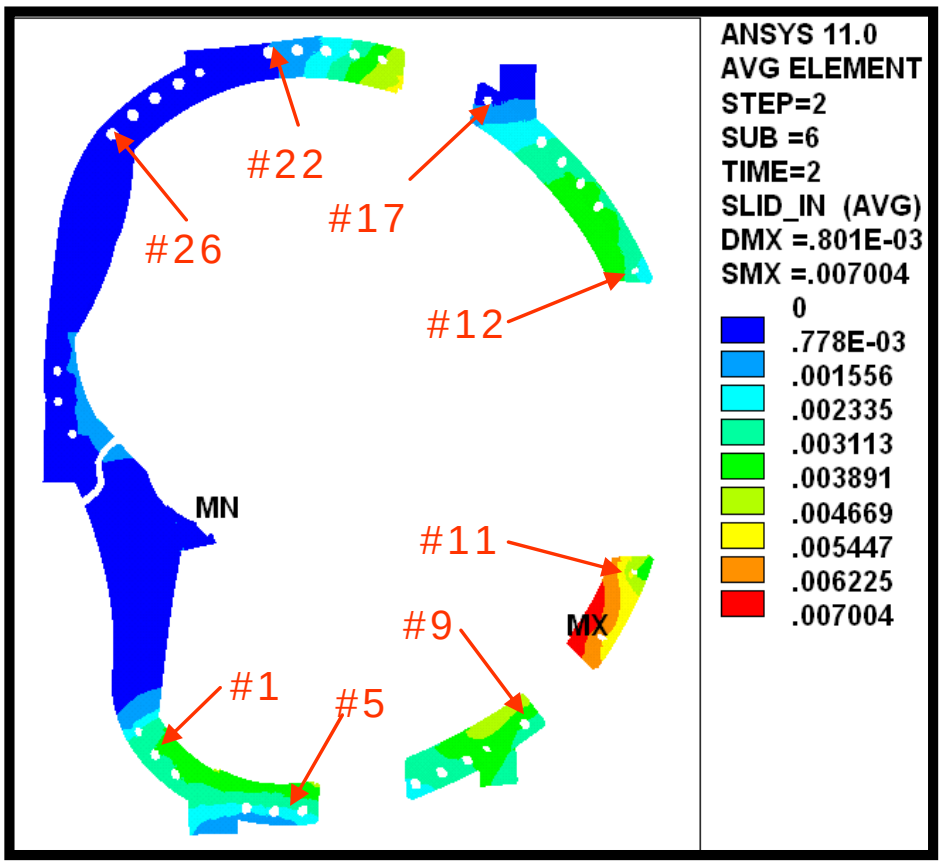

Fig. 24. A-B Bolt Preload & EM-Driven Shear Load (top) & Slippage (inches) (bottom)

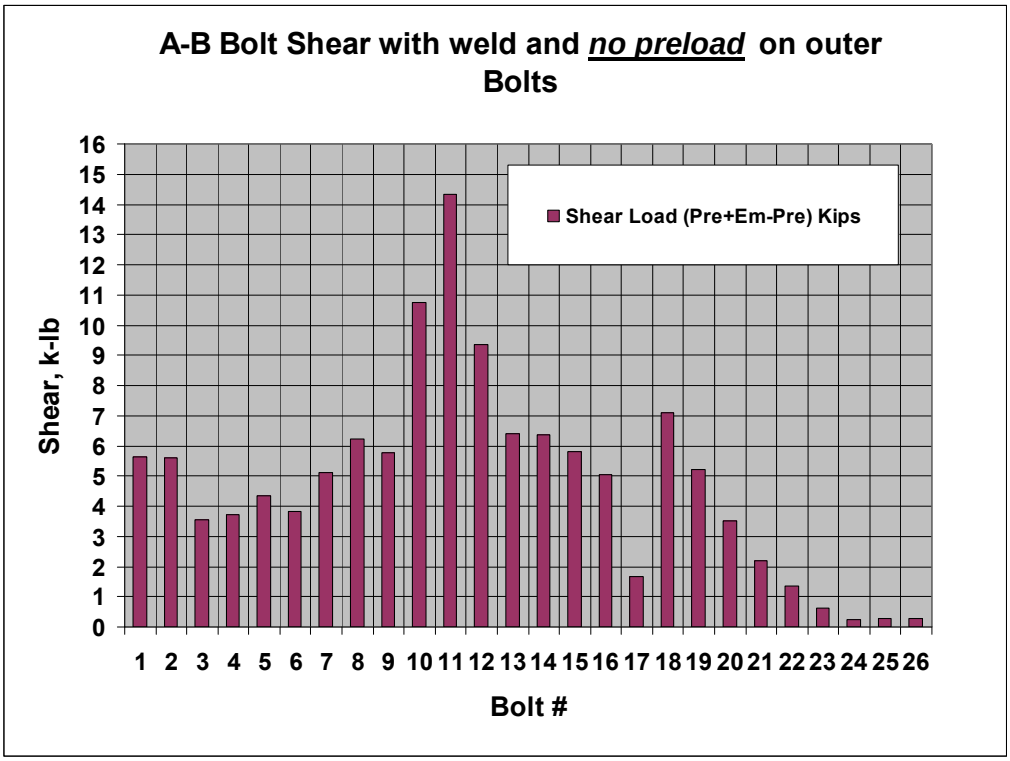

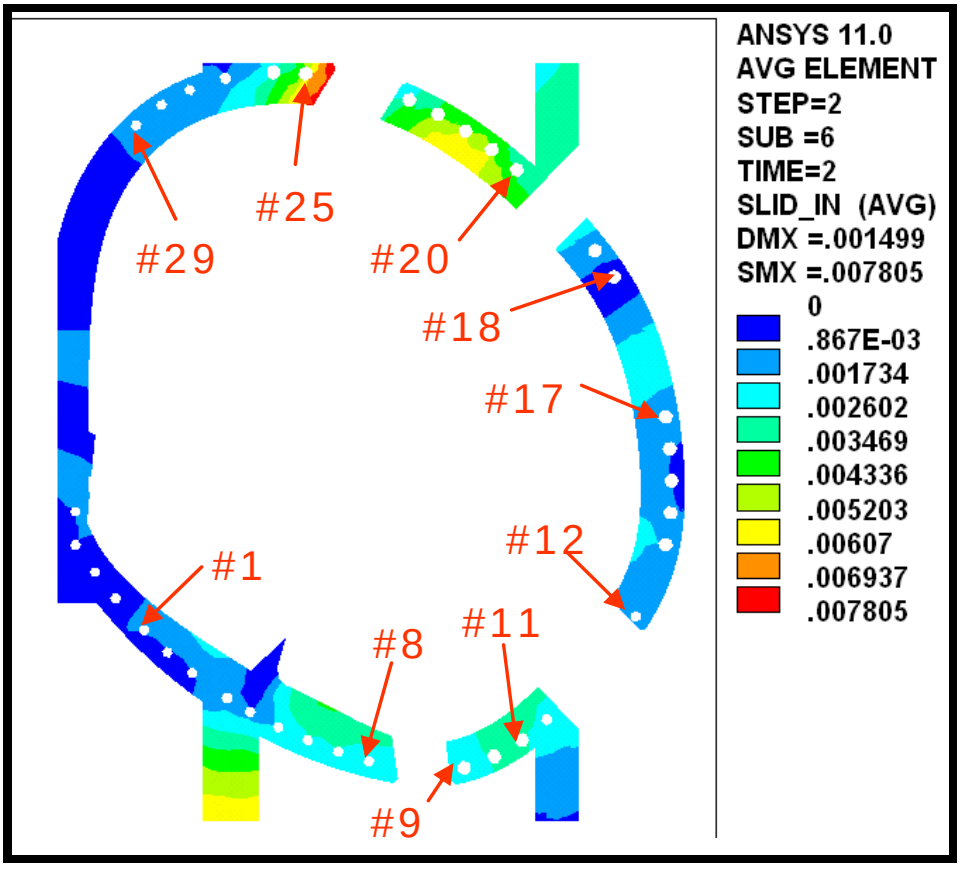

Fig. 25. A-B Bolt Preload & EM-Driven Shear Load (top) & Slippage (inches) (bottom)

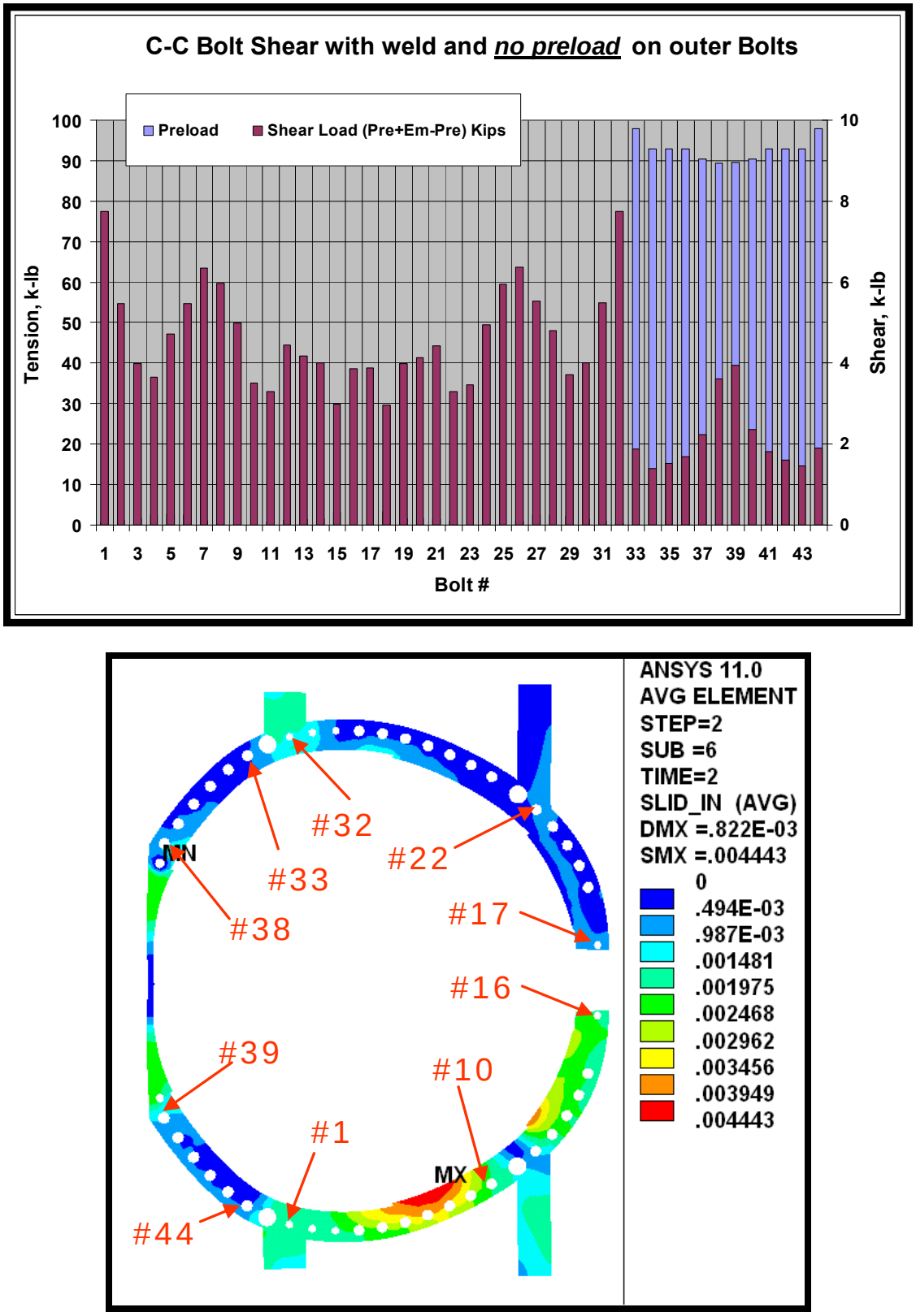

Fig. 26. A-A Bolt Preload & EM-Driven Shear Load (top) & Slippage (inches) (bottom)

5. Individual Bolt models (Type 1 and Type 2)

5.1.1 Stiffness, Stress and Equivalent Models, Type-1 & Type-2 Bolted Joints (circa Nov 2006)

Design sketches of the Type-1 and Type-2 bolted connections are shown in Fig. 5.1-1. Detailed models are developed and used to determine their effective stiffness and local stresses from a unit shear load as shown in Figs. 5.1-2 and 5.1-3. When a unit load of 25 kip is applied to each joint type flange, bolt stresses develop as shown in Fig. 5.1-4. These results assume that Stycast fills a 30 mil annular gap around G11 collars. Recent design modifications eliminate the Stycast and change the collar material to SS. No revision to the detailed model has been made to evaluate this design change.

Notice that a 25 kip shear load produces bolt stresses of 107 ksi & 124 ksi in the Type-1 & Type-2 bolted joints, respectively. With an expected shear load of 13 kip, the bolt stresses will be 56 ksi and 64 ksi, excluding stress concentrations at the thread. Stresses of this order will require a fatigue evaluation for this high-cycle application.

Figs. 5.1-5 & 5.1-6 show equivalent joint modeling for inclusion in the global model. Notice that if the bolts are subjected to transverse slip, then the equivalent stiffness is like a 2.75" to 2.9" diameter rod in bending. If the joints are locked by friction, then the joint stiffness is determined by the actual bolt diameter (e.g., 1.375").

Fig. 5.1-1 Type-1 (through) & Type-2 Bolted (tapped) Joints

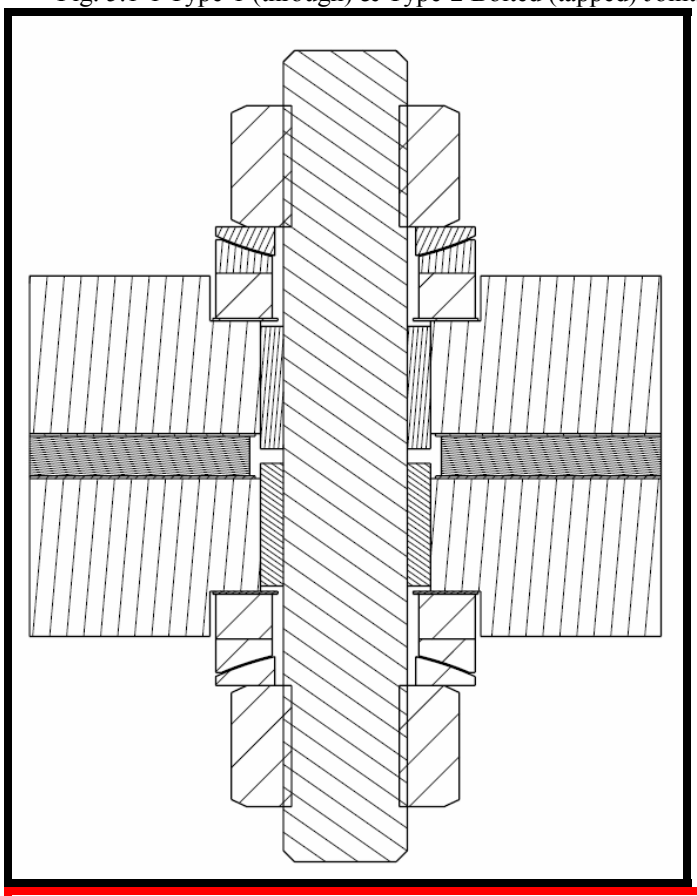

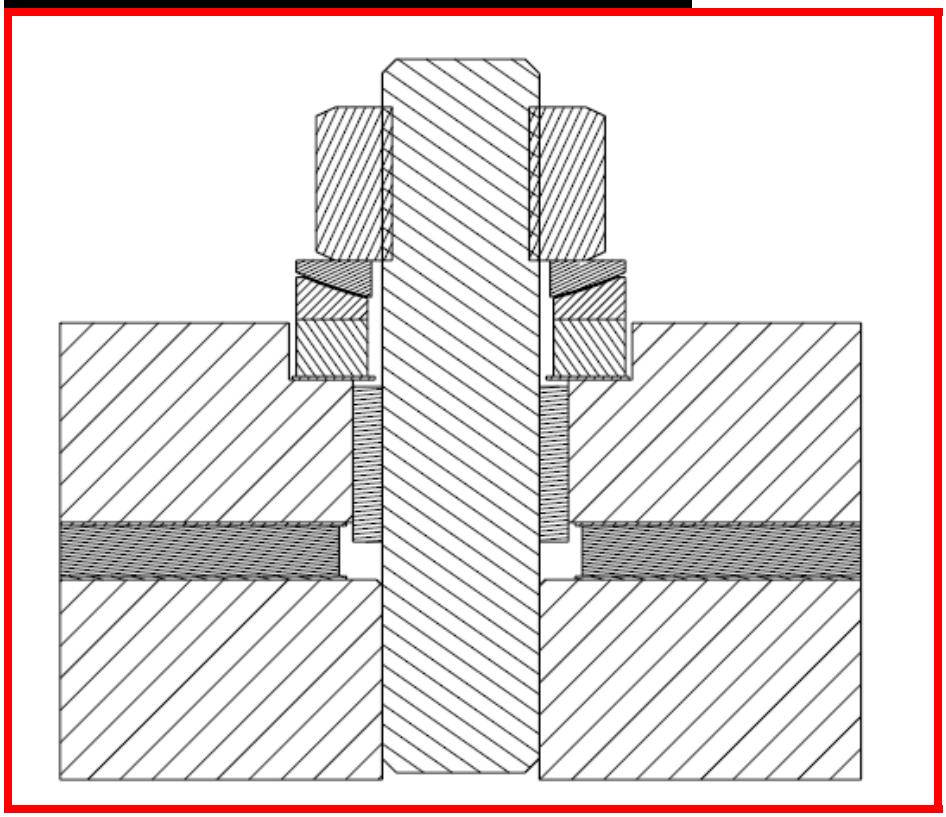

Fig. 5.1-2 Type-1 Stiffness Calculation

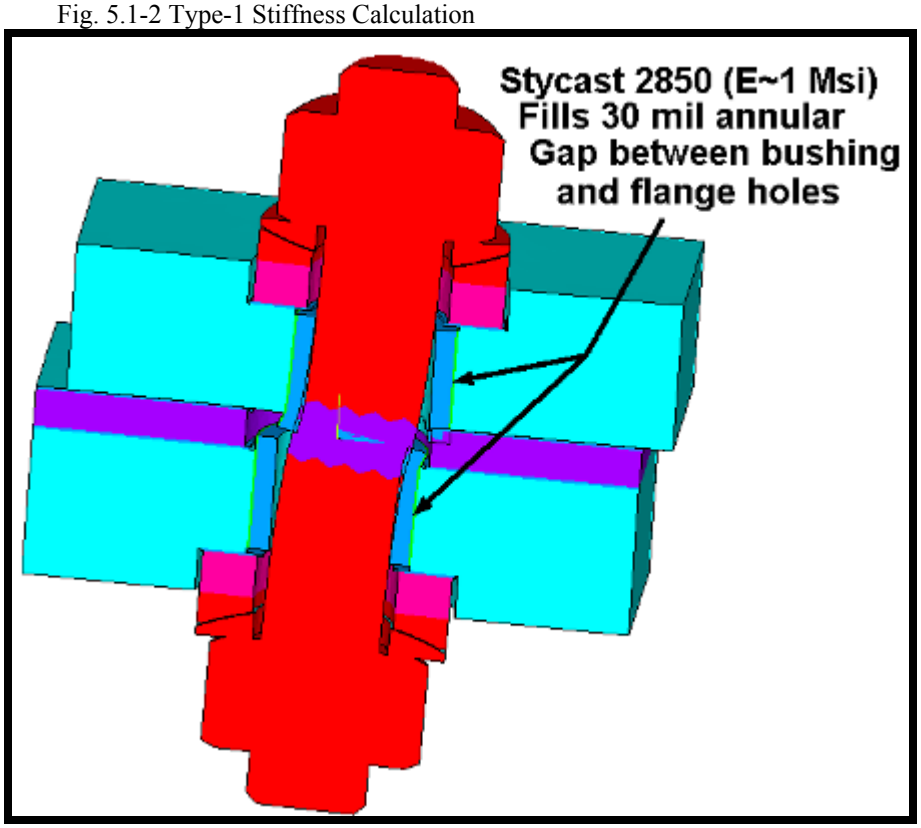

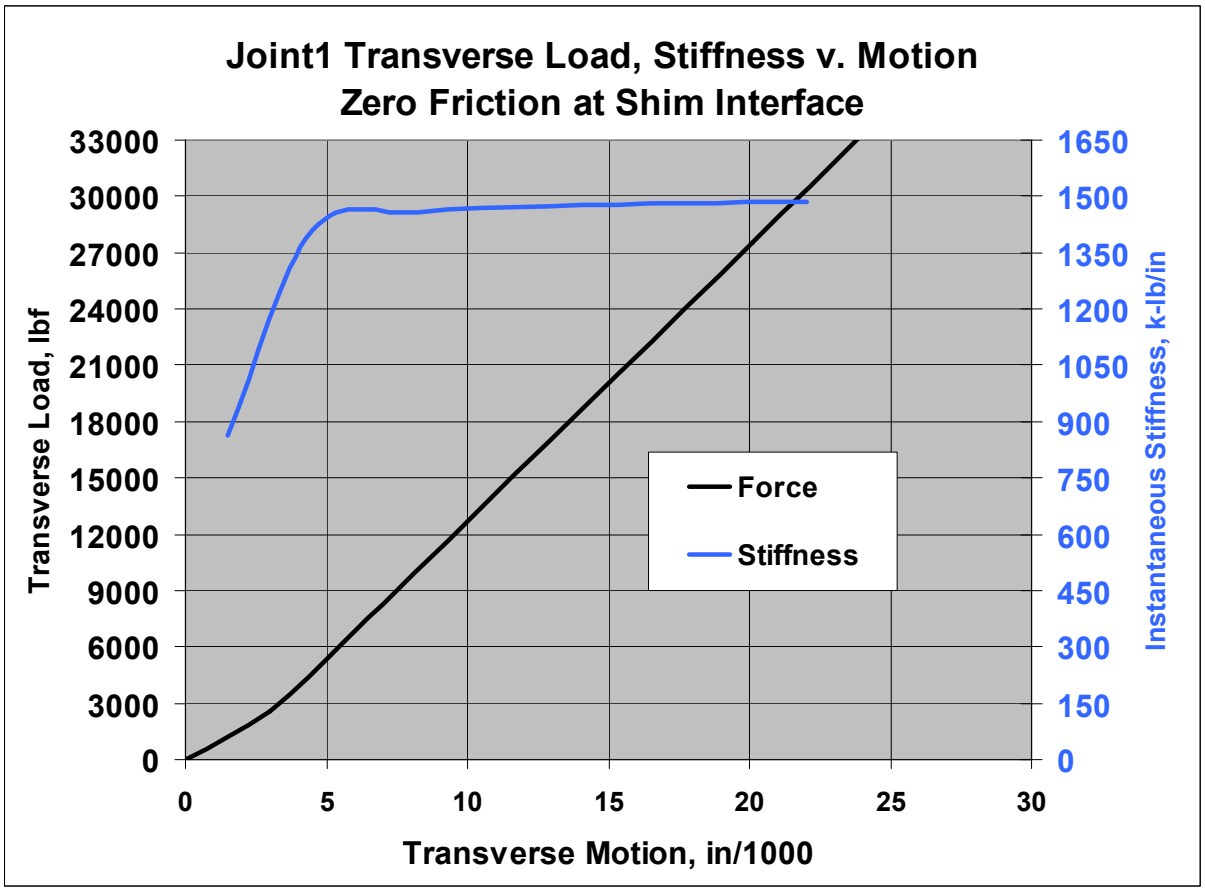

Fig. 5.1-3 Type-2 Stiffness Calculation

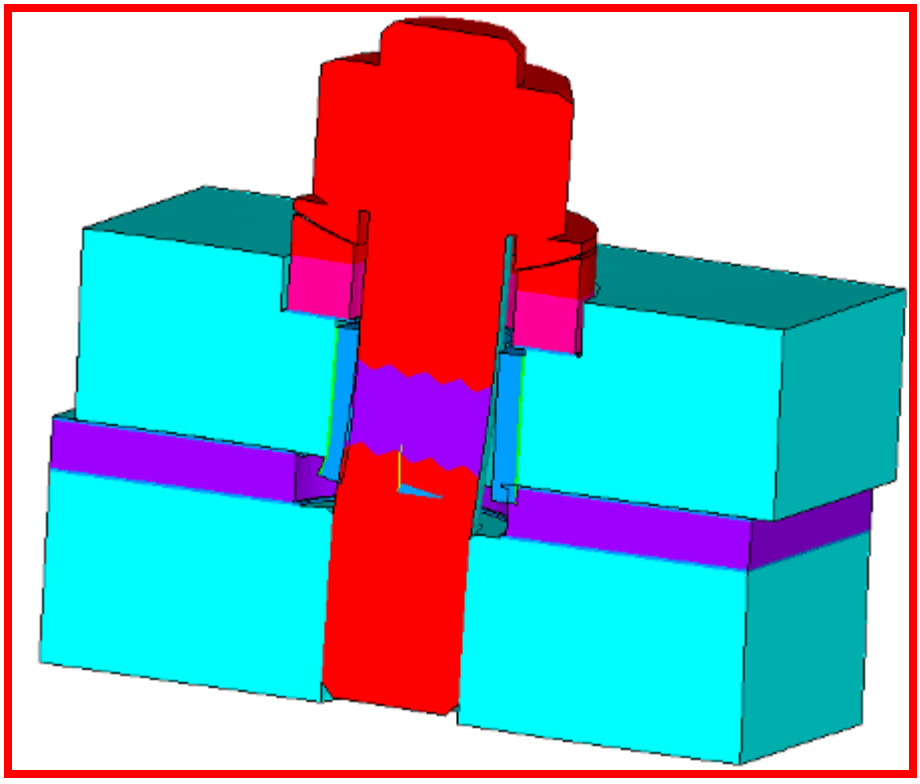

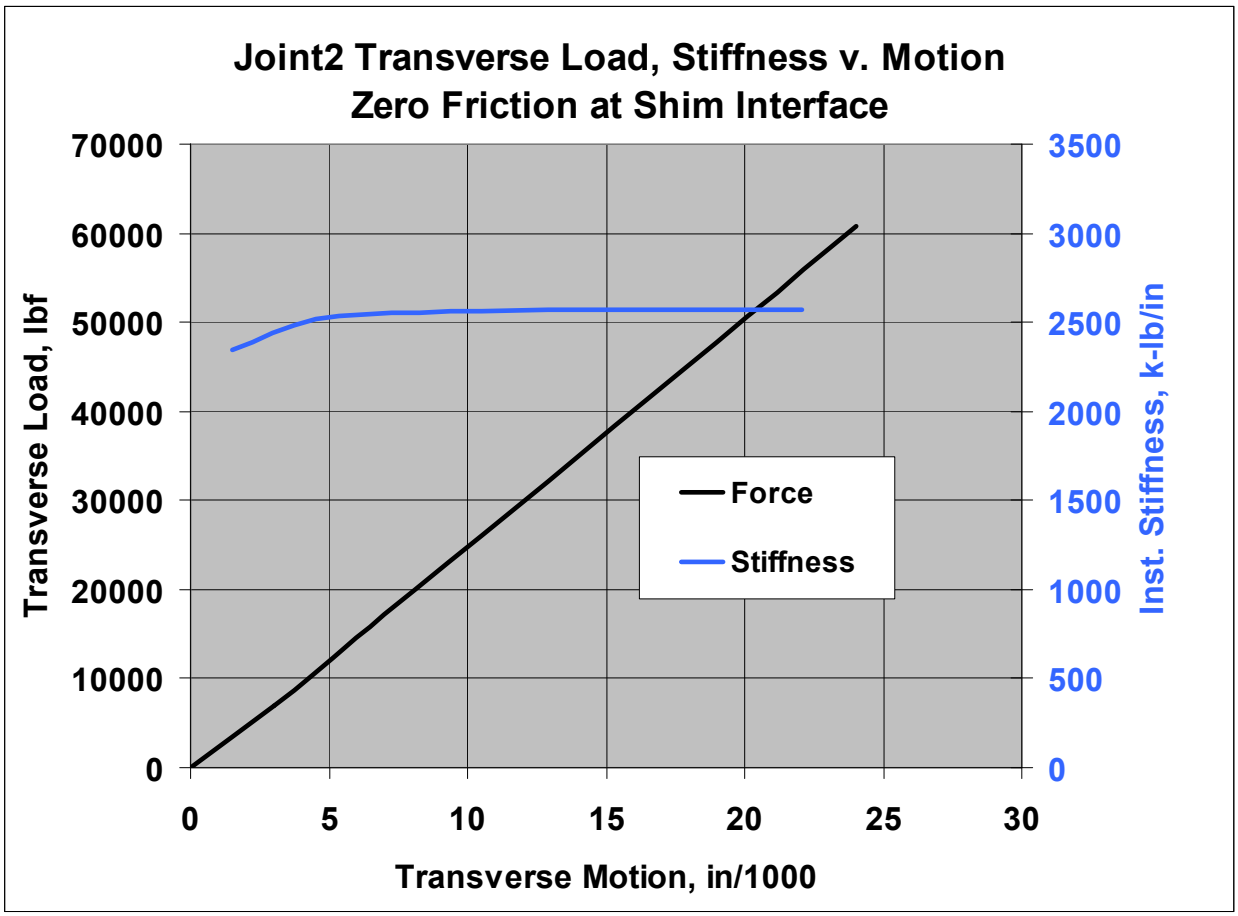

Fig. 5.1-4 Fastener Stress from 25 kip shear load

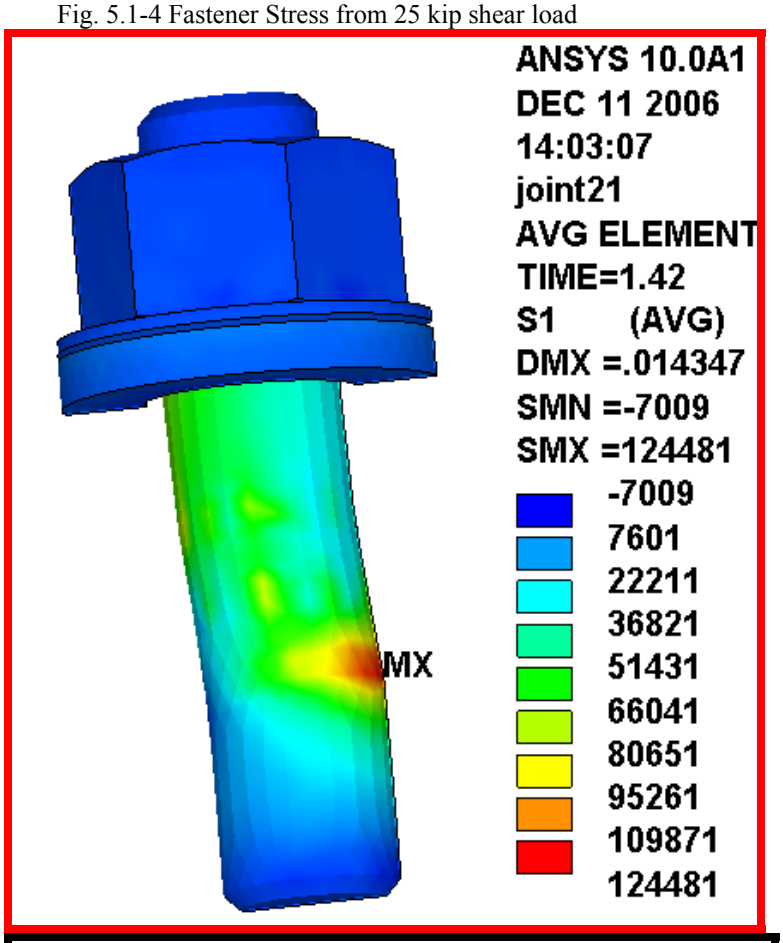

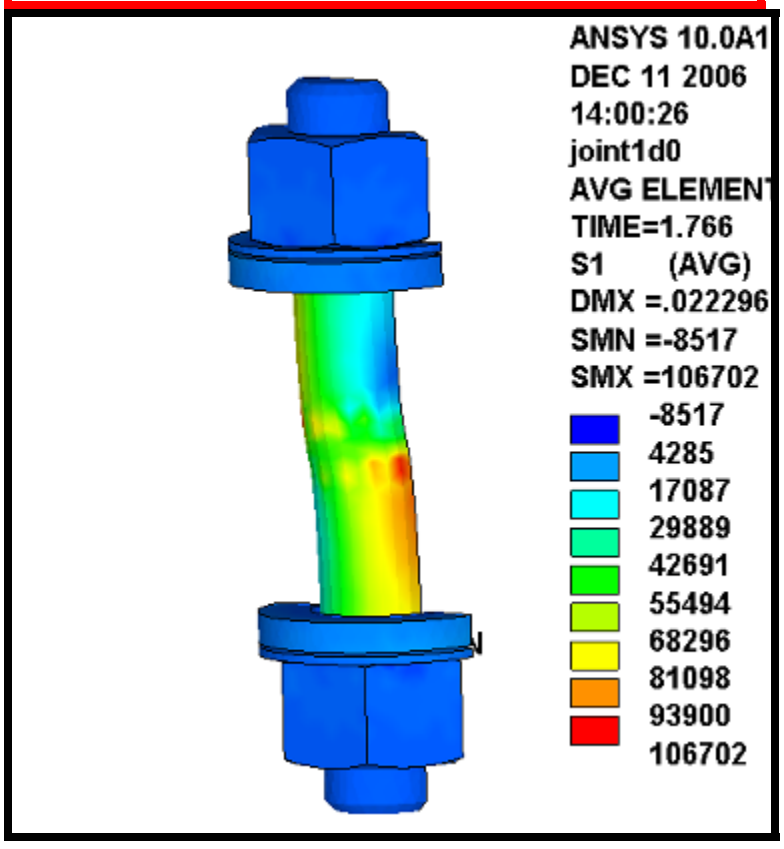

Fig. 5.1-5 Equivalent Type-1 Bolted Connection (2.9" dia. bolt in bending)

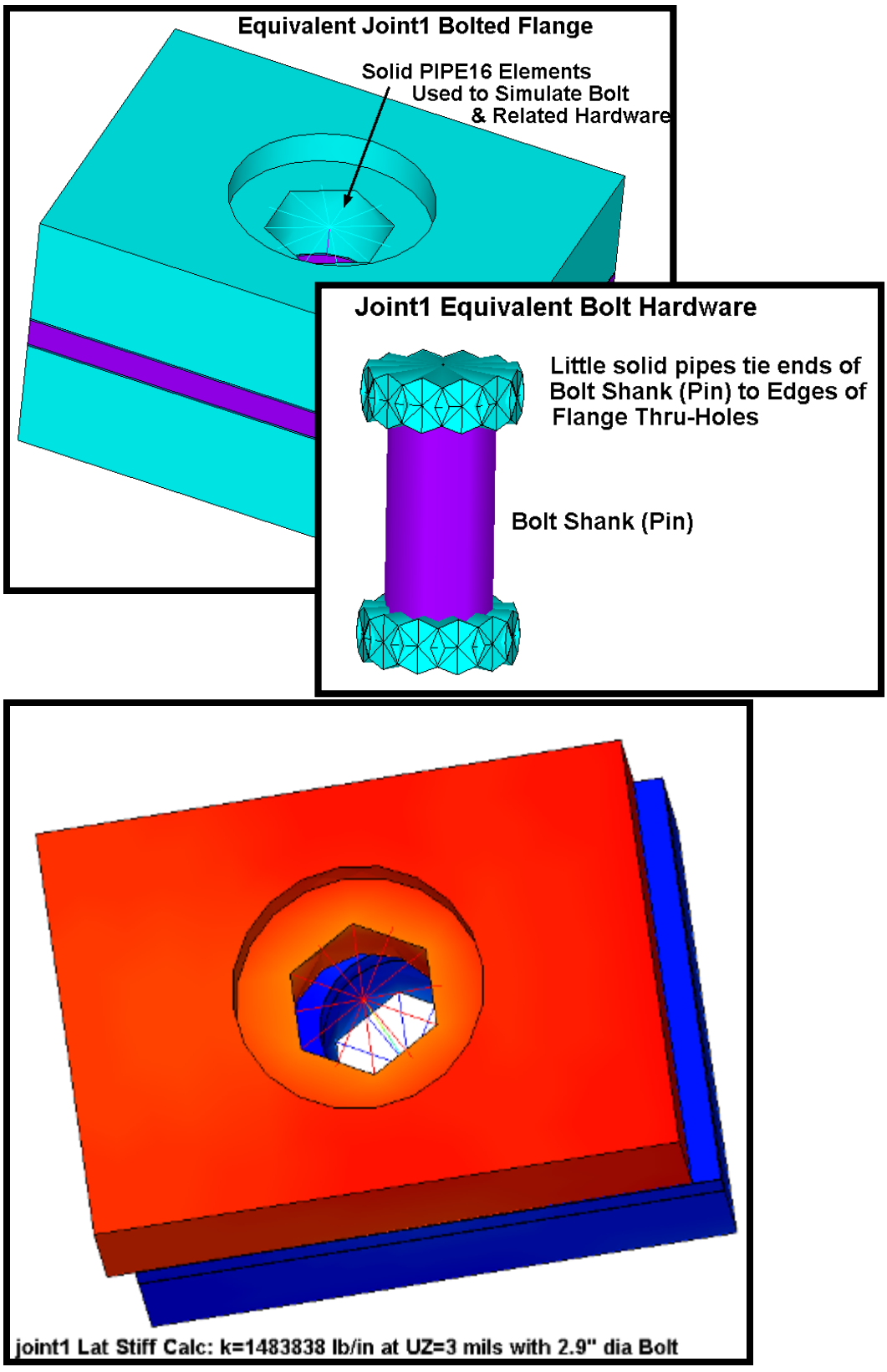

Fig. 5.1-6 Equivalent Type-3 Bolted Connection (2.75" dia. bolt in bending)

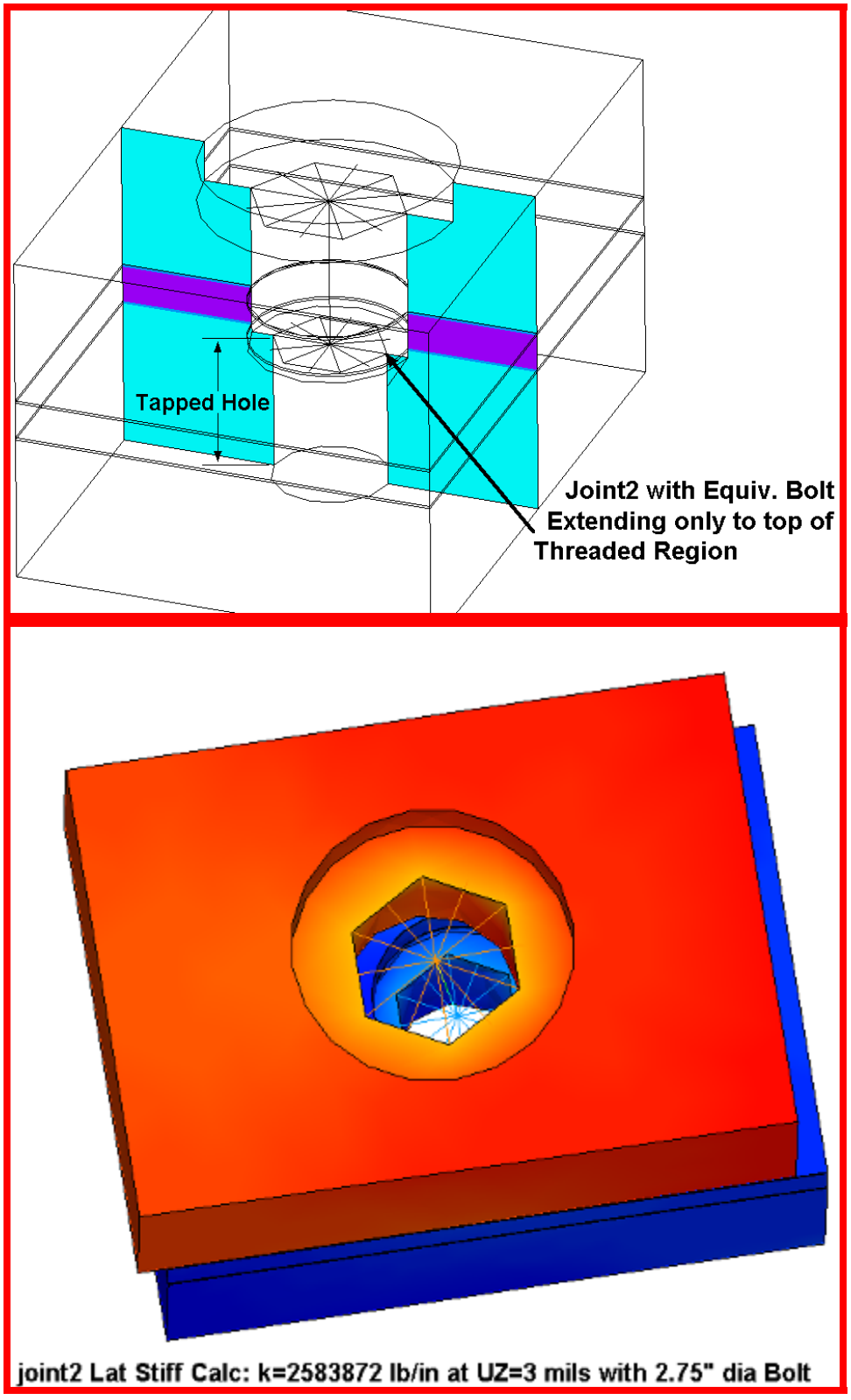

5.2 Stresses in the Revised Type-1 & Type-2 Bolted Joints (circa May 2007)

Slight modifications to the reference Type 1 & Type 2 bolted joints (shown in Fig. 5.2-1) have lead to a re-analysis of these mechanical fasteners. In this section, solid models from ORNL are cut in half (for computational efficiency), contact elements are added, material properties, boundary conditions and loads are applied and stresses are reported for a **20 kip** unit shear load. Details are discussed below.

ANSYS models of the Type 1 & Type 2 joints are developed from ORNL SAT files (courtesy K. Freudenberg). Half-symmetry model plots are shown in Figs. 5.2-2 through 5.2-4, and correspond to the Type 1 (through-bolt), Type 2 (tapped hole), and Type 2a (extended steel bushing, tapped hole). Standard contact elements are judiciously placed between the shims and flanges, and between the bolt shank and the bushings & shim hole. All other interfaces should never slide or break contact, and so "gluing" these volumes before meshing improves the computational efficiency of the model without detracting from its accuracy. Two different bushing materials are considered; G-11CR and SS.

The joints are preloaded by imposing an elevated reference temperature on the slice of bolt shank material shown as blue in the model plots. This typically requires one solution cycle since calculating the reference temperature required to produce the desired 72 kip (48.5 ksi) preload would be difficult to estimate for this geometry.

After establishing the proper preload, the joints are loaded by applying a shear load of 10 kip to the half-model, which is equivalent to 20 kip per joint. Friction is neglected since the intent of the analysis is to determine stresses produced by the shear load appearing on the bolts, as determined by the global model results of section 3.2. Therefore, the two load cases per analysis are executed:

- Load Step 1 (time=1.0): Bolt Preload ~72 kip, 0.0 kip Shear Load
- Load Step 2 (time=2.0): Bolt Preload plus 20 kip Shear Load

While the static tensile stress in the bolt is important, the cyclic EM loading is likely to be the more critical design factor. When evaluating the effects of changes in a stress-state, the stress range is the salient parameter. Load Step 1 results are subtracted from Load Step 2 results to produce a stress range. This operation subtracts-out the preload stress which does not change during the shear load application cycle.

Fig. 5.2-5 shows plot of the 1st principal stress range in the Type-1 bolt as a result of this load step subtraction operation. These contour plots also show the "Stress Linearization Path." This "Path" is placed at a critical location within the bolt shank, where large bending stresses coincide with the geometric stress concentration of the threads. You will notice that the path does not occur at the location of the maximum stress in the model. By studying Fig. 5.2-1 we see the extent of the threads, where these local tensile

stresses will be amplified by the thread stress concentration factor. Model stresses are higher at other locations within the shank, but there are no threads at those locations to intensify the stress.

Similar 1st principal stress plots are shown in Figs. 5.2-6 for the Type-2 (G-11 & Metallic bushings) and Fig. 5.2-7 for the Type-2a (extended metallic bushing) configurations. Notice that the Path occurs right at the maximum stress location for these Type-2 and Type 2a joints, since it happens to coincide with bolt thread.

The following (5) plots show the axial stress profile as a function of distance along the path for each configuration. The plots reveal some noteworthy results:

- The stress profile indicates a predominantly Bending component (no surprise)
- The MEM+BEND stress and TOTAL stress are essentially the same for the Type-1 joint
- There is a significant PEAK stress component {TOTAL-(MEM+BEND)}in the Type-2 & 2a joints based on the bolt-hole geometric discontinuity.

Since the model does not explicitly include the bolt threads, their influence has to be added by amplifying the local MEM+BEND stress. This is perfectly consistent with the ASME Code approach and the textbook definition of a Stress Intensification Factor (SIF). Incidentally, the SIF of these bolt threads will be a function of the thread form. Rolled threads have a lower SIF than cut threads. However, in the absence of a precise value, the ASME Code recommends a bolt thread SIF (k_{thread}) of 4.0 as shown in Fig. 5.2-13.

Below each stress profile or "section" plot is a listing of the categorized stresses for each stress component. We need to amplify a particular stress component by the thread SIF. Amplifying SY is a logical choice since the thread concentration is normal to this stress component. However, amplifying S1 (max tensile stress) is also appropriate and conservative, if not essentially the same as SY. In addition, it would be difficult to ignore the Peak stress component that the model is able to capture, which also contributes to the total stress at this max stress location. Therefore, the total stress range which is used to evaluate the fatigue life of the bolts is defined as follows:

$$\Delta S_{tot} = (k_{thread})(\Delta S1) + PEAK$$

Table 5.2-1 lists the numerical values of this operation and the Total Intensified Stress Range. Keep in mind that these values are based on a 20 kip unit shear load.

Table 5.2-1 Joint Fastener Fatigue Evaluation, 20 kip Shear Load Range

Joint Type	Type 1		Type 2		Type 2a
Bushing Material	G-11CR	SS	G-11CR	SS	SS
Un-Intensified Stress Range per 20 kip Shear Load (ΔS1), ksi	30.4	17.9	50.4	42.9	35.4
Thread Stress Intensification Factor	4	4	4	4	4
Peak Stress Range per 20 kip Shear Load, ksi	0.3	0.0	47.4	41.5	26.3
Total Intensified Stress Range per 20 kip Shear Load, ksi	122	72	249	213	168

Now, these stresses must be compared to a design-basis fatigue curve of the bolt material at the 77K operating temperature. Fig. 5.2-14 shows fatigue data for our A286 bolt material at RT, 77K and 4K (Reference: N. Suzuki, "Low-Cycle Fatigue Characteristics of Precipitation-Hardened Superalloys at Cryogenic Temperatures," Journal of Testing and Evaluation, JTEVA, Vol. 28, No. 4, July 2000. pp. 257-266.). The 77K curve is digitized in an Excel spreadsheet, and curve-fit to AN^B. The coefficient A is divided by 2 to make a design-basis fatigue curve. The equation is then used to estimate the number of cycles to failure as a function of the bolt shear load for each of the (5) configurations listed in Table 4.2-1. Results are plotted and shown in Fig. 4.2-15.

Clearly, Type 1 joints can support higher cyclic shear loads than Type 2 joints. Using SS bushings instead of G-11CR bushings improves the fatigue life of both Type 1 & Type 2 joint designs. In addition, modifying the Type 2 design by extending the bushing into a counter-bore in the adjacent flange face increases the shear capacity over the reference Type 2 design. The plot shows that only the Type 2 joint with a G-11 bushing does not provide sufficient fatigue strength to survive the estimated 9 kip load range for 100,000 EM cycles. The plot can also be used to evaluate the acceptability of any design for any number of cycles.

Fig. 5.2-1 May 2007 Joint Designs, Type 1 (top) & Type 2 (bottom)

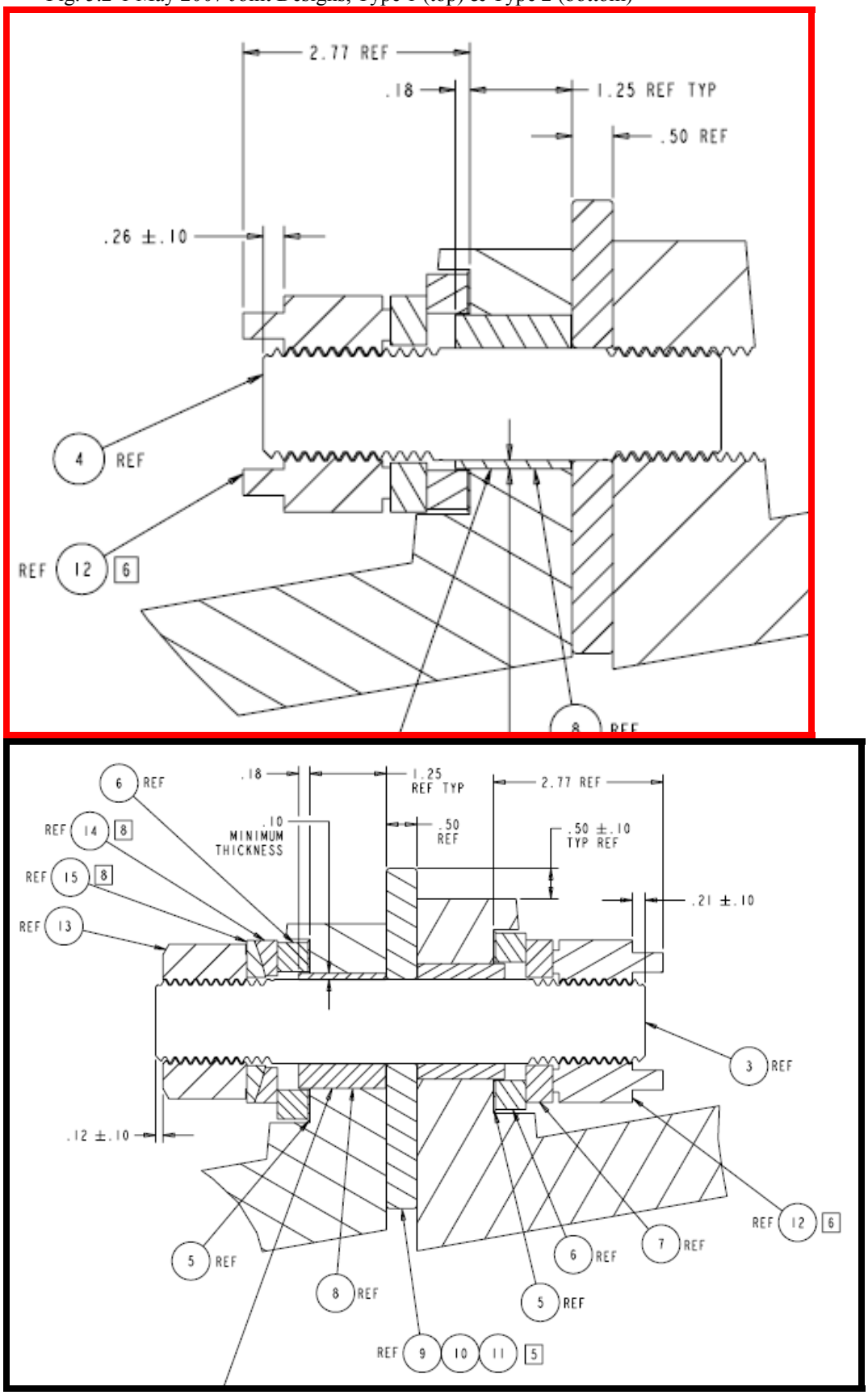

Fig. 5.2-2 ANSYS Model, Type 1 Bolted Connection

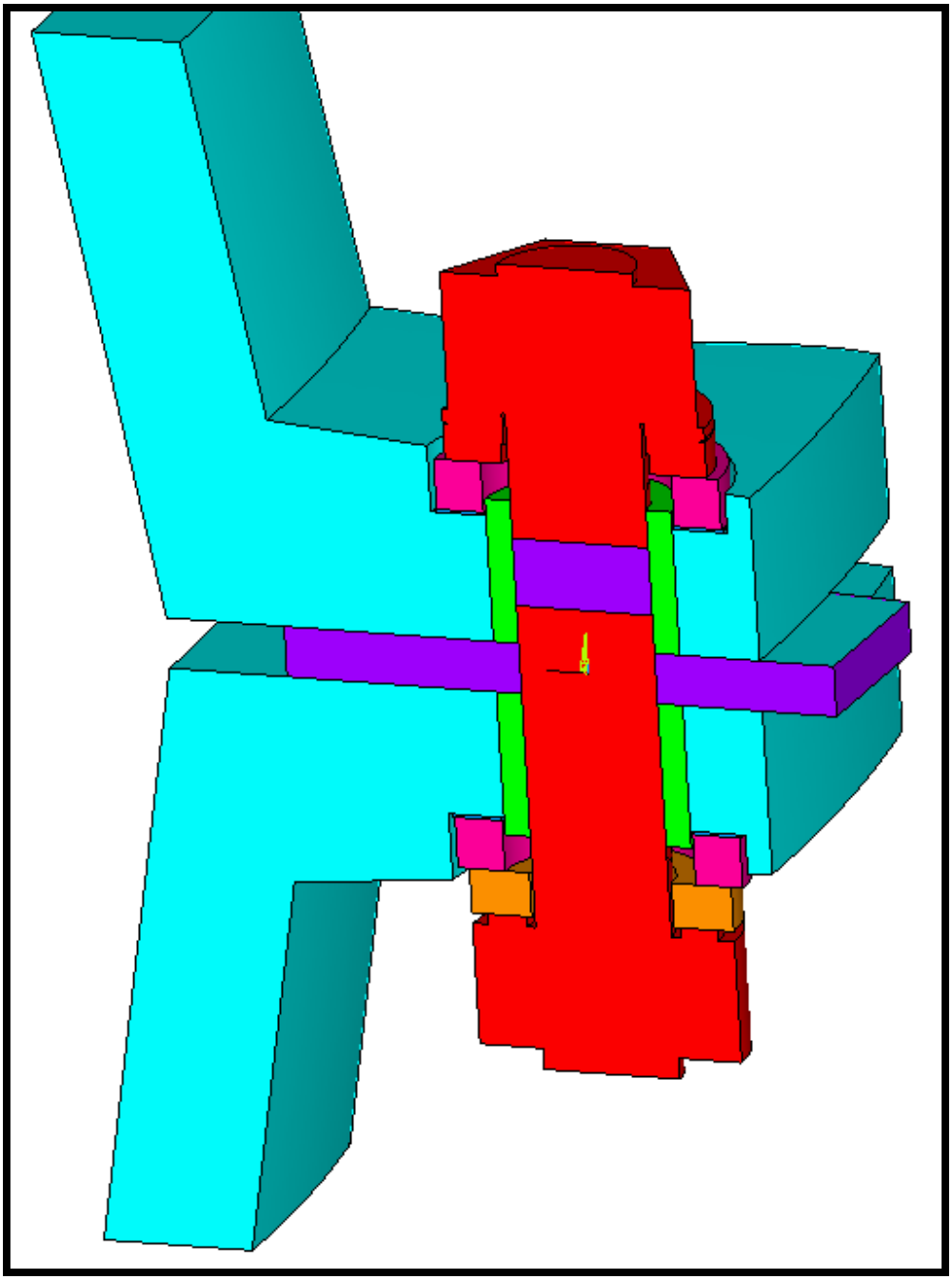

Fig. 5.2-3 ANSYS Model, Type 2 Bolted Connection

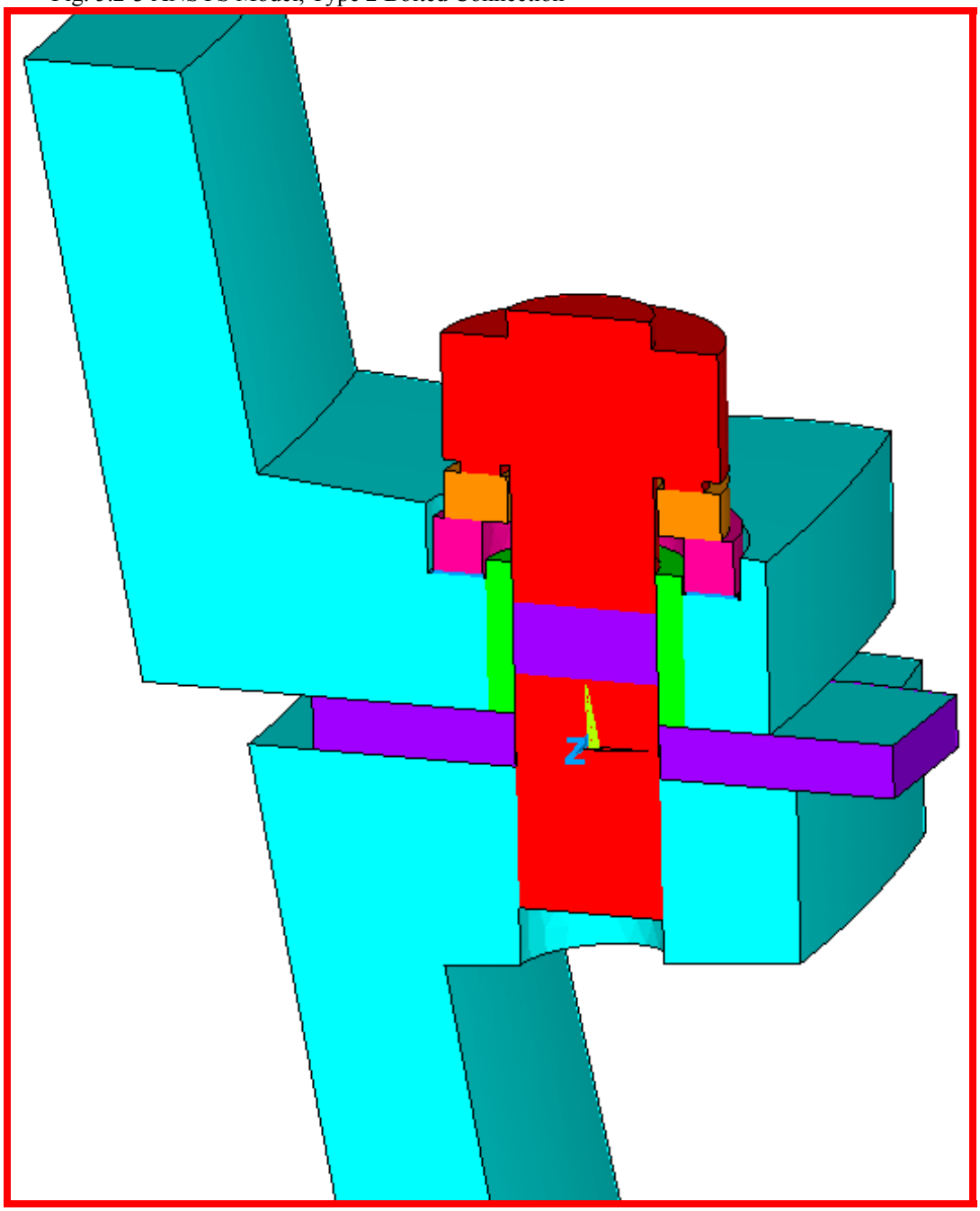

Fig. 5.2-4 ANSYS Model, Type 2a Bolted Connection, Extended Metallic Bushing

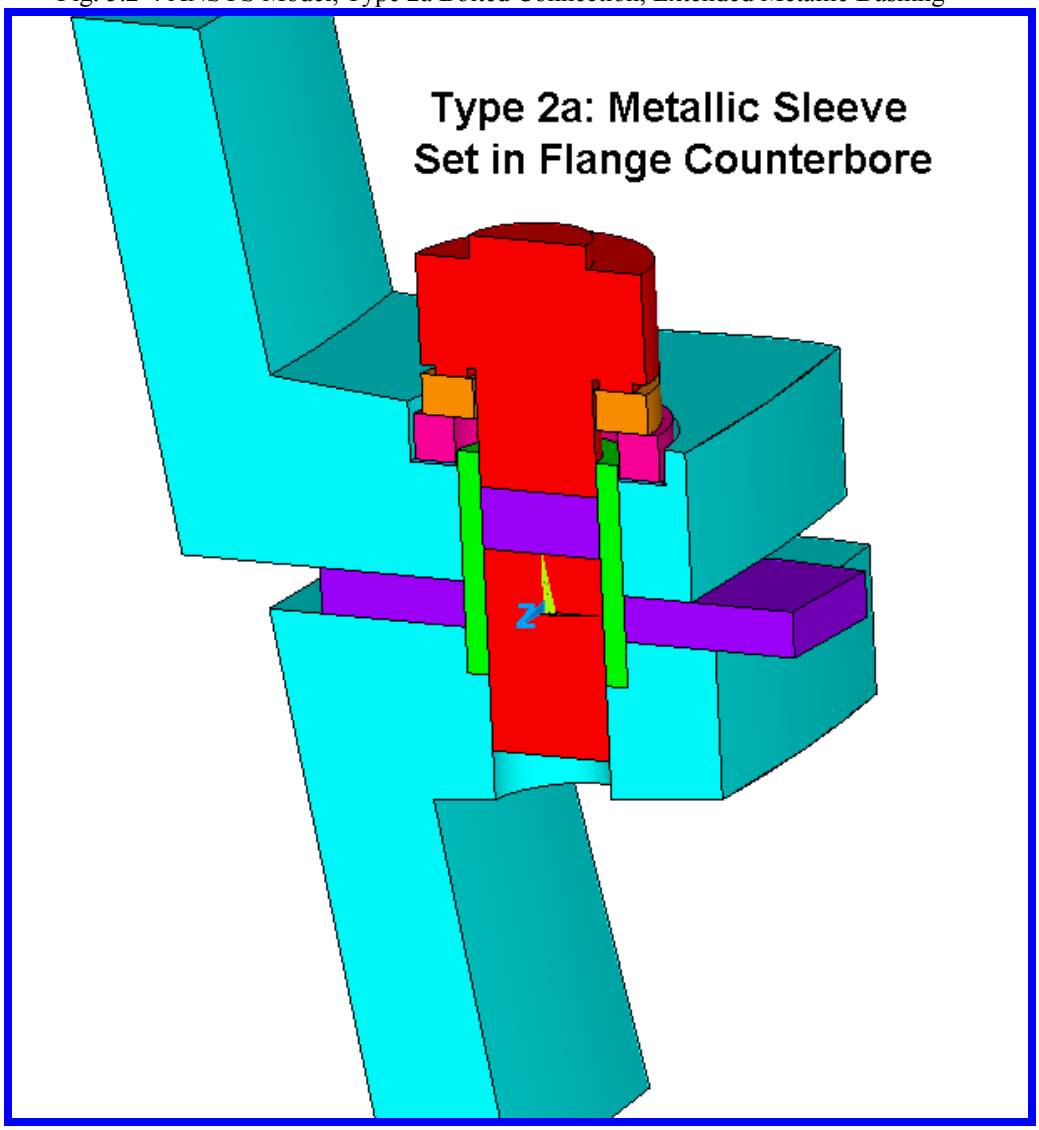

Note: There are no contact elements between the bolt shank and bushing ID for this Type 2a configuration. The intention of this bolting structure is to isolate the bolt from stresses due to shear and local contact. In this case, the metallic bushing is designed to carry the shear load.

Fig. 5.2-5 1st Principal Stress Range in Type 1 Bolt from 20 kip Shear Load G-11 Bushing (top), Metallic Bushing (bottom)

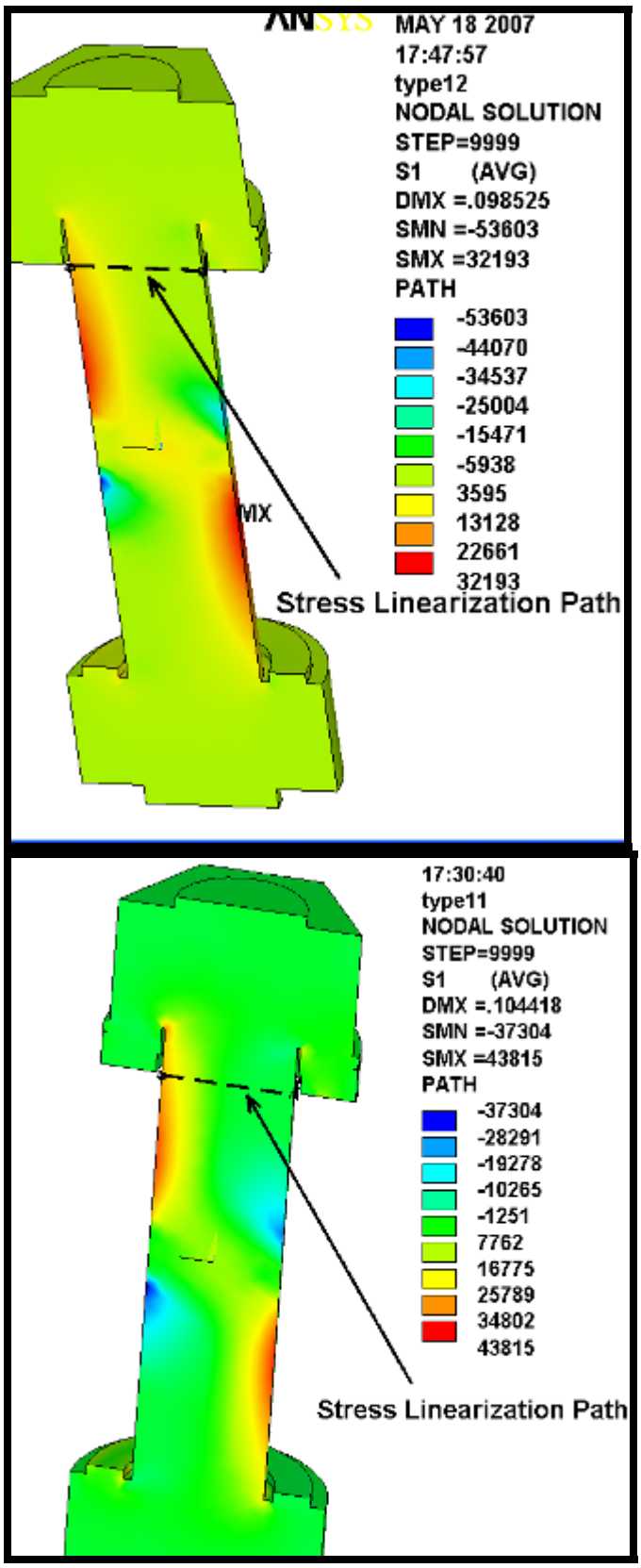

Fig. 5.2-6 1st Principal Stress Range in Type 2 Bolt from 20 kip Shear Load G-11 Bushing (top), Metallic Bushing (bottom)

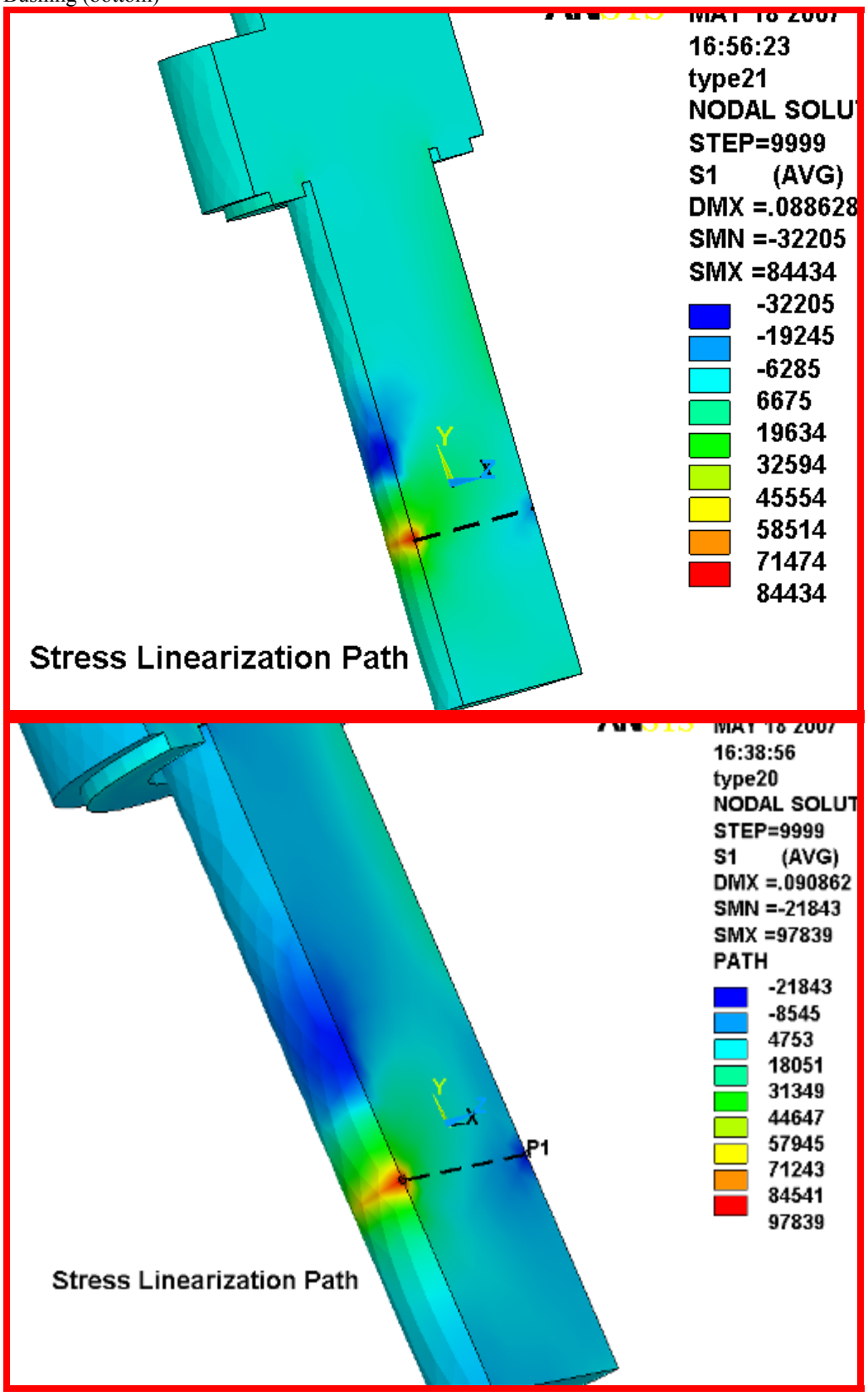

Fig. 5.2-7 1st Principal Stress Range in Type 2a Bolt from 20 kip Shear Load Extended Metallic Bushing

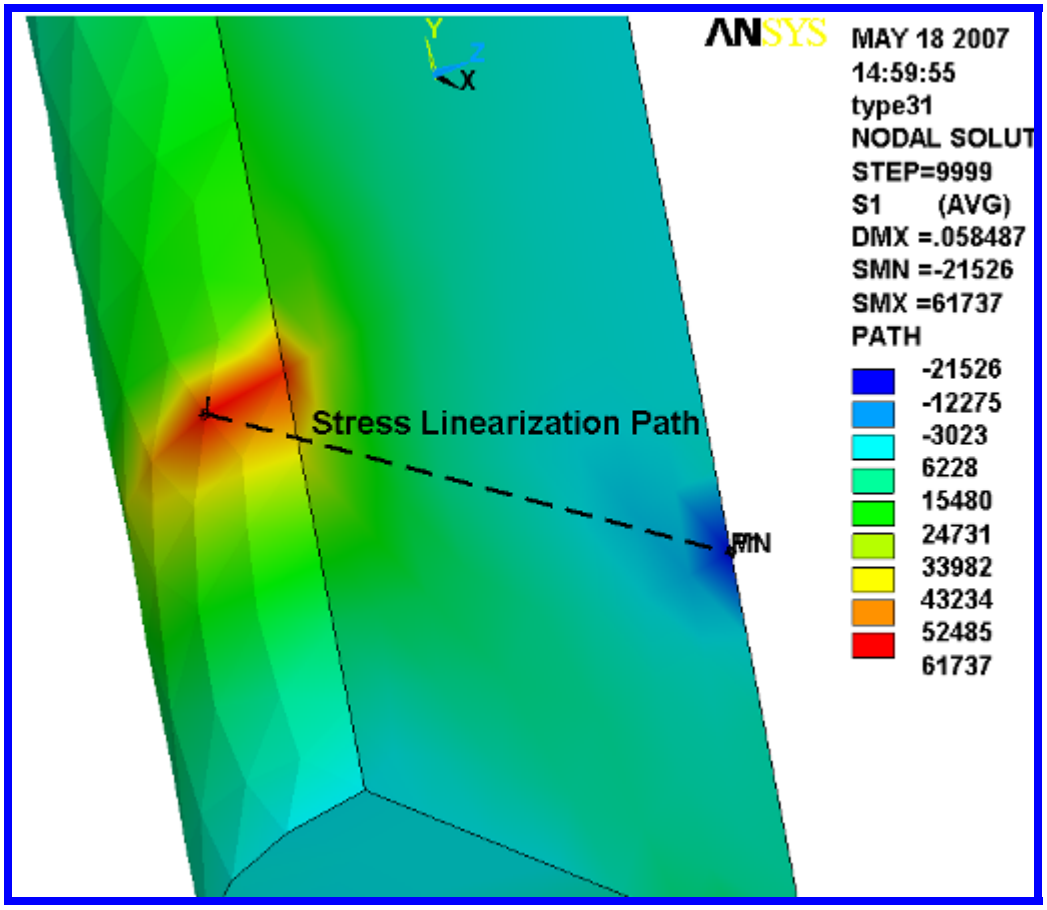

Fig. 5.2-8 Type 1 Section Stress Profile, G-11 Bushing

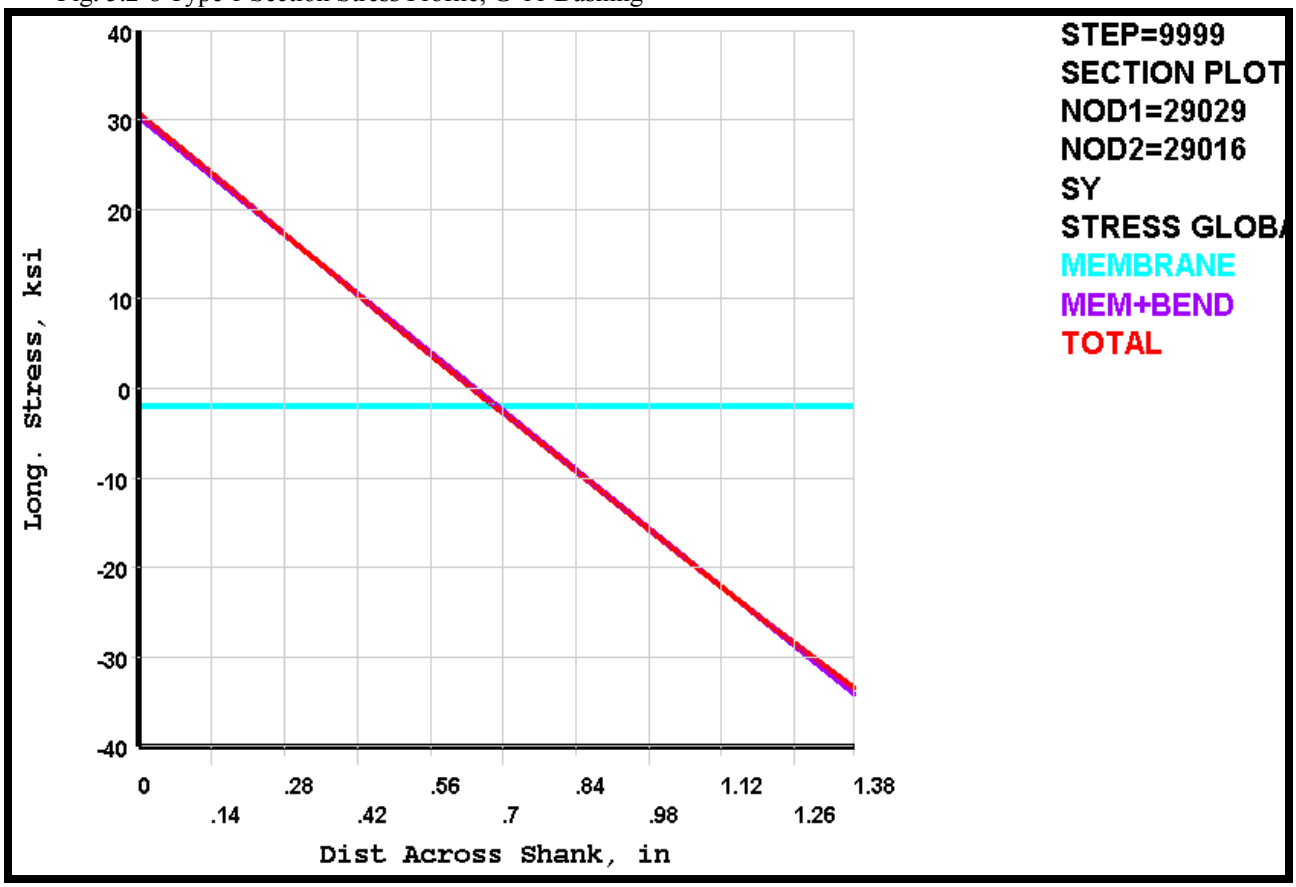


```
                ** MEMBRANE PLUS BENDING **  I=INSIDE C=CENTER
O=OUTSIDE
      SX           SY           SZ          SXY          SYZ
SXZ
 I   1.573       0.3030E+05    721.7       -1654.        9.750      -
0.1127
 C  -11.86        -1914.       -63.53      -1473.        2.267       -
1.354
 O  -25.28       -0.3413E+05   -848.7      -1293.       -5.217       -
2.596
      S1           S2           S3          SINT         SEQV
 I  0.3039E+05    721.7       -88.40       0.3048E+05  0.3008E+05
 C   790.4       -63.53       -2717.        3507.       3168.
 O   23.64        -848.7      -0.3418E+05  0.3420E+05  0.3378E+05

                ** TOTAL **  I=INSIDE C=CENTER O=OUTSIDE
      SX           SY           SZ          SXY          SYZ
SXZ
 I  -27.02       0.3069E+05    466.5       -10.28       -1.327
11.06
 C  -43.60        -2182.       -104.6      -2464.       -2.889
9.850
 O   22.69       -0.3347E+05   -452.3      -13.39        8.259
13.59
      S1           S2           S3          SINT         SEQV
TEMP
 I  0.3069E+05    466.7       -27.27       0.3072E+05  0.3047E+05
0.000
```

```
 C   1573.      -104.7      -3799.       5372.       4760.
 O   23.08      -452.7     -0.3347E+05  0.3350E+05  0.3326E+05
0.000
```

Fig. 5.2-9 Type 1 Section Stress Profile, Metallic Bushing

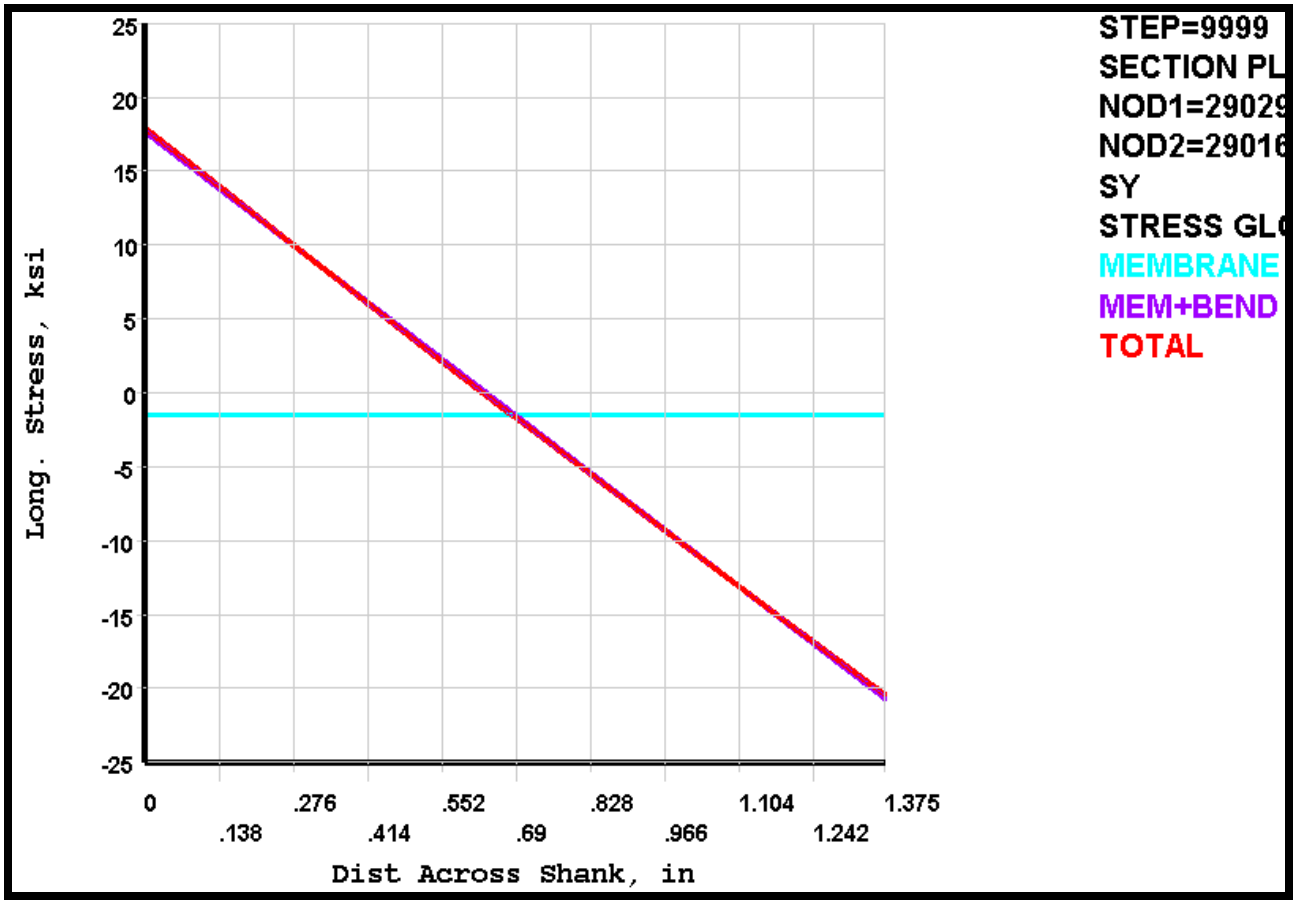


```
                ** MEMBRANE PLUS BENDING **  I=INSIDE C=CENTER
O=OUTSIDE
      SX           SY           SZ          SXY          SYZ
SXZ
 I   28.58       0.1767E+05    343.8       -1781.        8.942
0.6724
 C   26.95       -1501.       -84.05       -1653.        2.717       -
1.073
 O   25.33      -0.2067E+05   -511.9       -1524.       -3.508       -
2.818
      S1           S2           S3          SINT         SEQV
 I  0.1785E+05    343.8       -149.4       0.1800E+05  0.1776E+05
 C   1084.       -84.06       -2558.        3641.       3220.
 O   137.0       -511.9      -0.2078E+05   0.2092E+05  0.2060E+05

                ** TOTAL **  I=INSIDE C=CENTER O=OUTSIDE
      SX           SY           SZ          SXY          SYZ
SXZ
 I  -13.44       0.1792E+05    235.3        4.414      -0.8974
6.801
 C   45.76       -1649.       -115.4       -2615.       -1.723
6.860
 O   12.15      -0.2042E+05   -298.2       -9.731        3.657
6.875
      S1           S2           S3          SINT         SEQV
TEMP
```

```
 I  0.1792E+05   235.4      -13.63      0.1793E+05  0.1781E+05
0.000
 C   1947.      -115.4       -3550.       5498.       4810.
 O   12.31      -298.4     -0.2042E+05  0.2043E+05  0.2028E+05
0.000
```

Fig. 5.2-10 Type 2 Section Stress Profile, G-11 Bushing

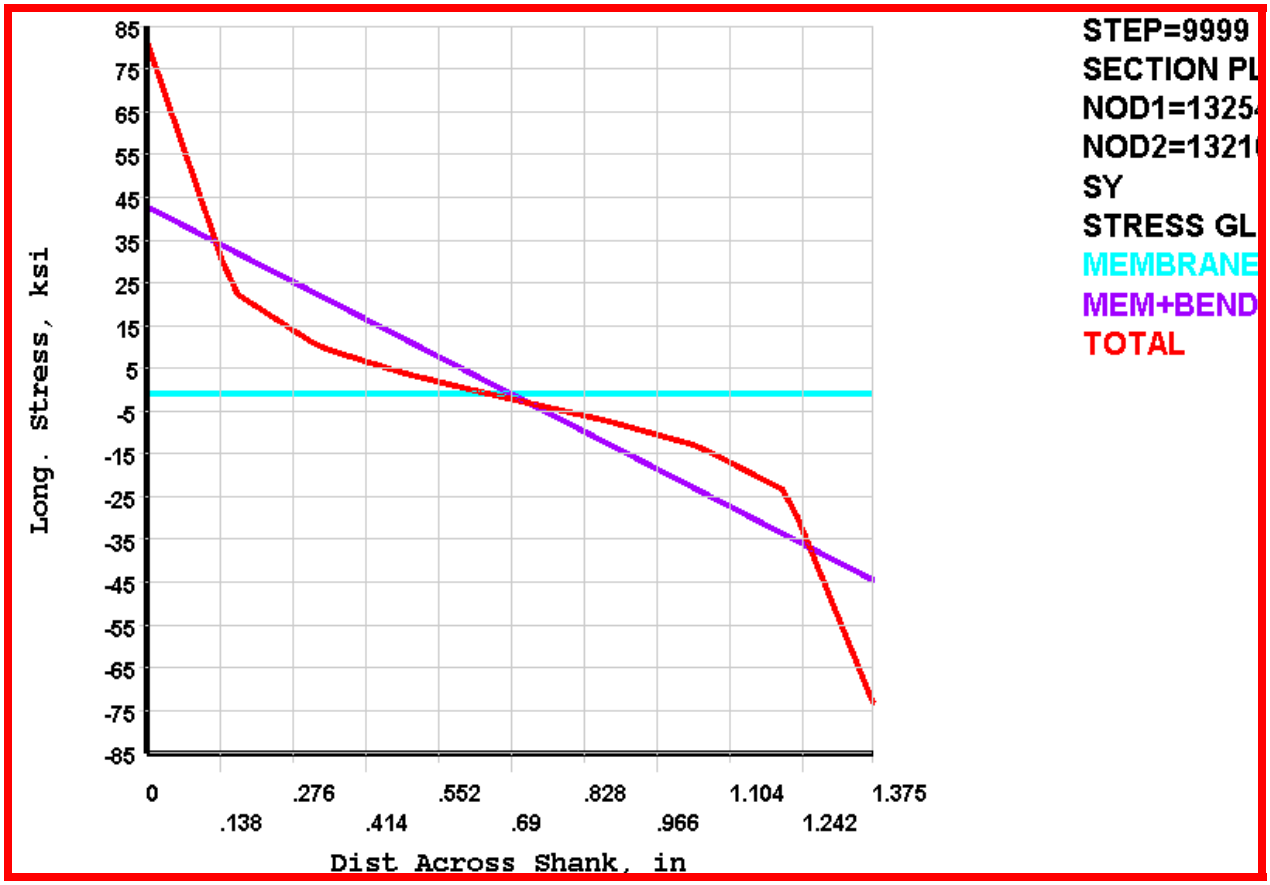


```
                ** MEMBRANE PLUS BENDING **  I=INSIDE C=CENTER
O=OUTSIDE
      SX            SY            SZ           SXY           SYZ
SXZ
 I  0.2945E+05  0.4281E+05  0.1865E+05  0.1259E+05  -395.8       -
43.14
 C   2610.       -848.9       489.6      0.1099E+05  -9.107       -
86.52
 O -0.2423E+05 -0.4450E+05 -0.1767E+05   9386.       377.6       -
129.9
      S1            S2            S3           SINT          SEQV
 I  0.5038E+05  0.2189E+05  0.1863E+05  0.3175E+05  0.3025E+05
 C  0.1200E+05   489.4     -0.1024E+05  0.2224E+05  0.1927E+05
 O -0.1766E+05 -0.2055E+05 -0.4819E+05  0.3053E+05  0.2919E+05

                ** TOTAL **  I=INSIDE C=CENTER O=OUTSIDE
      SX            SY            SZ           SXY           SYZ
SXZ
 I  0.4460E+05  0.8141E+05  0.3299E+05  0.2953E+05  -1163.       -
1249.
 C   1394.       -2113.       42.81       8763.      -13.10
40.58
 O -0.3290E+05 -0.7316E+05 -0.2834E+05  0.2367E+05   1042.       -
1418.
      S1            S2            S3           SINT          SEQV
TEMP
```

```
 I  0.9784E+05  0.3301E+05  0.2815E+05  0.6969E+05  0.6739E+05
0.000
 C   8578.       42.89      -9297.      0.1787E+05  0.1548E+05
 O -0.2184E+05 -0.2840E+05 -0.8414E+05  0.6230E+05  0.5929E+05
0.000
```

Fig. 5.2-11 Type 2 Section Stress Profile, Metallic Bushing

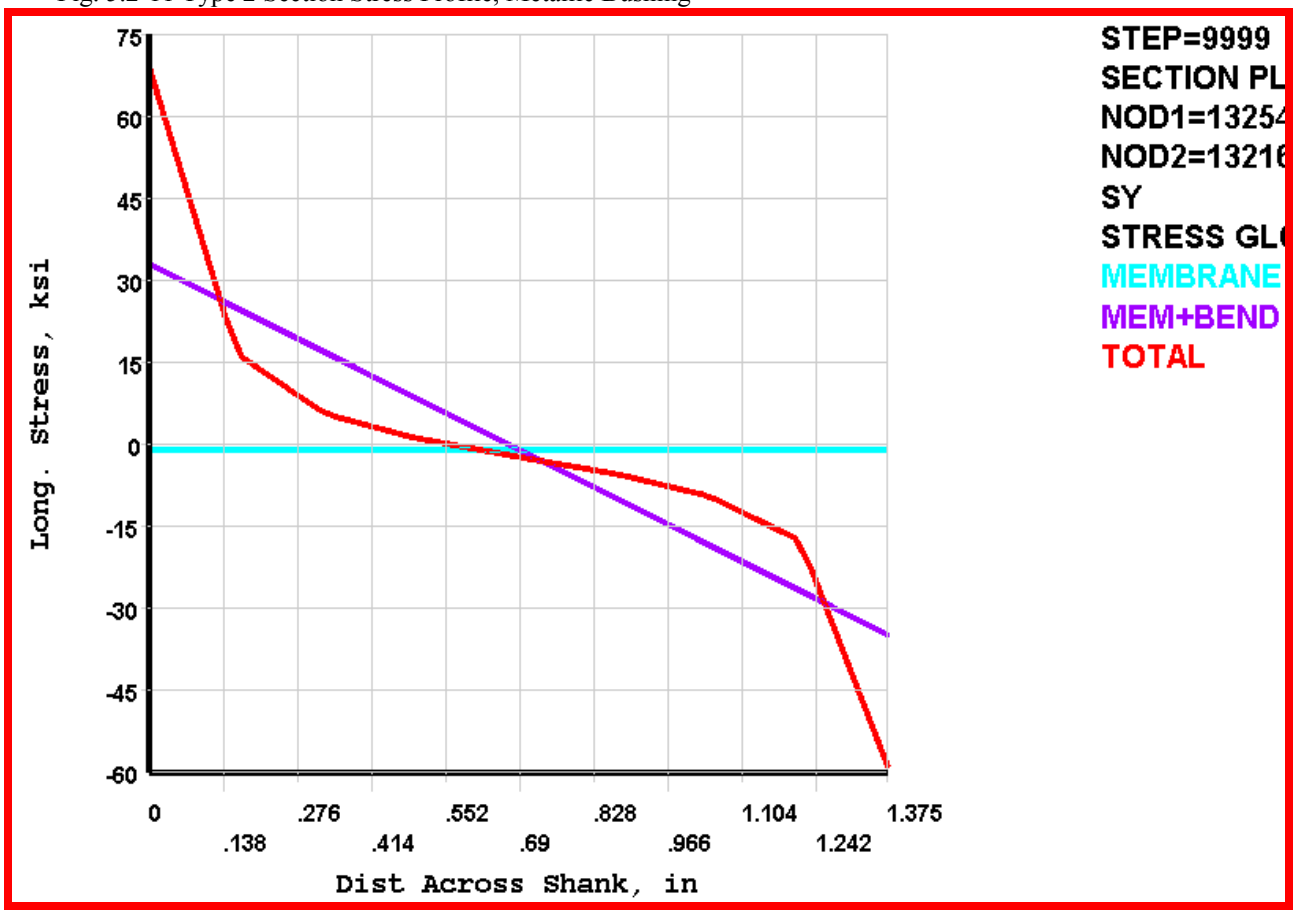


```
                ** MEMBRANE PLUS BENDING **  I=INSIDE C=CENTER
O=OUTSIDE
       SX            SY            SZ           SXY           SYZ
SXZ
 I  0.2632E+05  0.3294E+05  0.1584E+05  0.1286E+05  -337.0       -
32.61
 C   2301.       -923.6       655.2      0.1107E+05  -10.89       -
68.57
 O -0.2171E+05 -0.3478E+05 -0.1453E+05   9285.       315.3       -
104.5
       S1            S2            S3           SINT          SEQV
 I  0.4291E+05  0.1640E+05  0.1578E+05  0.2713E+05  0.2683E+05
 C  0.1188E+05   655.0      -0.1050E+05  0.2238E+05  0.1938E+05
 O -0.1452E+05 -0.1690E+05 -0.3961E+05  0.2509E+05  0.2399E+05

                ** TOTAL **  I=INSIDE C=CENTER O=OUTSIDE
       SX            SY            SZ           SXY           SYZ
SXZ
 I  0.4016E+05  0.6896E+05  0.2870E+05  0.2613E+05  -992.3       -
1087.
 C   690.7       -2303.       219.3       9920.       -16.71
38.51
 O -0.2834E+05 -0.5885E+05 -0.2332E+05  0.1995E+05   882.0       -
1187.
       S1            S2            S3           SINT          SEQV
TEMP
```

```
 I  0.8443E+05  0.2871E+05  0.2468E+05  0.5976E+05  0.5785E+05
0.000
 C   9226.       219.4     -0.1084E+05  0.2006E+05  0.1741E+05
 O -0.1839E+05 -0.2338E+05 -0.6874E+05  0.5036E+05  0.4806E+05
0.000
```

Fig. 5.2-12 Type 2a Section Stress Profile, Metallic Bushing

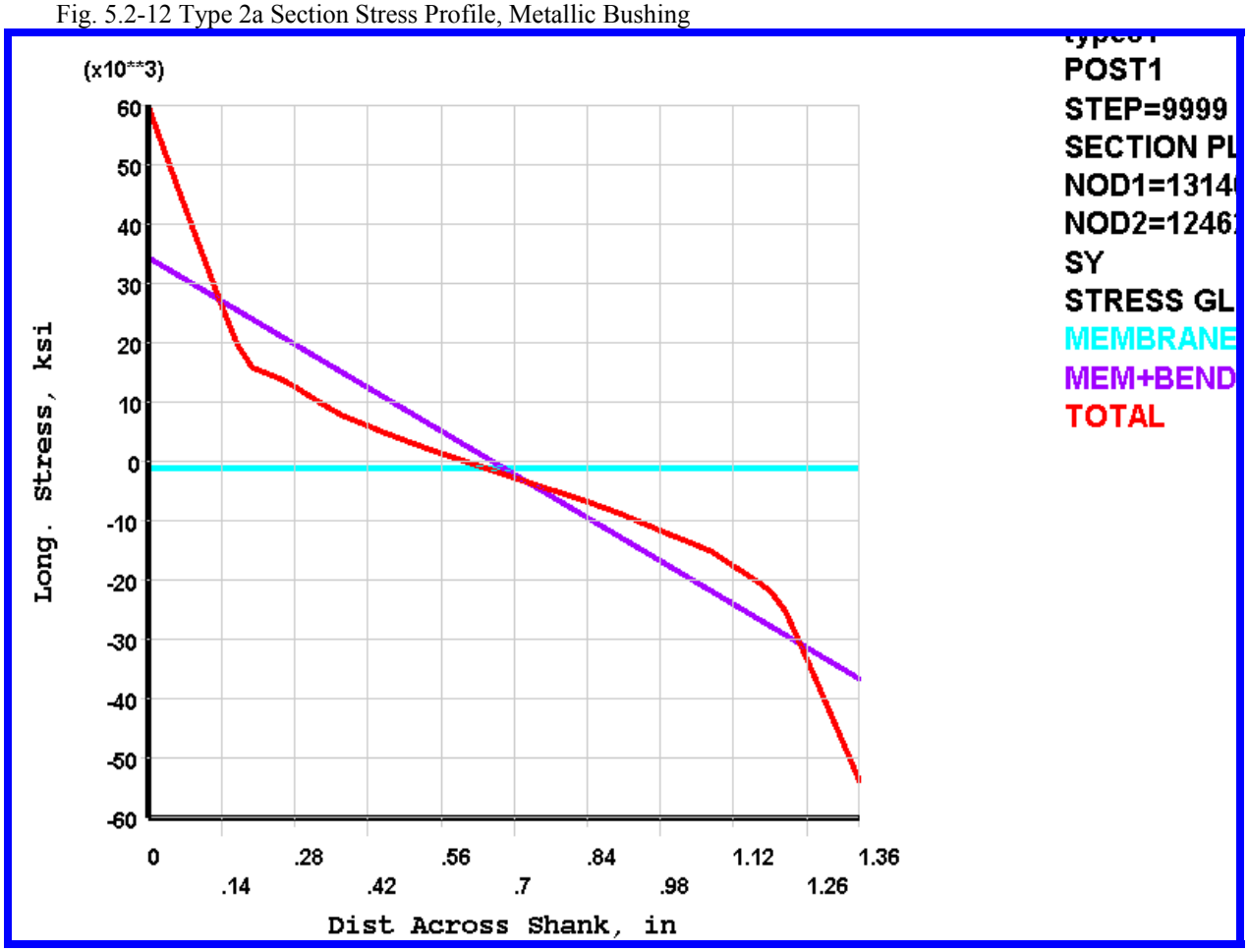


```
                ** MEMBRANE PLUS BENDING **  I=INSIDE C=CENTER
O=OUTSIDE
       SX            SY            SZ           SXY           SYZ
SXZ
 I  0.2494E+05  0.3430E+05  0.1689E+05    3258.         799.6
1310.
 C    4517.       -1151.        1488.        1346.         187.1
613.0
 O -0.1590E+05 -0.3660E+05 -0.1392E+05   -566.5       -425.4       -
83.92
       S1            S2            S3           SINT          SEQV
 I  0.3539E+05  0.2405E+05  0.1668E+05  0.1871E+05  0.1633E+05
 C    4938.         1370.        -1455.         6394.         5550.
 O -0.1391E+05 -0.1589E+05 -0.3662E+05  0.2272E+05  0.2179E+05

                ** TOTAL **  I=INSIDE C=CENTER O=OUTSIDE
       SX            SY            SZ           SXY           SYZ
SXZ
 I  0.3710E+05  0.5968E+05  0.2774E+05    6984.         1081.
1822.
 C    3307.       -2161.        879.0       -183.4         66.68
506.1
 O -0.2153E+05 -0.5378E+05 -0.2247E+05    437.9       -78.75       -
46.18
```

```
      S1           S2           S3          SINT         SEQV
TEMP
 I  0.6174E+05  0.3539E+05  0.2740E+05  0.3434E+05  0.3112E+05
0.000
 C   3413.       781.2      -2170.       5583.       4838.
  O -0.2153E+05 -0.2248E+05 -0.5378E+05  0.3226E+05  0.3179E+05
                                0.000
```

Fig. 5.2-13 ASME Code Base Thread Stress Intensification Factor (NB-3232.3 (c))

NB-3230 STRESS LIMITS FOR BOLTS

NB-3231 Design Conditions

(a) The number and cross-sectional area of bolts required to resist the design pressure shall be determined in accordance with the procedures of Appendix E, using the larger of the bolt loads given by the equations of Appendix E as a design mechanical load. The allowable bolt design stresses shall be the values given in Table I-1.3, for bolting materials.

(b) When sealing is effected by a seal weld instead of a gasket, the gasket factor, m, and the minimum design seating stress, y, may be taken as zero.

(c) When gaskets are used for preservice testing only, the design is satisfactory if the above requirements are satisfied for $m=y=0$, and the requirements of NB-3232 are satisfied when the appropriate m and y factors are used for the test gasket.

NB-3232 Normal Conditions

Actual service stresses in bolts, such as those produced by the combination of preload, pressure and differential thermal expansion may be higher than the values given in Table I-1.3.

NB-3232.1 Average Stress. The maximum value of service stress, averaged across the bolt cross-section and neglecting stress concentrations, shall not exceed two times the stress values of Table I-1.3.

NB-3232.2 Maximum Stress (Except As Restricted by NB-3232.3). The maximum value of service stress at the periphery of the bolt cross-section (resulting from direct tension plus bending) and neglecting stress concentrations shall not exceed three times the stress values of Table I-1.3. Stress intensity, rather than maximum stress, shall be limited to this value when the bolts are tightened by methods other than heaters, stretchers or other means which minimize residual torsion.

NB-3232.3 Fatigue Analysis of Bolts. Unless the components on which they are installed meet all the conditions of NB-3222.4*(d)* and thus require no fatigue analysis, the suitability of bolts for cyclic operation shall be determined in accordance with the procedures of the following subsubparagraphs.

(a) Bolting Having Less Than 100,000 psi Tensile Strength. Bolts made of materials which have specified minimum tensile strengths of less than 100,000 psi shall be evaluated for cyclic operation by the methods of NB-3222.4*(e)*, using the applicable design fatigue curve of Fig. I-9.4 and an appropriate fatigue strength reduction factor (see NB-3232.3*(c)*).

(b) High-Strength Alloy-Steel Bolting. High-strength alloy-steel bolts and studs may be evaluated for cyclic operation by the methods of NB-3222.4*(e)* using the design fatigue curve of Fig. I-9.4 provided:

(1) The maximum value of the service stress (see NB-3232.2) at the periphery of the bolt cross-section (resulting from direct tension plus bending) and neglecting stress concentration shall not exceed 2.7 S_m, if the higher of the two fatigue design curves given in Fig. I-9.4 is used. (The 2 S_m limit for direct tension is unchanged.)

(2) Threads shall be of a V-type having a minimum thread root radius no smaller than 0.003 in.

(3) Fillet radii at the end of the shank shall be such that the ratio of fillet radius to shank diameter is not less than 0.060.

(c) Fatigue-Strength-Reduction Factor (see NB-3213.17). Unless it can be shown by analysis or tests that a lower value is appropriate, the fatigue-strength-reduction factor used in the fatigue evaluation of threaded members shall not be less than 4.0. However, when applying the rules of NB-3232.3*(b)* for high-strength alloy-steel bolts, the value used shall not be less than 4.0.

(d) Effect of Elastic Modulus. Multiply S_{alt} (as determined in NB-3216.1 or NB-3216.2) by the ratio of the modulus of elasticity given on the design fatigue curve to the value of the modulus of elasticity used in the analysis. Enter the applicable design fatigue curve at this value on the ordinate axis and find the corresponding number of cycles on the axis of abscissas. If the operational cycle being considered is the only one which produces significant fluctuating stresses, this is the allowable number of cycles.

(e) Cumulative Damage. The bolts shall be acceptable for the specified cyclic application of loads and thermal stresses provided the cumulative usage factor, U, as determined in NB-3222.4*(e)(5)* does not exceed 1.0.

NB-3233 Upset Conditions

The stress limits for Normal Conditions (see NB-3232) apply.

NB-3234 Emergency Conditions

The stress limits of NB-3232.1 and NB-3232.2 apply.

NB-3235 Faulted Conditions

The limits of NB-3225 apply.

Fig. 5.2-14 Fatigue Data for A286 (N. Suzuki) & Proposed NCSX Design-Basis Fatigue Curve

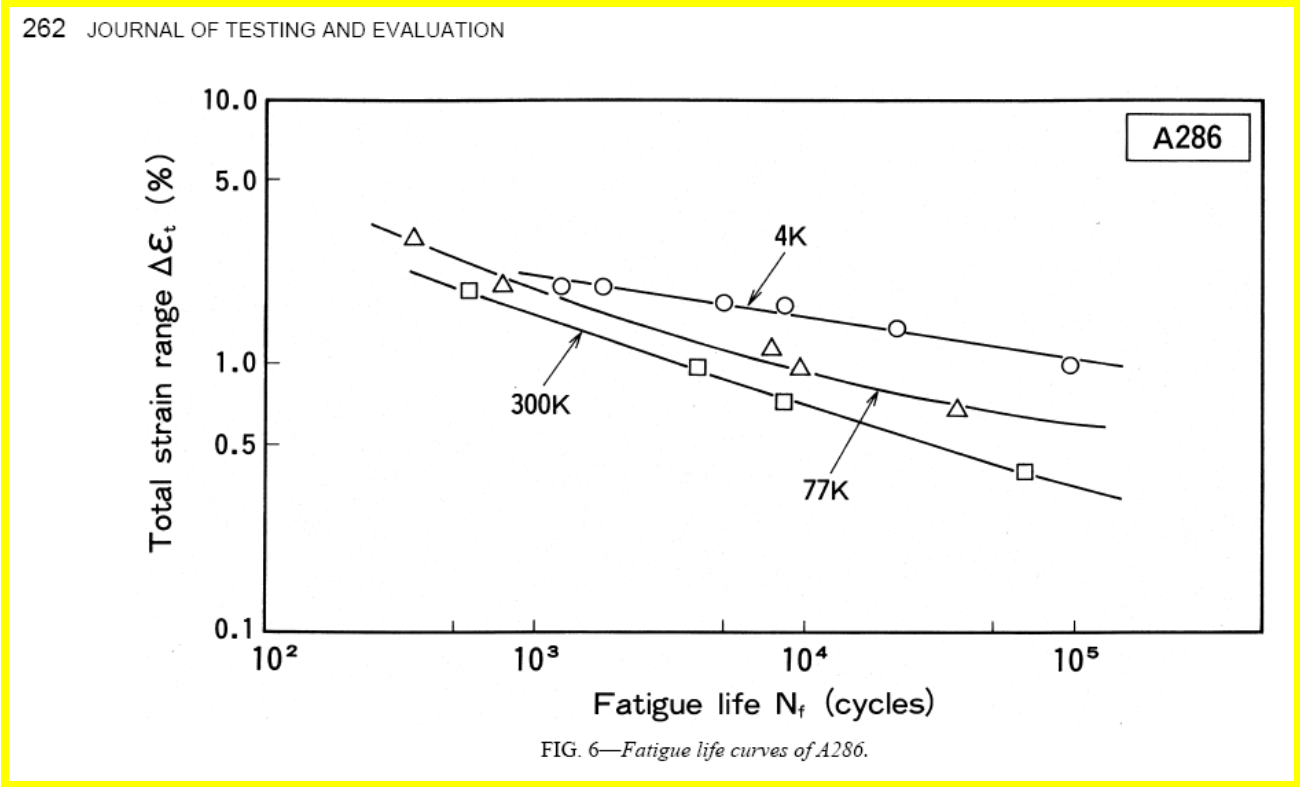

Notes:

1. Suzuki reports an elastic modulus of 223 GPa for A286 at 77K.

2. Total Stress Range = Elastic Modulus x Total Strain Range

3. NCSX Structural Design Criteria requires reducing test data by a factor of 2 to obtain a design-basis fatigue curve.

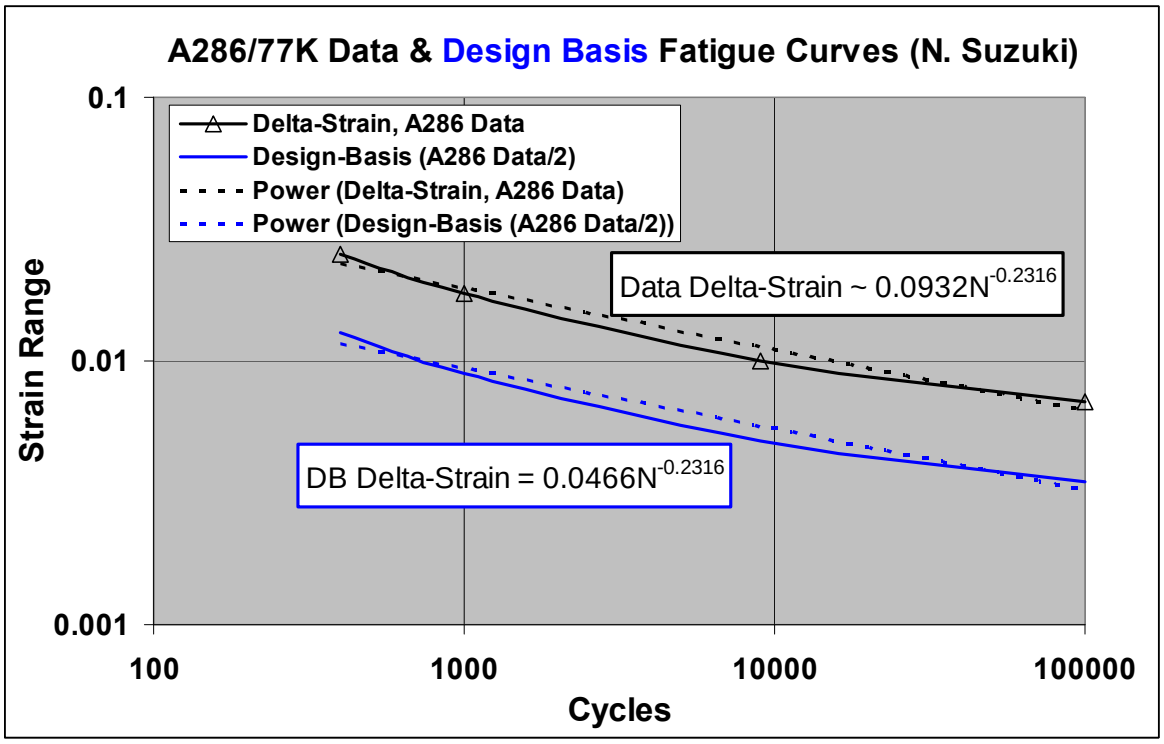

Fig. 5.2-15 Allowable Number of Shear Load Cycles (N) v. Bolt Shear Load for each of the (5) Bolted Joint Configurations

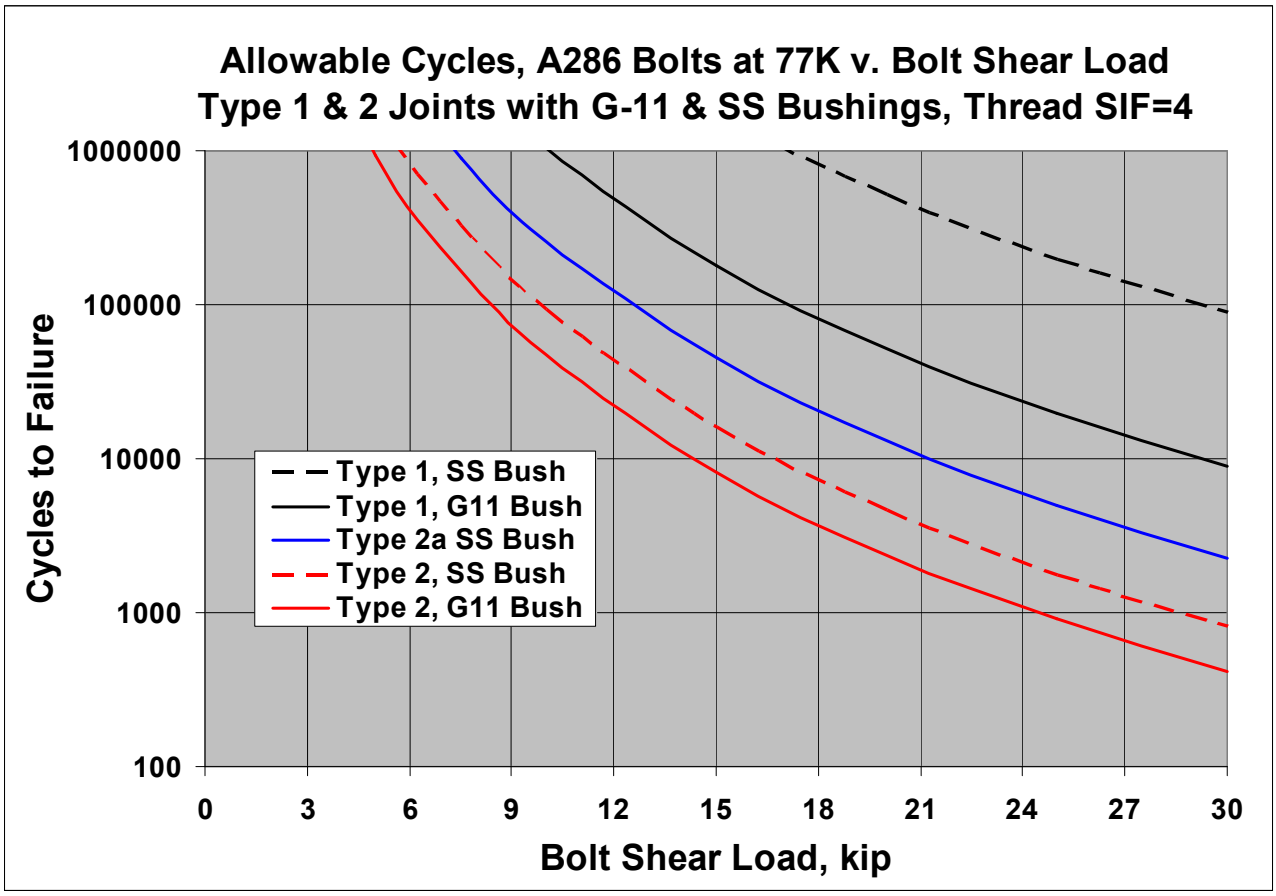

Assumptions:

1. Stresses scale with applied bolt shear load.

2. Stress Intensification Factor of 4.0 applicable to bolt threads.

3. Cycles to Failure obtained from Design-Basis fatigue curve-fit and FE model stresses.

5.3 Stresses in the Revised Type-1 & Type-2 Bolted Joints (circa July 2007)

The recent release of the final reference Type 1 & Type 2 bolted joint design details (UT-Battelle ORNL drawing SE 140-190 Rev 2, parts shown in Fig. 4.3-1) indicates one minor which necessitates a re-analysis of these mechanical fasteners. The shims have a clearance hole of 1.5" diameter. (They used to be a tight-fit to the bolt). The analysis methodology follows the approach presented in section 5.2. Even the models are carried over from the section 5.2 analyses, with this simple shim hole change (see Figs. 5.3-2 & 5.3-3).

Fig.5.3-4 shows a stress contour plot of the Type 1 bolt subjected to a 20 kip shear load. The contours correspond to the stress range (Load Step 2 minus Load Step 1) and therefore reflect the stress range from the shear load only. Paths P1 and P2 define the sections through the highest thread stress (2" from the ends of the bolt). Although the plot shows the 1st principal stress, we must be mindful of the 3rd principal stress which would be "tensile" if the shear load sign was applied as a negative value.

Table 5.3-1 lists the section stress range from this 20 kip shear load across the P2 and P3 bolt sections. Recall from section 4.2 that the Total bolt stress range is defined by the following equation with an adjustment proposed here to include ΔS3 also:

$$\Delta S_{tot} = (k_{thread})(\Delta S1) + PEAK \text{ or } (k_{thread})(\Delta S3) + PEAK$$

Similar results are shown in Fig. 5.3-5 and Table 5.3-2 for the Type 2 joint with the following exception. There is only one critical bolt section which occurs at the surface of the tapped hole.

Table 5.3-3 lists the numerical values associated with this equation and the Total Intensified Stress Range. Keep in mind that these values are based on a 20 kip unit shear load and can come from ΔS1 or ΔS3.

Table 5.3-3 Total Intensified Joint Fastener Stress from 20 kip Shear Load Range

Joint Type	Type 1	Type 2
Un-Intensified Stress Range, ksi	-35.4	-50.5
Thread Stress Intensification Factor	4	4
Peak Stress Range, ksi	-1.1	-40.0
Total Intensified Stress Range, ksi	143	242

These revised total intensified stress values are used in a spread sheet along with A286 fatigue data to create the design-basis shear load fatigue curve shown in Fig. 5.3-6. Focusing on the project's 100000 cycle design life, we see that the Type 1 joint shear loads should not exceed ~15 kip, while the Type 2 joint shear loads should not exceed ~9 kip. While the clearance hole in the shim has almost no impact on the Type 2 joint, it results in a slight reduction in the shear capacity of the type 1 joint.

Fig. 5.3-1 July 2007 Joint Designs, Type 1 (top) & Type 2 (bottom)

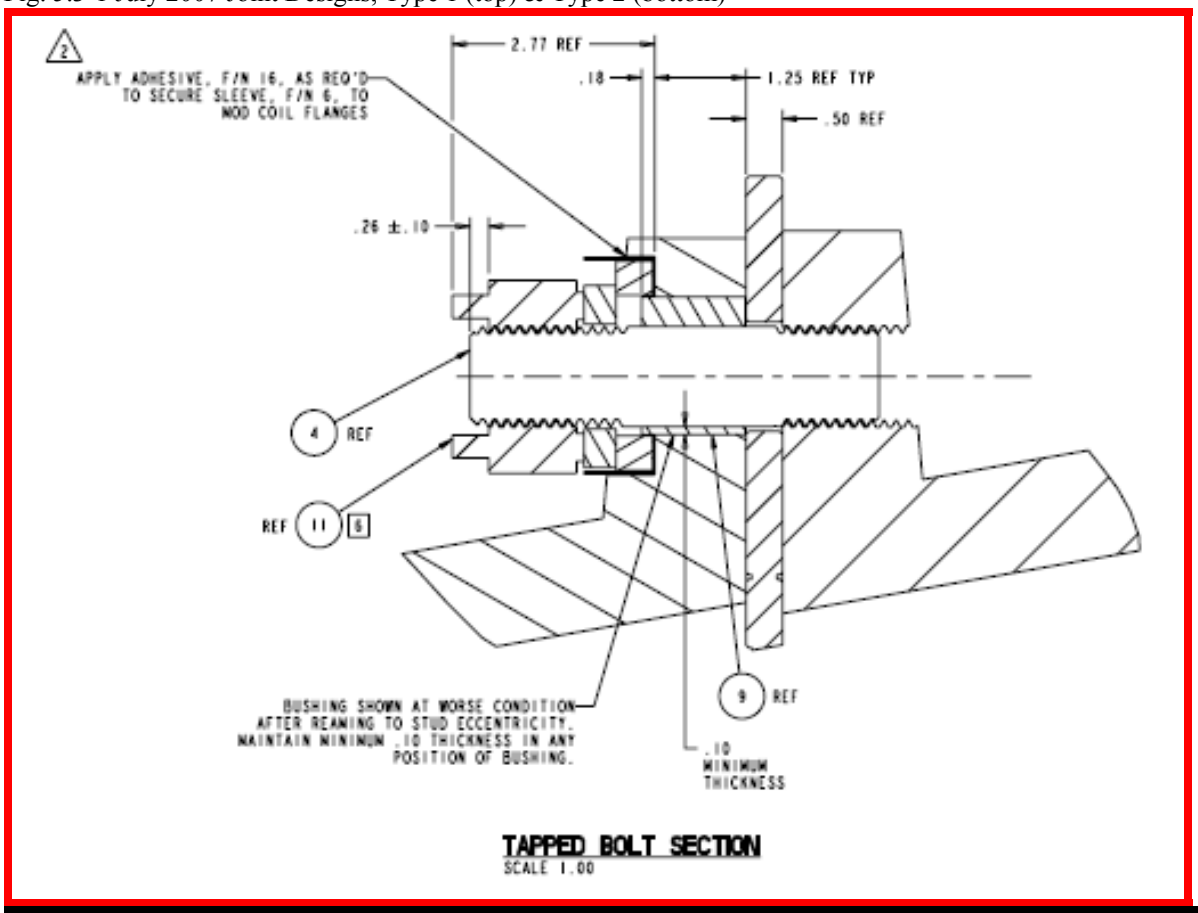

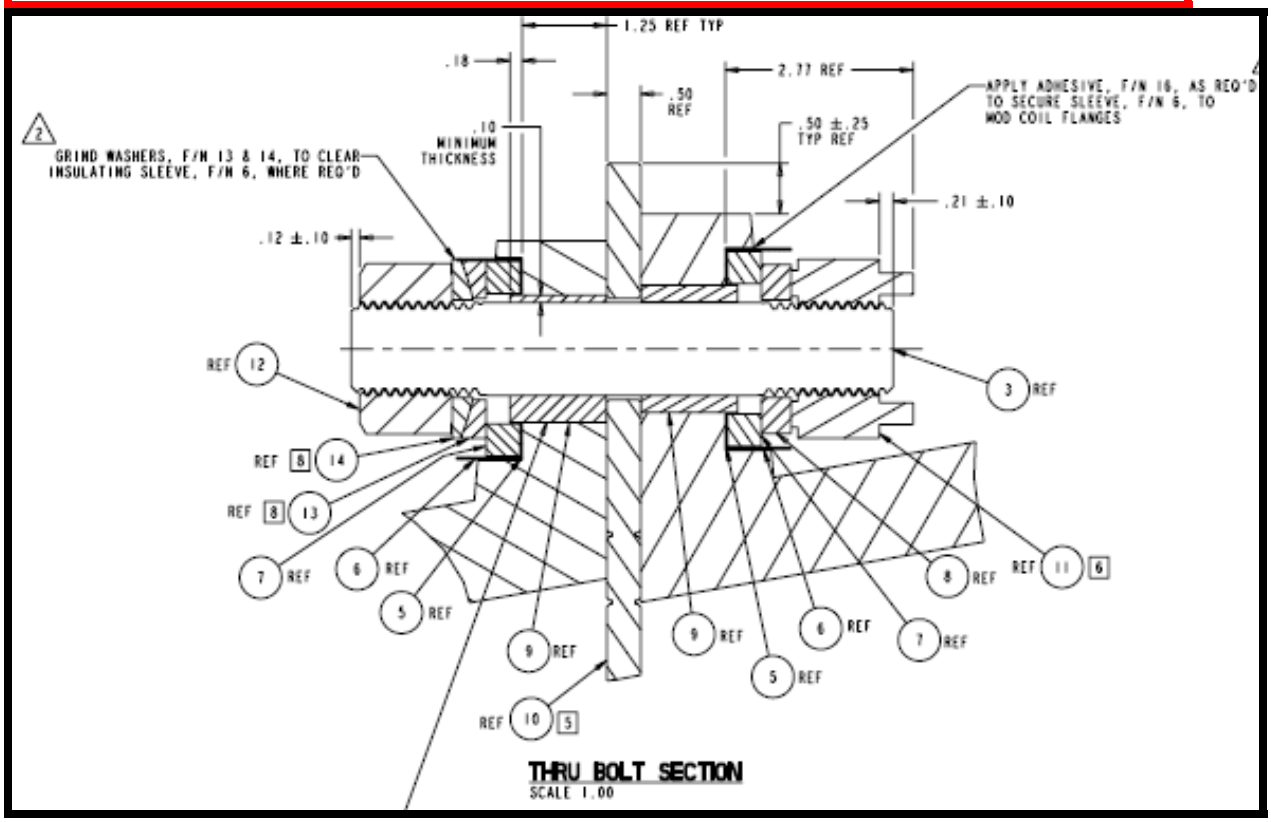

Fig. 5.3-2 ANSYS Model, Type 1 Bolted Connection

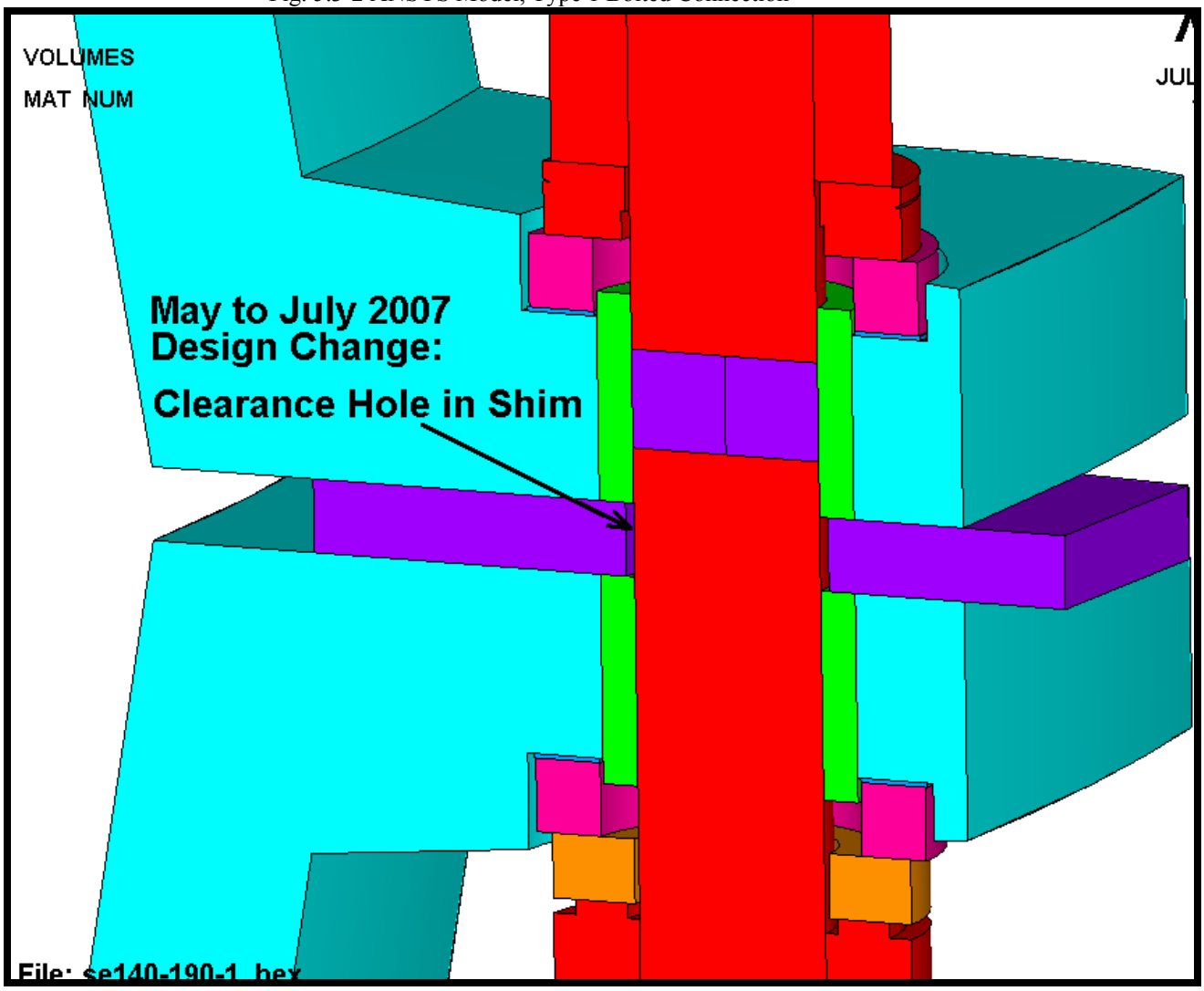

Fig. 5.3-3 ANSYS Model, Type 2 Bolted Connection

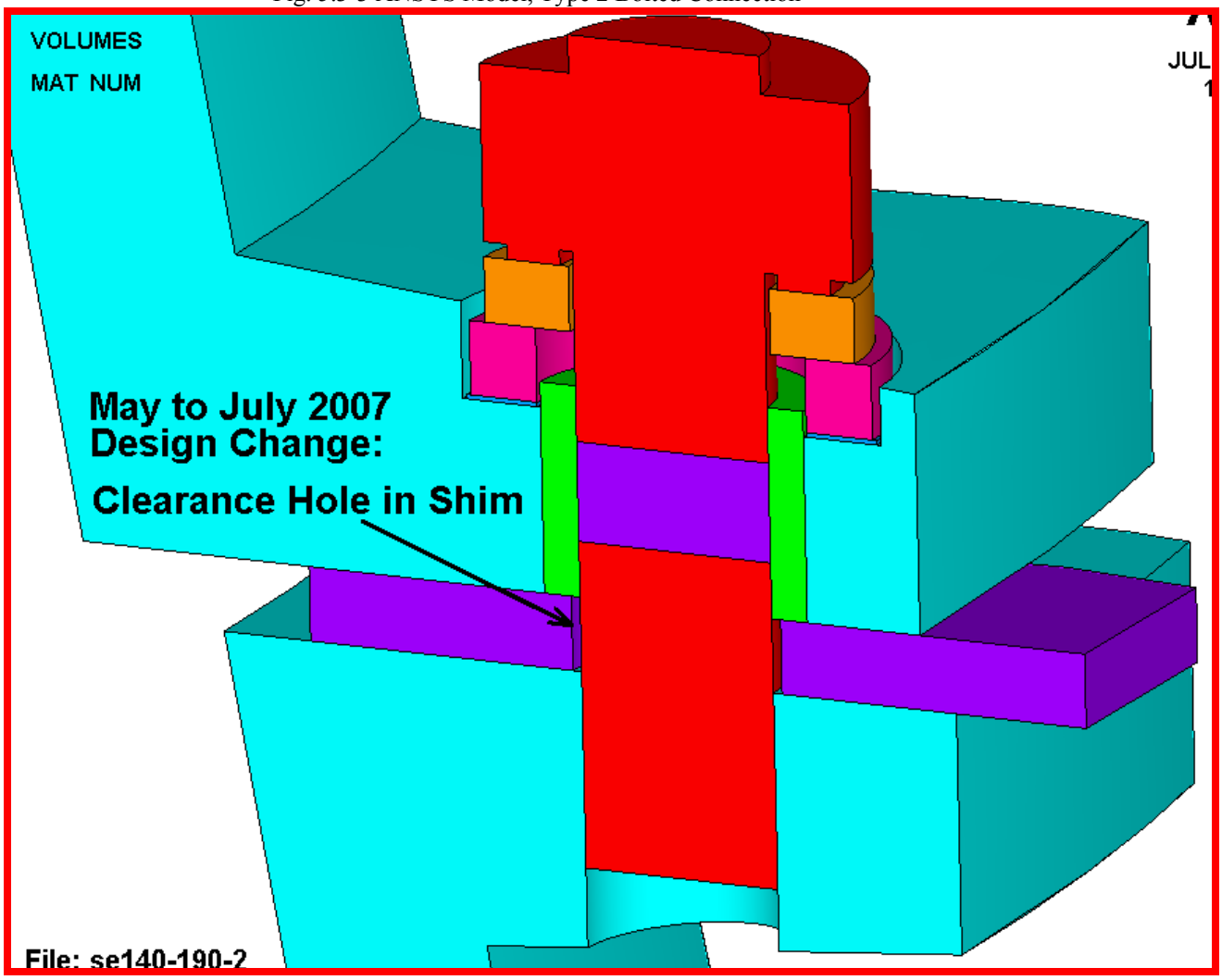

Fig. 5.3-4 1st Principal Stress Range in Type 1 Bolt from 20 kip Shear Load

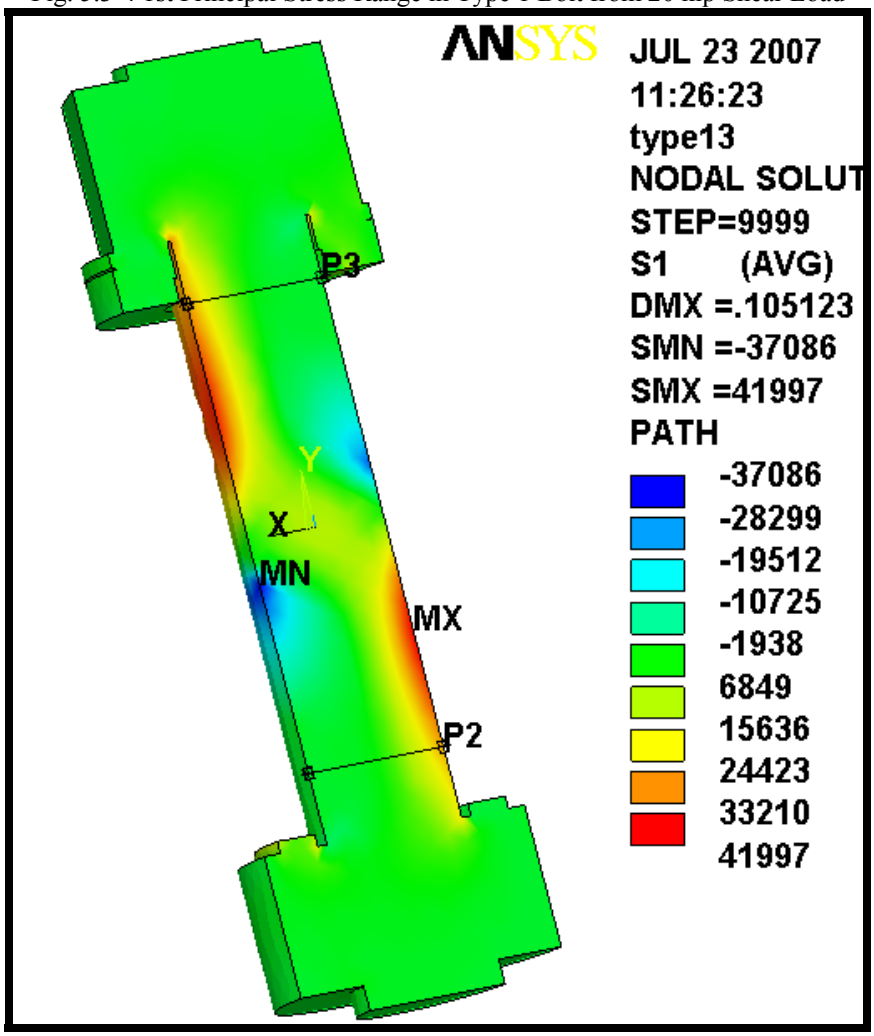

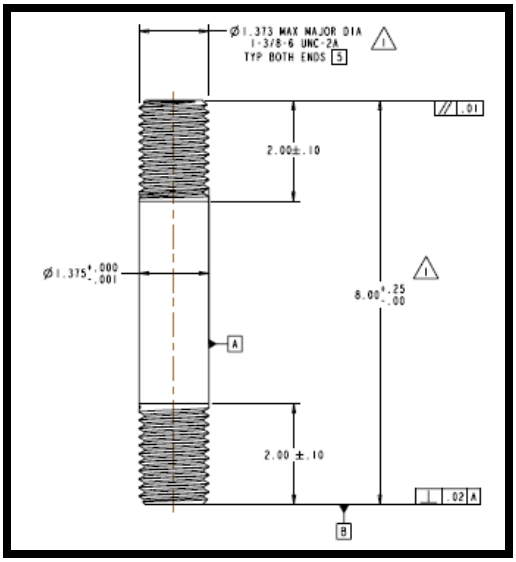

Note: Sections taken 2" from bolt ends (per SE 140-191 Rev1)

Table 5.3-1 Type 1 Section Stress Range from 20 kip Shear Load, G-11 Bushing

Linearized (Membrane + Bending) Stress Across Section P2

```
              ** MEMBRANE PLUS BENDING **  I=INSIDE C=CENTER
O=OUTSIDE
      SX           SY           SZ          SXY          SYZ
SXZ
 I   4.203     -0.3430E+05  -572.2      -2085.       7.300      -
3.512
 C  -55.31      -2521.       18.66      -2314.       1.576      -
1.693
 O  -114.8      0.2926E+05   609.5      -2542.      -4.148
0.1249
      S1           S2           S3          SINT         SEQV
 I   130.5       -572.2     -0.3443E+05  0.3456E+05  0.3421E+05
 C   1334.        18.65      -3910.       5243.       4725.
 O  0.2948E+05   609.5       -333.2      0.2981E+05  0.2935E+05

              ** PEAK **  I=INSIDE C=CENTER O=OUTSIDE
      SX           SY           SZ          SXY          SYZ
SXZ
 I   7.727        718.6        252.2       2069.       -6.175      -
2.994
 C  -59.75       -254.8       -20.80      -1297.       8.614      -
1.127
 O   101.7        394.3       -169.8       2501.       -25.14     -
0.9168
      S1           S2           S3          SINT         SEQV
 I   2462.        252.1       -1736.       4198.       3637.
 C   1144.       -20.82       -1458.       2602.       2257.
 O   2754.       -169.8       -2258.       5011.       4360.
```

Linearized (Membrane + Bending) Stress Across Section P3

```
      SX           SY           SZ          SXY          SYZ
SXZ
 I  -19.80      0.3047E+05   708.5      -1836.       10.32
0.1745
 C  -31.87      -2450.       -88.57     -1628.       2.318      -
1.448
 O  -43.95     -0.3537E+05  -885.7      -1420.       -5.681     -
3.070
      S1           S2           S3          SINT         SEQV
 I  0.3058E+05   708.5       -130.0      0.3071E+05  0.3030E+05
 C   787.3      -88.57       -3269.       4056.       3697.
 O   13.09      -885.7      -0.3543E+05  0.3544E+05  0.3500E+05

              ** PEAK **  I=INSIDE C=CENTER O=OUTSIDE
      SX           SY           SZ          SXY          SYZ
SXZ
 I  -6.206        354.1       -238.3       1828.       -11.85
10.73
 C  -48.88       -225.4       -50.34      -1074.       -5.461
11.61
 O   67.58        603.5        419.8       1406.       13.68
17.46
      S1           S2           S3          SINT         SEQV
 I   2010.       -238.1       -1663.       3673.       3208.
```

C	940.8	-50.48	-1215.	2156.	1869.
O	1768.	419.5	-1096.	2864.	2481.

Fig. 5.3-5 1st Principal Stress Range in Type 2 Bolt from 20 kip Shear Load

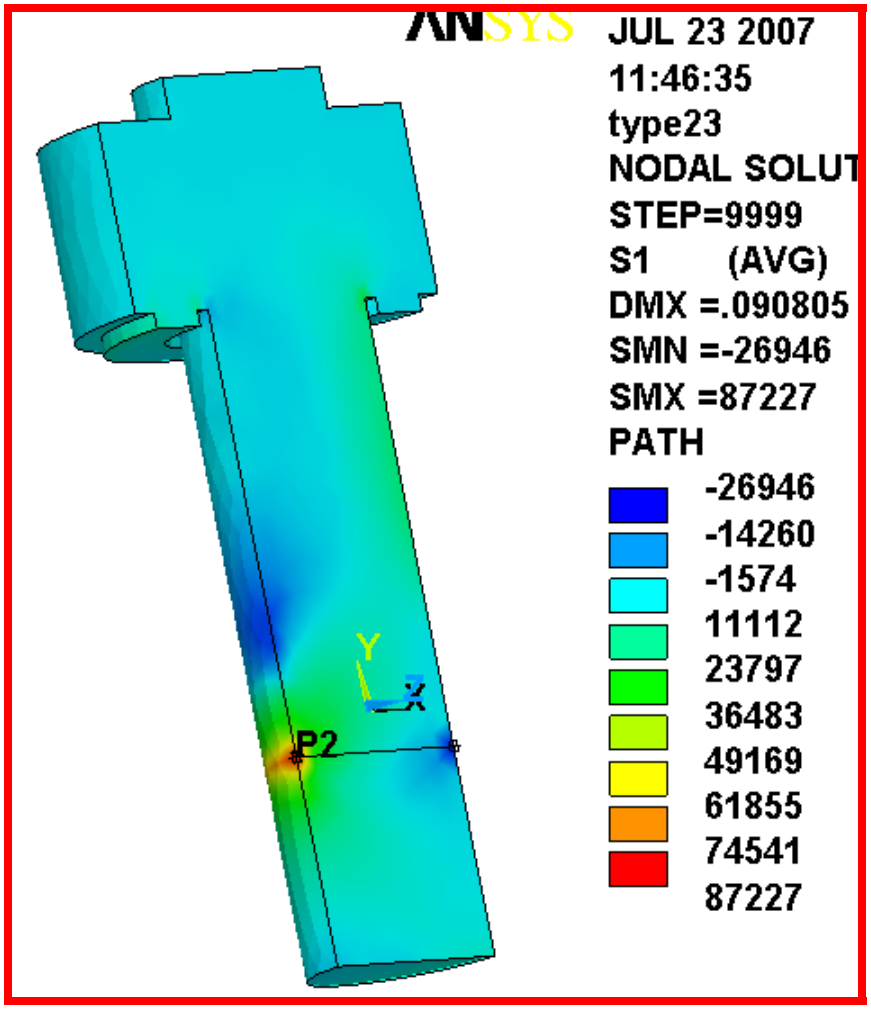

Note: Sections taken at edge of hole (also max stress location) since threads are certain to be there.

Table 5.3-2 Type 2 Section Stress Range from 20 kip Shear Load, G-11 Bushing

Linearized (Membrane + Bending) Stress Across Section P2

```
              ** MEMBRANE PLUS BENDING **  I=INSIDE C=CENTER
O=OUTSIDE
      SX           SY           SZ          SXY          SYZ
SXZ
 I -0.2595E+05 -0.4633E+05 -0.1892E+05  0.1013E+05   824.6      -
171.2
 C   2114.       -2644.        105.2      0.1075E+05   72.58      -
67.66
 O  0.3017E+05  0.4105E+05  0.1913E+05  0.1136E+05  -679.4
35.87
      S1           S2           S3          SINT         SEQV
 I -0.1889E+05 -0.2178E+05 -0.5054E+05  0.3165E+05  0.3031E+05
 C  0.1074E+05   106.1     -0.1127E+05  0.2201E+05  0.1907E+05
 O  0.4821E+05  0.2306E+05  0.1908E+05  0.2913E+05  0.2736E+05

              ** PEAK **  I=INSIDE C=CENTER O=OUTSIDE
      SX           SY           SZ          SXY          SYZ
SXZ
 I -0.1089E+05 -0.3404E+05 -0.1273E+05  0.1285E+05   2072.      -
1305.
 C  -892.1       -88.25       -107.5      -1794.      -95.14
108.6
 O  0.1352E+05  0.3147E+05  0.1203E+05  0.1388E+05  -998.8      -
930.4
      S1           S2           S3          SINT         SEQV
 I  -5161.     -0.1253E+05 -0.3997E+05  0.3481E+05  0.3177E+05
 C   1362.       -121.0       -2329.       3692.       3217.
 O  0.3908E+05  0.1198E+05   5952.      0.3313E+05  0.3057E+05
```

Fig. 5.3-6 Allowable Number of Shear Load Cycles (N) v. Bolt Shear Load circa July 2007 Bolted Joint Configurations

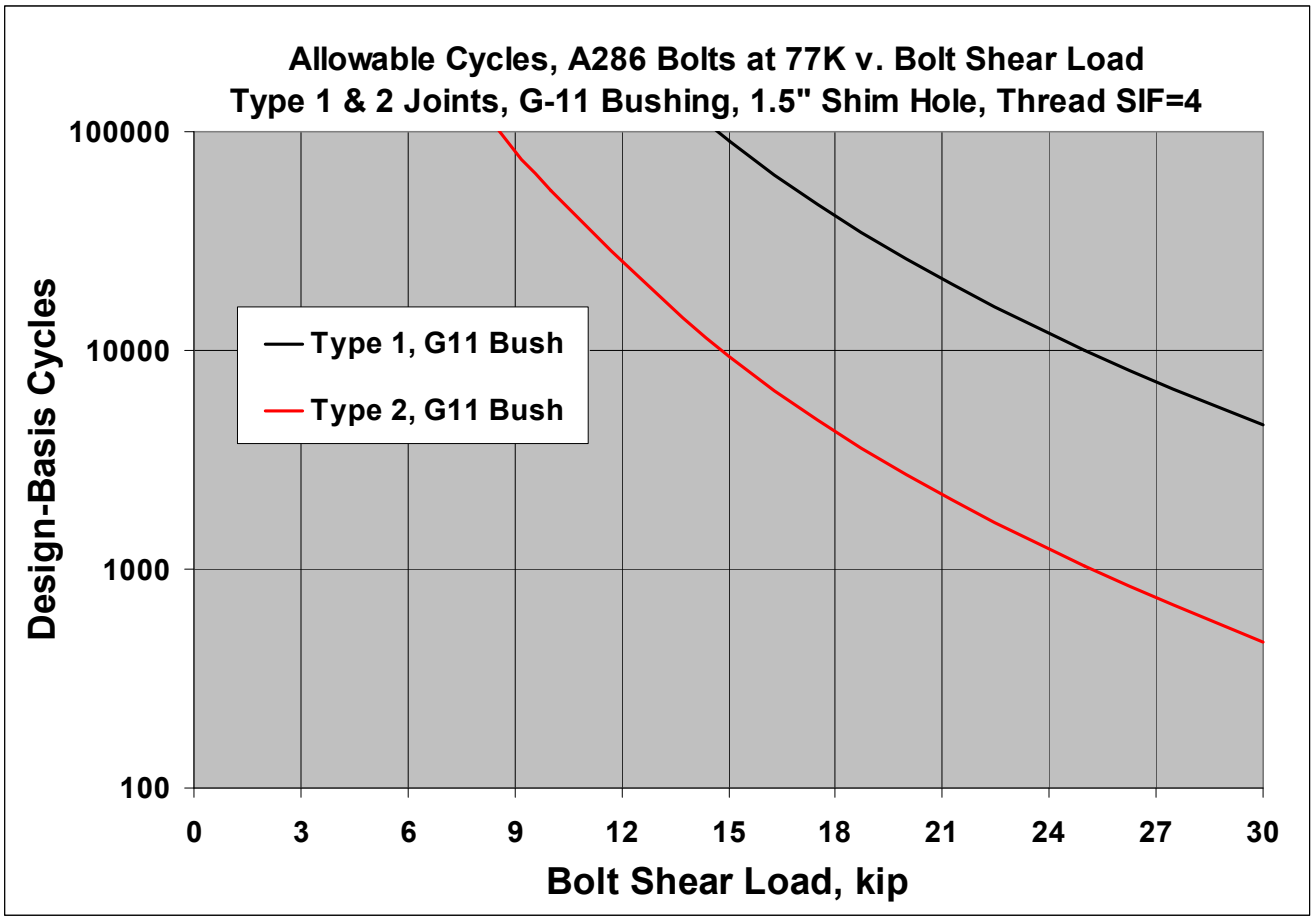

Assumptions:
1. Stresses scale with applied bolt shear load.
2. Stress Intensification Factor of 4.0 applicable to bolt threads.
3. Design-Basis Cycles obtained from Design-Basis fatigue curve-fit and FE model stresses.

References

[1] ANSYS Inc, 275 Technology Drive, Canonsburg, PA 15317
[2] K.D.Freudenberg "Non-Linear Modular Coil Analysis" NCSX-CALC-14-002-001, July 2007.
[3] W.D. CAIN, "MAGFOR: A Magnetics Code to Calculate Field and Forces in Twisted Helical Coils of Constant Cross-Section", 10th IEEE/NPSS Symposium on Fusion Engineering, 1983
[4] H.M. Fan. "Nonlinear Analysis of Modular Coil and Shell Structure" NCSX-CALC-14-001-001, February 2006

A. Attachments

A.1 Bonded Interfaces

The analysis begins with a simulation assuming all coil-to-coil flange interfaces are bonded. This provides an estimate of the shear loads which must be carried by friction and bolts, with particular attention given to the inboard leg region. A postprocessing macro is developed to integrate the two in-plane shear components over small regions and turn them into shear stress as a function of poloidal angle shown in Figs. A.1-1 through A.1-4. The plots show the magnitude of the shear stress at each interface. Interfaces A-A, A-B & C-C must transmit a peak shear stress of ~10 MPa, while B-C has a peak of ~18 MPa. Of course, the shear areas differ substantially, so the magnitude of the shear forces is different for each interface.

Fig. A.1-1 Subdivision of A-A Inboard Leg and Integrated Shear Stresses

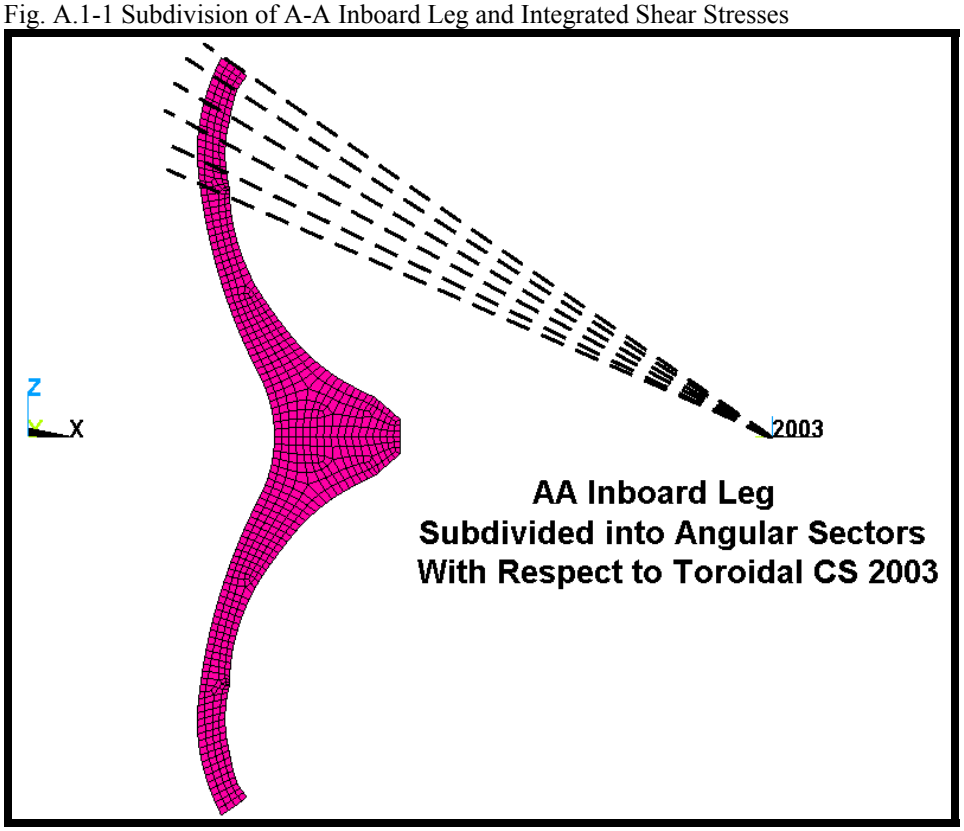

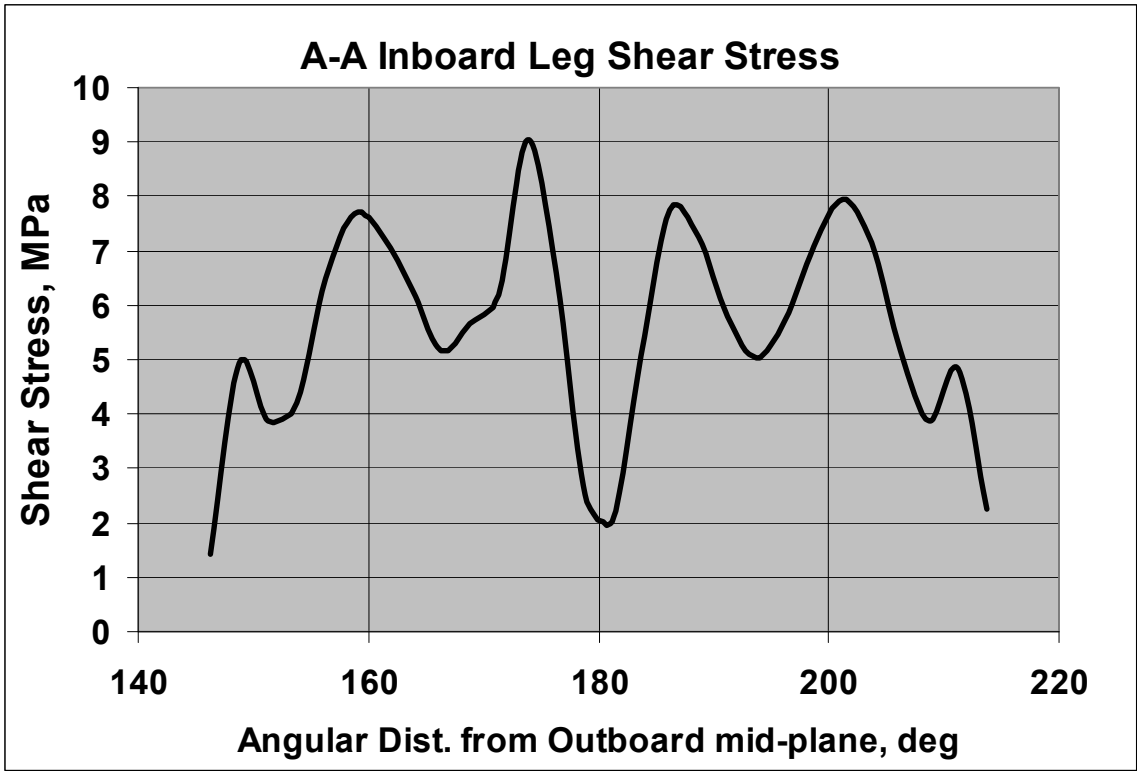

Fig. A.1-2 Subdivision of A-B Inboard Leg (Similar to A-A) and Integrated Shear Stresses

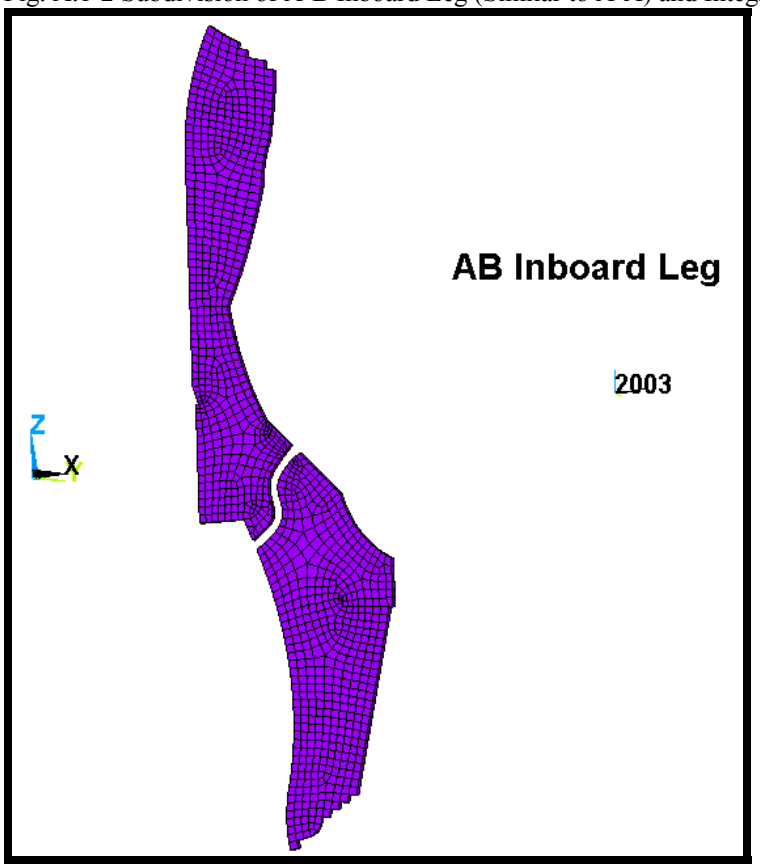

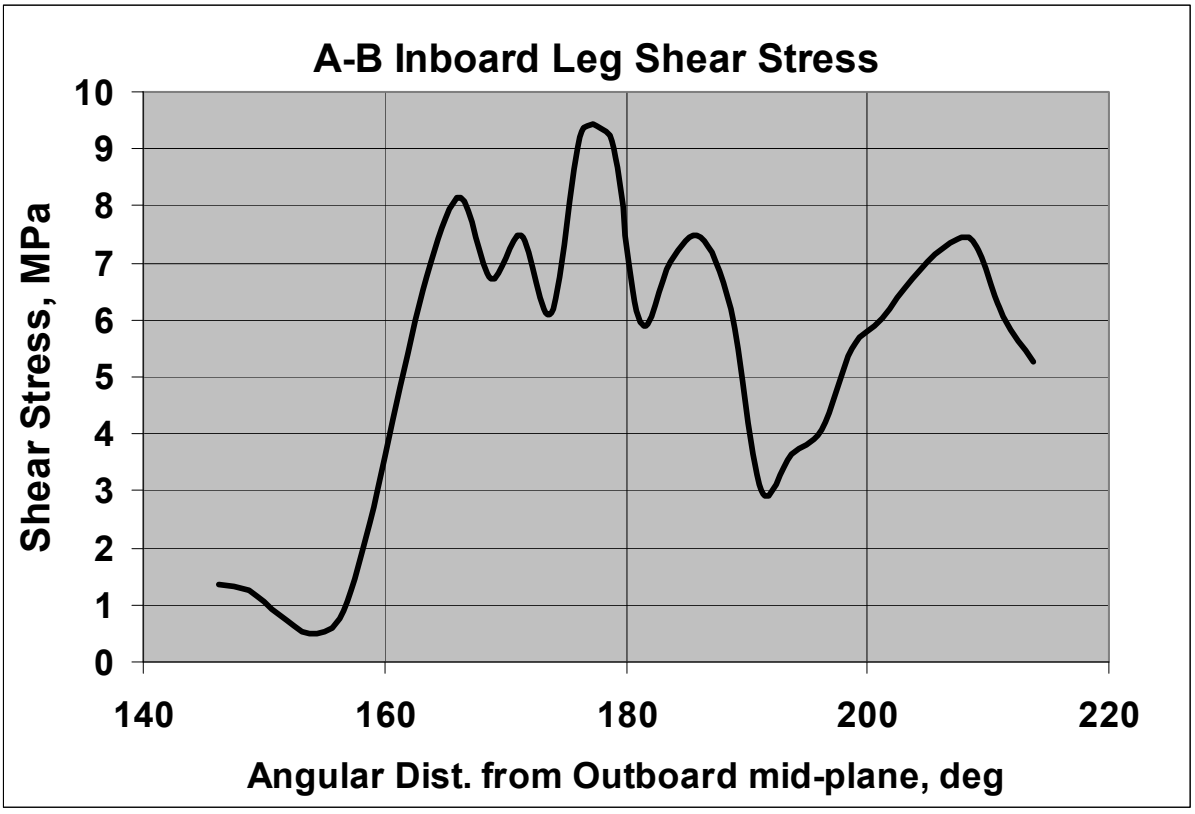

Fig. A.1-3 Subdivision of B-C Inboard Leg (Similar to A-A) and Integrated Shear Stresses

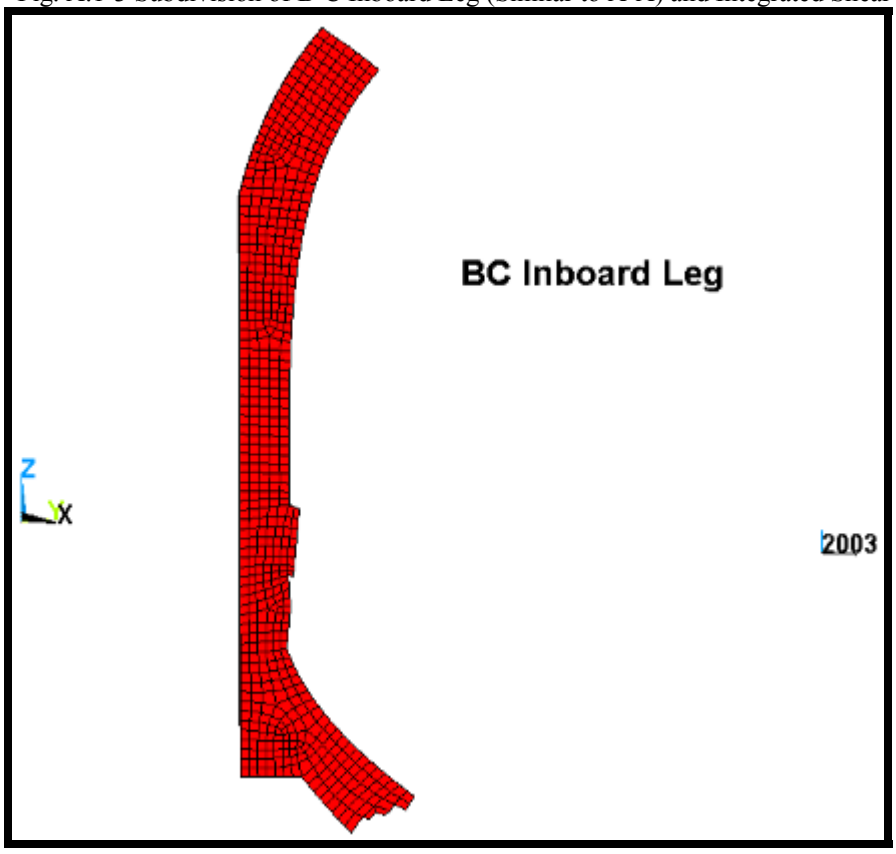

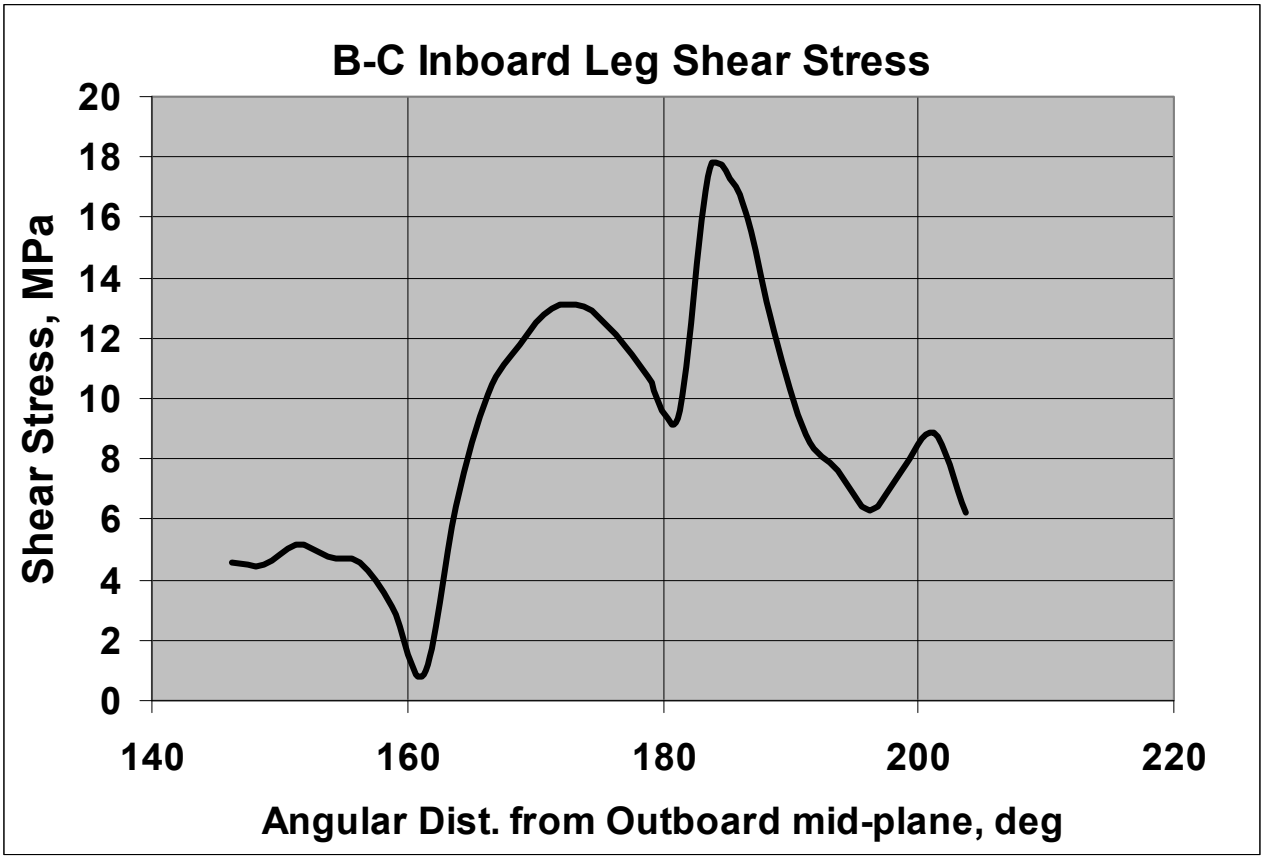

Fig. A.1-4 Subdivision of C-C Inboard Leg (Similar to A-A) and Integrated Shear Stresses

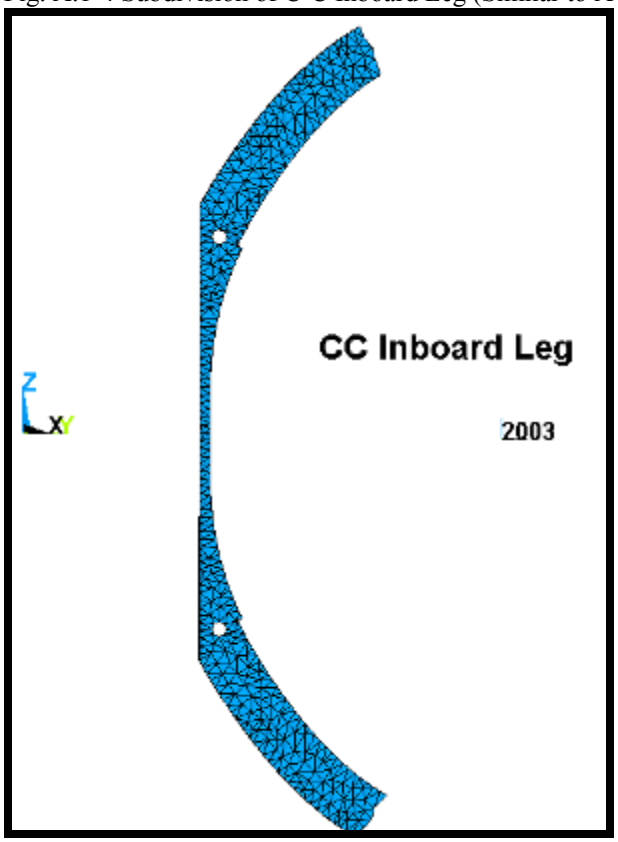

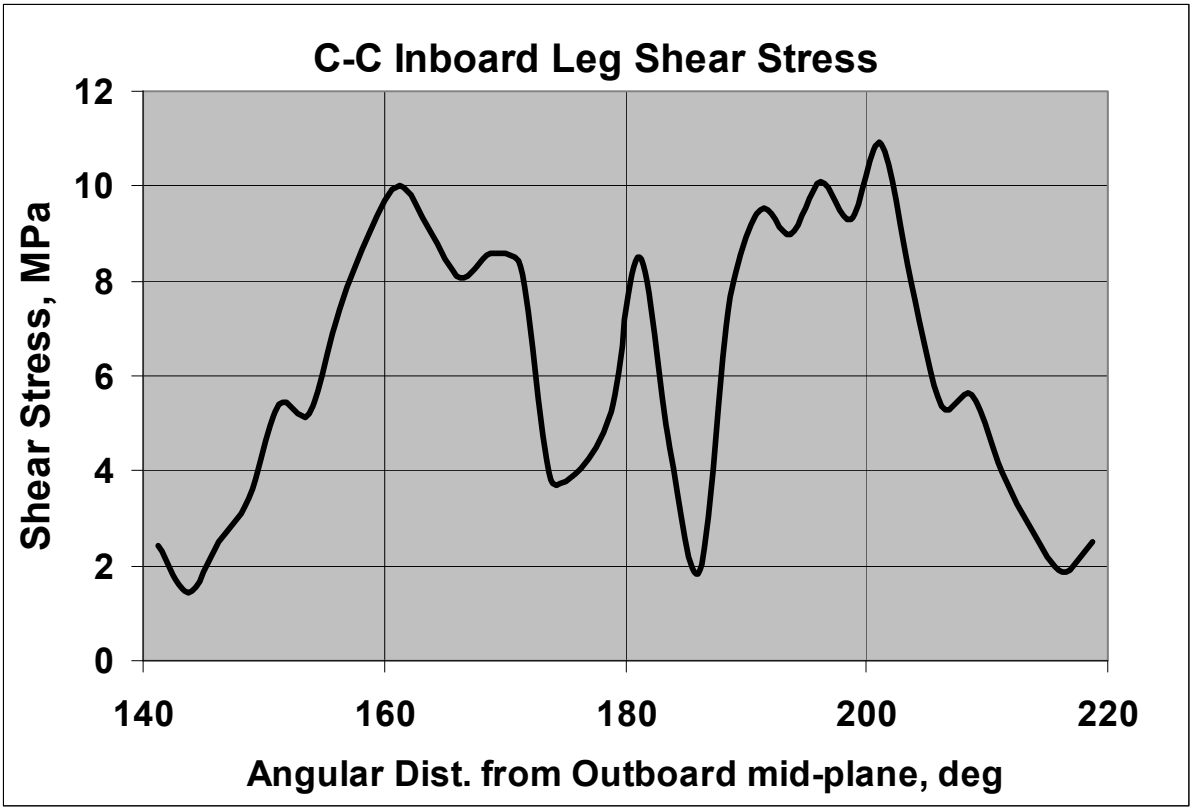

A.2 Using Larger C-C inner Leg Bolts

CC Connection with 1.5” bolts

NCSX NATIONAL COMPACT STELLARATOR EXPERIMENT

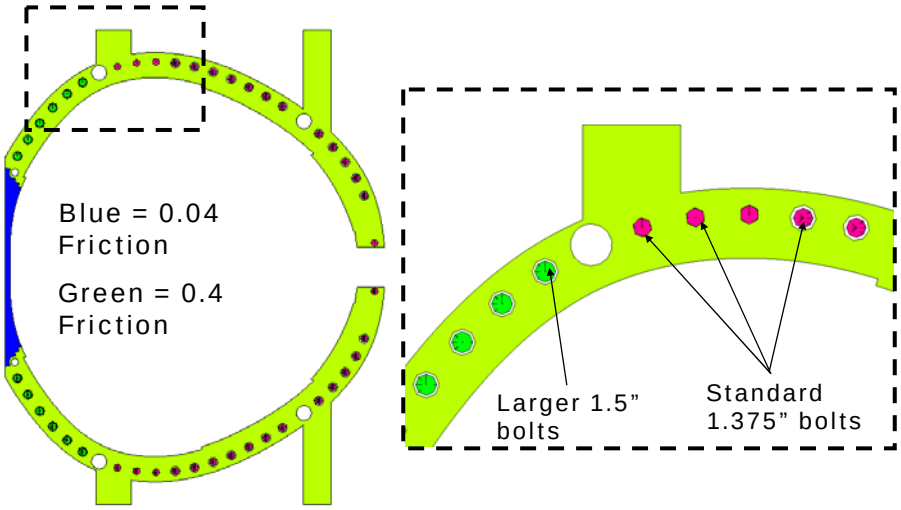

1.5” bolts will have approximately 90 Kips preload or 20% increase from 1.375” bolts.

6 ADDED 1.5” BOLTS

NCSX NATIONAL COMPACT STELLARATOR EXPERIMENT

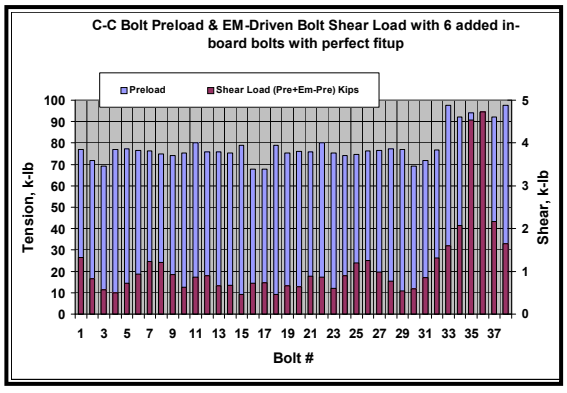

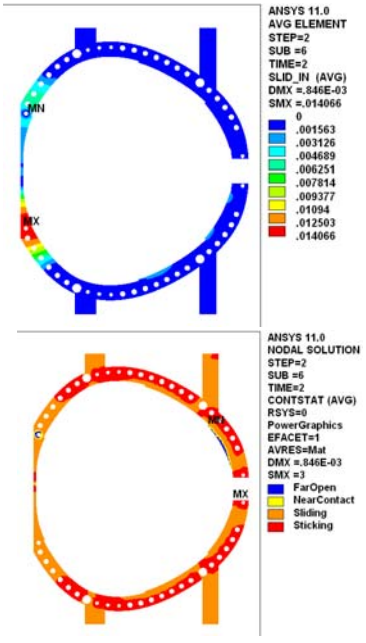

Friction = 0.04 on Inner-leg region, mu = 0.4 everywhere else

Outer Bolts #1 and #32 are now completely stuck. Inner leg slippage has been essentially eliminated.

Innermost inboard bolts (#35 - #36) are stuck according to the status plot.

12 ADDED 1.5” BOLTS

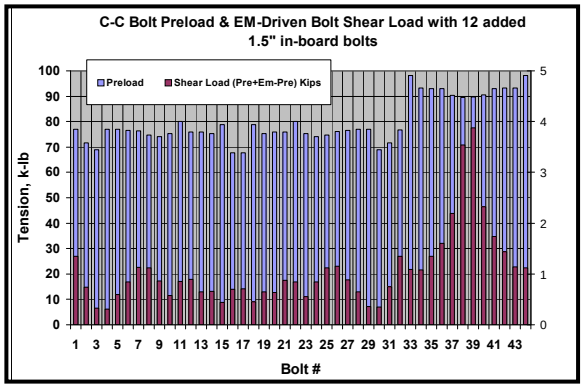

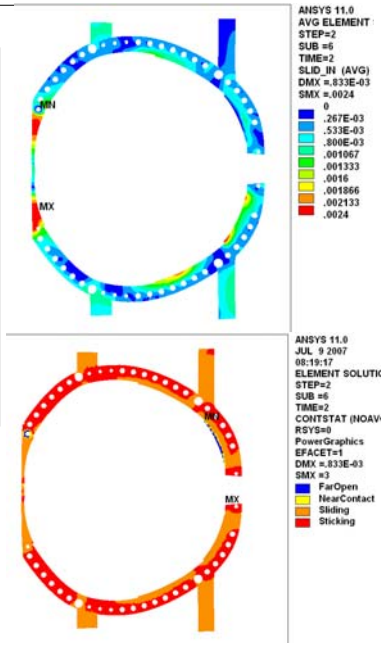

Friction = 0.04 on Inner-leg region, mu = 0.4 everywhere else

Outer Bolts #1 and #32 are now completely stuck. Inner leg slippage has been essentially eliminated.

Innermost inboard bolts (#38 - #39) are still stuck.

Three Innermost Bolts Added

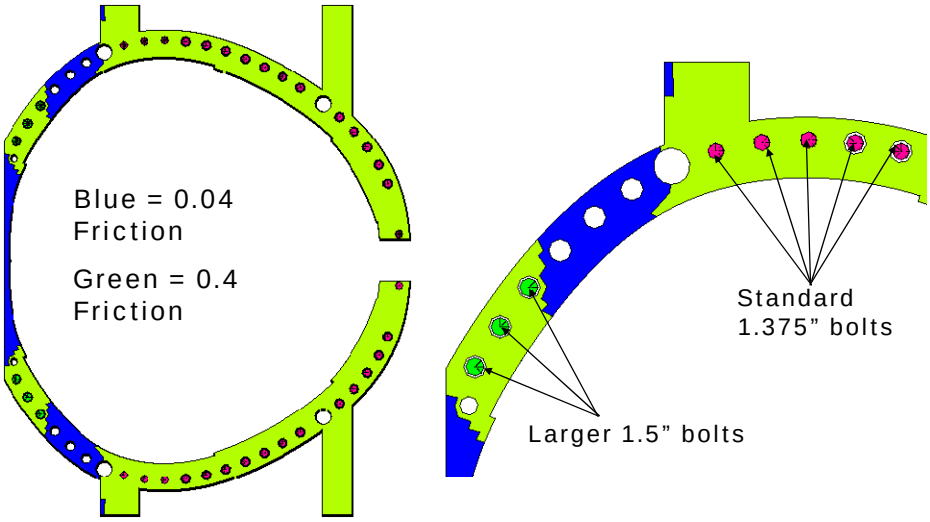

Reverse 6 ADDED 1.5” BOLTS

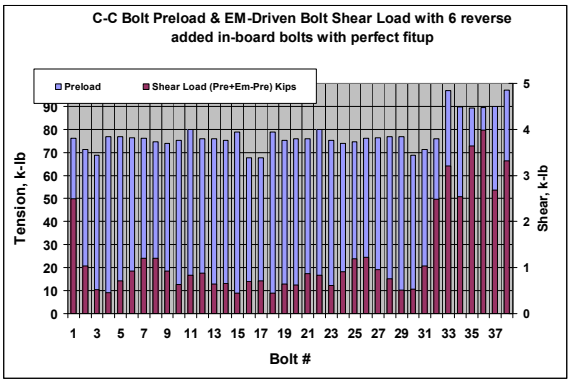

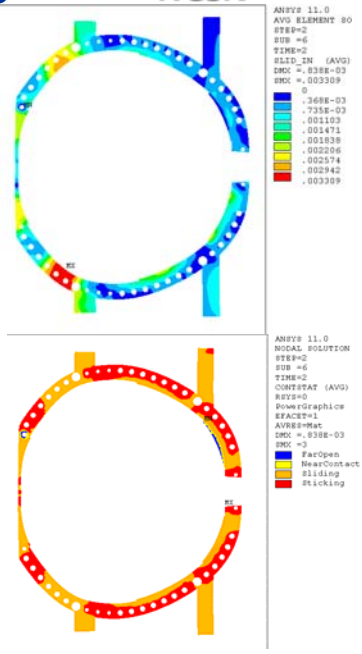

Friction = 0.04 on Inner-leg region,
mu = 0.4 everywhere else

Outer Bolts #1 and #32 are now completely stuck.
Inner leg slippage has been essentially eliminated.

Innermost inboard bolts (#35 - #36) are still stuck.

Study on the Inner Leg of CC

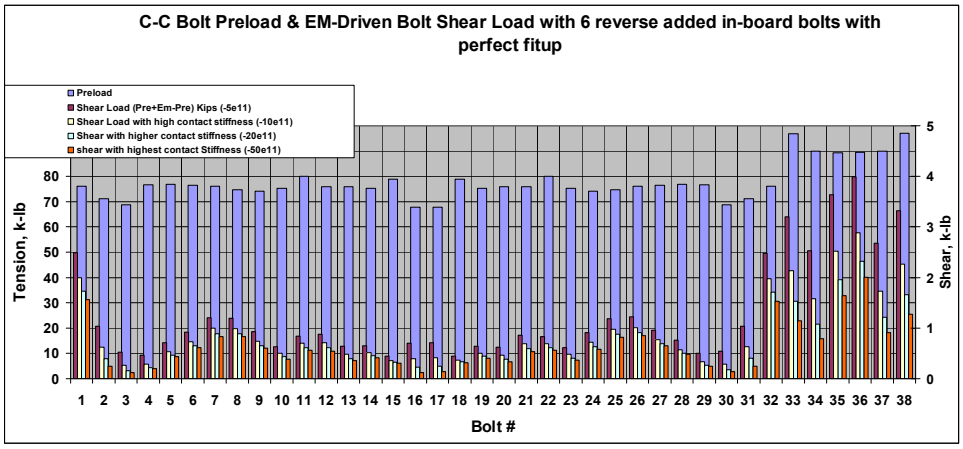

Inner Leg Bolts Only